Improving Specifications to Resist Frost Damage in Modern Concrete Mixtures

Pool Fund Study TPF-5-297

Led by Oklahoma DOT

Hope Hall, Justin Becker, Chad Staffileno, Mark Finnell, Lichun Chen, David Welchel,

Jacob Peery, Jake LeFlore, Dan Cook, M. Tyler Ley

Oklahoma State University

Stillwater, Oklahoma

Mehdi Khanzadeh Moradllo, Chunyu Qiao, Rita Maria Ghantous, Mitchell Keys,

Myo Zaw, Steven Reese, W. Jason Weiss

Oregon State University

Corvallis, Oregon

August 31, 2019

TABLE OF CONTENTS

1.0 INTRODUCTION

Concrete is widely known as the building material of choice when a long-lasting structure is desired. However, concrete can be damaged when it is 1) wet and 2) exposed to freezing temperatures [1, 2]. The damage that occurs due to freezing and thawing can lead to premature deterioration, costly repairs, and the need to replace concrete infrastructure components well before they reach the end of their expected lifetimes. This problem is widely known, and there are many specifications in place designed to minimize these problems. The most widely adopted approach to producing concrete with frost durability is to add an air-entraining admixture (AEA) while the concrete is being mixed. The AEA creates small, well-dispersed, air-filled bubbles in the fresh concrete. Because a large number of variables during batching, mixing, and placement impact how AEAs perform in concrete, in practice it can be challenging to provide a consistent air-void system in hardened concrete [5]. The concrete industry would greatly benefit from tools that would help ensure that this process is done correctly and the concrete that is produced will be freeze-thaw durable.

Current specifications for freeze-thaw durability were developed more than half a century ago. These specifications are based on the measurement of total air volume in fresh concrete [6, 7]. This is typically done by comparing the actual density to the theoretical, or by measuring the response of the concrete from an increase in pressure. While the specification and measurement of the total volume of air within concrete are useful, more in-depth research has shown that the size and spacing of the air-entrained bubbles are more important. For this paper, the size and spacing of the air bubbles will be combined into a term called the "air void system quality". Historically, the air void system quality is defined by "the Spacing Factor" [4, 9]. The ACI 201 technical committee has recommended that a spacing factor of 200 μm be used to provide concrete with satisfactory freeze-thaw durability [10]. The spacing factor can be determined by a hardened air void analysis or petrographic analysis completed as per ASTM C457 [11]. Unfortunately, the ASTM C457 method requires significant labor, specially trained staff and equipment, and can take between 7 to 14 days to complete. However, the biggest drawback of this testing is that it cannot be used on concrete before it has hardened. This means that several days of construction could proceed before this measurement would indicate that there was an issue. Because of these challenges, most specifications measure the total volume of air in the concrete while it is being placed and assume that the correlation between air volume and air quality suggested in the work from the 1950's is satisfactory.

Modern concrete mixtures commonly use Portland cement in combination with other types of supplementary cementitious materials; mixtures often contain between two to five chemical admixtures; cement is made with new types of grinding aids that aim to reduce production energy and provide strength increases; and finally, modern construction practices are much more complex, as machines are used that pump, consolidate, and finish our concrete. There are numerous examples of how these changes have influenced the original relationship between air volume and air quality. Specific examples include different AEAs [12, 13, 15], admixture combinations [14, 15, 17] and pumping [18-21]. There has been little progress made because tools are not readily available to help investigate these issues. Because of these substantial differences in modern mixtures from those investigated in the 1950's, it is not clear if air volume specifications are still appropriate.

This highlights the need for a new tool to provide more insight into the quality of the air void system during construction so that near real-time changes can be made to ensure that concrete that is freeze-thaw durable is being used and provide useful insights into how different additives or processes impact the quality of the air void system.

1.1 Organization of this Document

This report aims to provide new insights into the measurement of air void systems in fresh concrete as well as new levels of understanding and prediction of freeze thaw durability of concrete structures. This was a collaborative research project between research teams led by Tyler Ley at Oklahoma State University and Jason Weiss at Oregon State University and Purdue University.

The document is broken into two primary sections: Measuring Air Void Systems in Fresh Concrete and Prediction of Freeze Thaw Durability. Each chapter is a summary providing the key conclusions and important

data from the work. An appendix for many of the chapters has also been included. In most cases each appendix is a peer reviewed journal paper that provides details about the methods and materials used as well as a much more in depth discussion of the results and the data. This means that if there a detail that a reader wants to know more about then they are encouraged to look at the corresponding appendix. The document was organized in this way so that a reader could quickly learn the key findings while also having access to all of the necessary details.

References

1.   Kosmatka, S.H. and M.L. Wilson, *Design and control of concrete mixtures*. 2016: Portland Cement Assoc.
2.   Pigeon, M. and R. Pleau, *Durability of concrete in cold climates*. 1995: CRC Press.
3.   Scherer, G.W. and J. Valenza, *Mechanisms of frost damage.* Materials science of concrete, 2005. **7**(60): p. 209-246.
4.   Backstrom, J., et al., *Void spacing as a basis for producing air-entrained concrete.* ACI Journ., 1954. **4**: p. 760-761.
5.   Whiting, D. and D. Stark, *Control of air content in concrete.* NCHRP report, 1983(258).
6.   Kleiger, P., *Studies of the Effect of Entrained Air on the Strength and Durability of Concrete made with Various Maximum Sizes of Aggregate*. 1952: Portland Cement Association.
7.   Kleiger, P., *Further Studies on the Effect of Entrained Air on Strength and Durability of Concrete with Various Sizes of Aggregates*. 1956: Portland Cement Association.
8.   211, A.C. *Standard Practice for Selecting Proportions for Normal, Heavyweight and Mass Concrete*. 1991. American Concrete Institute.
9.   Powers, T.C. and T. Willis. *The air requirement of frost resistant concrete*. in *Highway Research Board Proceedings*. 1950.
10.   201.2R, A.C. *Guide to Durable Concrete*. 2016. American Concrete Institute.
11.   ASTM-C457, *Standard Practice for Microscopical Determination of Air-Void Content and Parameters of the Air-Void System in Hardened Concrete*. 2017, ASTM International: West Conshohocken, PA.
12.   Gay, F. *A factor which may affect differences in the determined air content of plastic and hardened air-entrained concrete*. in *Proceedings of the Fourth International Conference on Cement Microscopy, Las Vegas, Int. Cem. Microscopy Assoc*. 1982.
13.   Gay, F.T. *The Effect of Mix Temperature on Air Content and Spacing Factors of Hardened Concrete Mixes with Standardized Additions of Air-Entraining Agent*. in *Proceedings, Seventh International Conference on Cement Microscopy, Fort Worth, International Cement Microscopy Assoc., Duncanville, TX*. 1985.
14.   Plante, P., M. Pigeon, and C. Foy, *The influence of water-reducers on the production and stability of the air void system in concrete.* Cement and Concrete Research, 1989. **19**(4): p. 621-633.
15.   Jana, D., B. Erlin, and M.F. Pistilli, *A closer look at entrained air in concrete.* Concrete international, 2005. **27**(7): p. 61-64.
16.   Freeman, J.M., *Stability and quality of air void systems in concretes with superplasticizers*. 2012, Oklahoma State University.
17.   Felice, R., J.M. Freeman, and M.T. Ley, *Durable Concrete with Modern Air-Entraining Admixtures.* Concrete international, 2014. **36**(8): p. 37-45.
18.   Pleau, R., et al., *Influence of pumping on characteristics of air-void system of high-performance concrete.* Transportation research record, 1995: p. 30-36.
19.   Janssen, D., K. Macdonald, and A. Gardiner. *Effects of pumping parameters on the stability of entrained air voids*. in *CONSEC'01: Third International Conference on Concrete Under Severe Conditions*. 2001.
20.   Elkey, W.D., D.J. Janssen, and K.C. Hover. *Effects of admixtures on air-void stability of concrete subjected to pressurization*. in *Concrete Under Severe Conditions 2*. 1998.
21.   Janssen, D.J., R.M. Dyer, and W.E. Elkey. *Effect of pumping on entrained air voids: role of pressure*. in *CONSEC 95 Concrete Under Severe Conditions*. 1995.

2.0 MEASURING AIR VOID SYSTEMS IN FRESH CONCRETE

2.1 DETERMINING THE AIR-VOID DISTRIBUTION IN FRESH CONCRETE WITH THE SEQUENTIAL AIR METHOD (SAM)

Modern tools are needed to build confidence that concrete construction will be long-lasting in freeze-thaw environments while also minimizing the amount of material that is rejected at the job site. Ideally, these tools could be used during both the development of the concrete mixtures and then again at the job site to evaluate the material. In addition, the measurements should be robust, accurate, and provide answers in a timely manner that correlate to historic measurements of freeze-thaw durability.

This chapter outlines a procedure that uses sequential pressures to determine the air void quality in fresh concrete using the SAM (AASHTO TP 118). The variability of the SAM was investigated. Also the SAM, hardened air-void analysis (ASTM C457), and rapid freeze-thaw testing (ASTM C666) were compared in both laboratory and field testing. Finally, a discussion is included over the potential use and impact of the method. The goal of this paper is to introduce and establish the validity of the SAM test method. Other papers over the mechanism and usage over a wider number of materials will proceed this paper.

2.1.2 Experimental Methods
All the admixtures used met the requirements of ASTM C260 and ASTM C494. The wood rosin (WROS) and synthetic (SYNTH) AEA are two popular commercial AEAs. Sixteen different mixture designs in the laboratory were investigated. Between five and fourteen dosages of AEA were investigated for each mixture to achieve a range of air contents from 2% to 10%. A subset of mixtures was investigated with either a polycarboxylate (PC) superplasticizer meeting ASTM C1017 or a midrange water reducer (WR) meeting ASTM C494. A dose of between 60 and 200 mL/100 kg was used to increase the slump of the mixture between 50 mm to 150 mm. All the concrete mixtures in this research used a Type I cement that met the requirements of ASTM C150. An ASTM C618 Class C fly ash was used in several of the mixtures with a 20% cement replacement by weight. Both the crushed limestone and the sand met ASTM C33 specifications and have proven to be freeze-thaw durable. The absorption of the crushed limestone and sand was 0.60% and 0.55% respectively.

2.1.2.1 Sampling & Testing Procedure
Testing of 303 concrete mixtures were completed both in the laboratory and field. Samples were made for both hardened air-void analysis (ASTM C457) and the SAM (AASHTO TP 118). A selection of these mixtures were sampled to also investigated rapid freeze-thaw testing (ASTM C666). Field testing was completed with 62 field mixtures from seven different sites in Oklahoma. The majority of these samples were taken from paving projects and more details can be found in other publications [1].

2.1.2.2 Sequential Air Method
The Sequential Air Method (AASHTO TP 118), also known as the SAM or Super Air Meter provides both the air content and spacing of air void system through the SAM Number. Similar to the ASTM C231 Type B meter with some modifications, the SAM device show in Figure 2.1.1 uses six restricted clamps to account for increased pressures and a digital pressure gauge for testing. The SAM can be used to test concrete before it hardens, which provides insight into the air void system to help design and evaluate the air void system of the hardened concrete. The test should take an experienced user between eight to 10 minutes to complete. The test applies three sequential pressures to the fresh concrete and the equilibrium pressures are recorded. The pressure is then released and the same steps are applied again to the fresh concrete. The SAM Number is calculated by taking the numerical difference between the final pressure steps. The difference between the pressure responses is an indication of the air void size and spacing in the concrete. Figure 2.1.2 shows a typical data set and a video of the test is available [2].
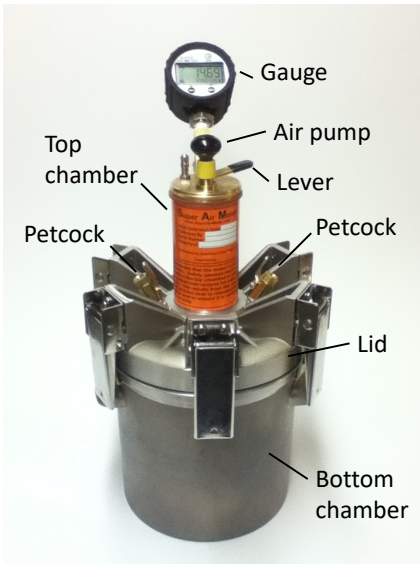
Figure 2.1.1 – The device used to complete the SAM.
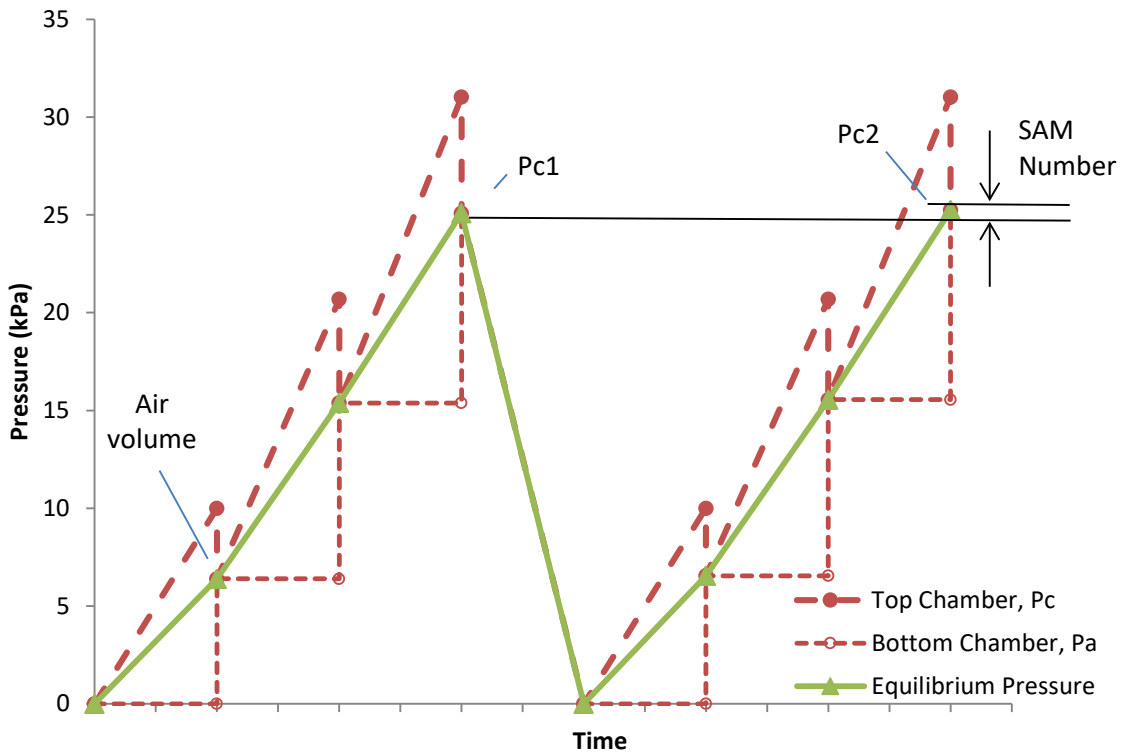
Figure 2.1.2 A graphical representation of the pressures in the top and bottom chamber in the SAM.

2.1.3 Results

2.1.3.1 Comparing SAM Number to Spacing Factor

Figure 2.1.3 shows the correlation between the SAM Number and the Spacing Factor for 303 laboratory and field concrete mixtures that were completed by two different labs. These mixtures consisted of 176 laboratory mixtures completed at Oklahoma State University, 65 laboratory mixtures completed at FHWA Turner Fairbanks, and 62 field mixtures from seven different field projects in Oklahoma. While the data in Figure 2.1.3 is scattered, there does seem to be a correlation between the Spacing Factor and SAM Number. Figure 2.1.3 shows the suggested Spacing Factor of 200 µm from ACI 201.2R-16 [3] along with a SAM Number of 0.20. It

4

is interesting that when a SAM Number of 0.20 is used that this correlated with a spacing factor of 200 μm for 88% of the comparisons. If the user is interested in determining a Spacing Factor of 250 μm then a SAM Number of 0.25 correctly separates 85% of the comparisons. This almost perfect correlation between the numbers does not continue for a Spacing Factor of 300 μm as a SAM Number of 0.33 shows the best correlation for just over 75% of the data. By using this single SAM Number as a threshold value it allows the user to determine in a single measurement if a Spacing Factor is above or below a target value. This concept of using a single critical value is common place in determining freeze-thaw durability and assists practitioners with implementation.
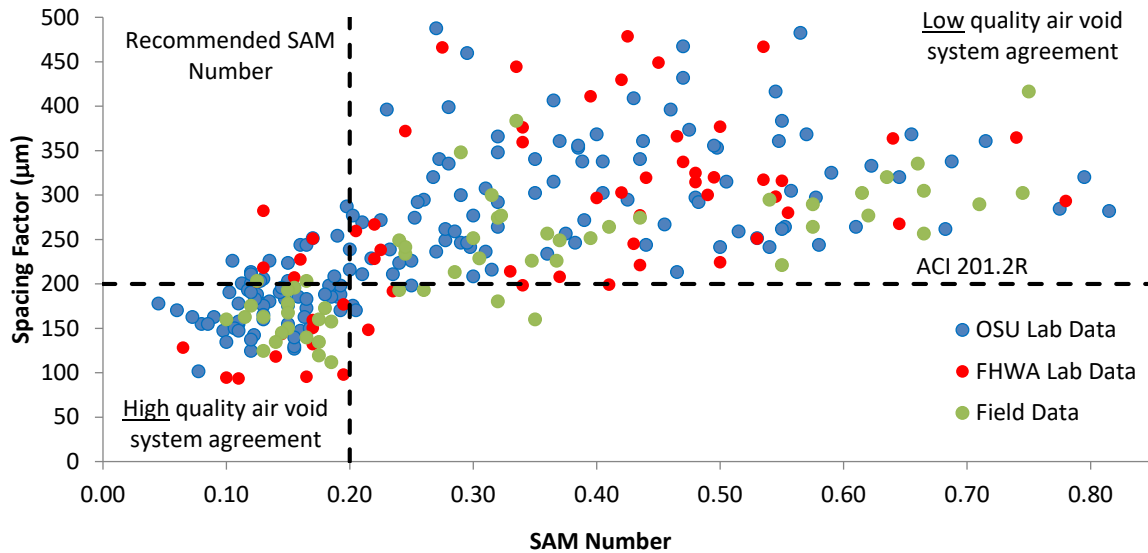
Figure 2.1.3 – The SAM Number versus the Spacing Factor for 303 laboratory and field mixtures completed by two different research groups. A SAM Number of 0.20 was able to correctly identify if the Spacing Factor was above or below 200 μm for 88% of the data.

2.1.3.2 Comparing SAM and Durability Factor in ASTM C666

Since a good correlation was found between the Spacing Factor and SAM Number one would expect a good correlation between SAM Number and the results from the freeze-thaw testing. However, the best correlation between the SAM Number and Durability Factor may not be the same. Figure 2.1.4 shows the relationship between Durability Factor and SAM Number for 68 different concrete mixtures. Again, a single SAM Number of 0.32 was used to investigate the data. A SAM Number of 0.32 was chosen as the limit as it provides a conservative estimate and it correctly separated nearly 90% of the investigated mixtures. Furthermore, if one was using these results to create a specification then it may be appropriate to use a SAM Number that is even lower in order to provide some safety factor against failure.
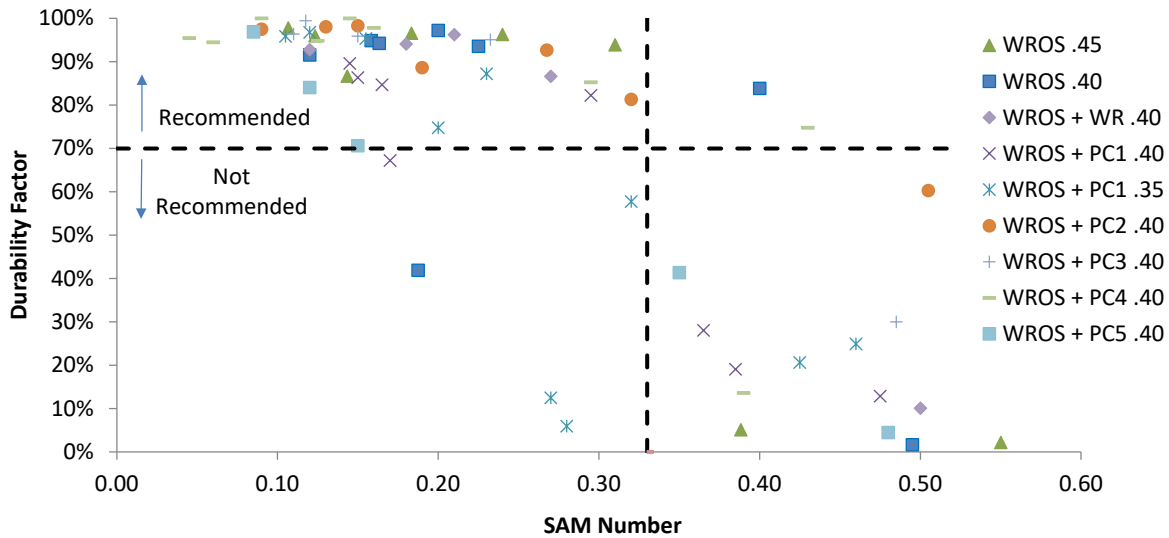
Figure 2.1.4 – SAM Number versus Durability Factor for 68 mixtures. A SAM Number of 0.32 identified whether the concrete would have a Durability Factor above 70% for 90% of the mixtures investigated.

2.1.3.3 Variability of SAM

It is important that the variation of a testing method is well understood. To investigate the variability of the test method 170 concrete mixtures were completed with two different SAM meters and two operators simultaneously completing the measurement. The measured SAM Number from each meter is shown in Figure 2.1.5. A line of equity has also been added to the graph. Ideally all of the mixtures would fall on the line but as can be seen, there is some variance. This difference in measurements could be caused by variations from operators, materials, or the method itself.
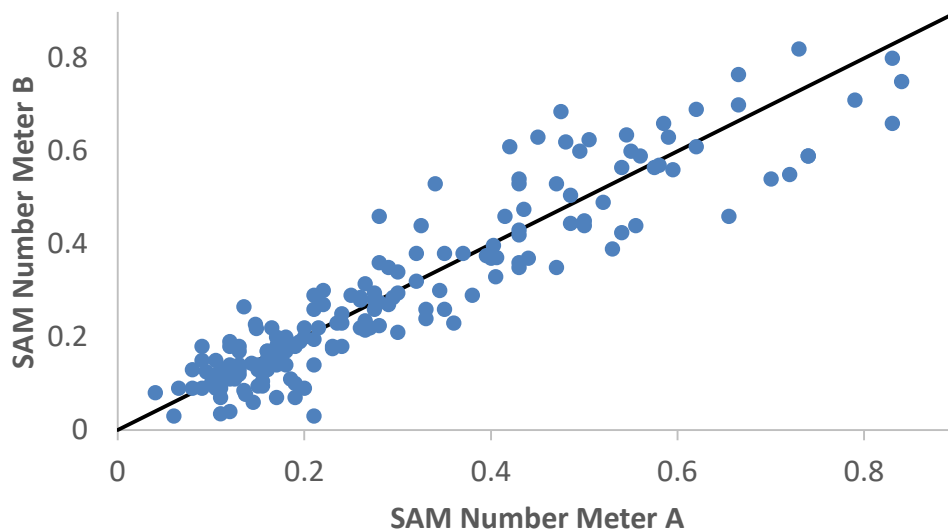
Figure 2.1.5 – A comparison of the SAM Number from two different meters measured on the same concrete mixtures. A line of equity is shown for comparison.

2.1.3.4 Variability of Measurements

Table 2.1.1 shows that all three tests have a COV between 15.2% and 22.7% with the SAM Number showing the lowest COV. Because the COVs between these three tests are so similar this could mean that the air void

6

quality in concrete is more variable than other parameters that are more commonly measured such as the compression strength or unit weight. This is also supported by the observation that the variation of the SAM Number was significantly reduced when only investigating water in the test method.

Table 2.1.1 – A comparison of the coefficient of variation, agreement with Durability Factor as found in this paper, and the time required to complete the test.

Test Method	Parameter	COV	Agreement with DF of 70 In ASTM C 666	Time to complete the test
SAM	SAM Number[1]	15.2%	90%	10 min
ASTM C457	Spacing Factor[2]	20.1%	67%	7 days
ASTM C666	Durability Factor[3]	22.7%	-	3.5 months

[1]Assumes a SAM Number of 0.32 and a standard deviation of 0.049 from this paper

[2]From ASTM C457

[3]From ASTM C666 with a durability factor of 75 and Method B

2.1.4 Conclusion

This work presents a new method to measure the air void quality in fresh concrete by using sequential pressures. The test can determine both the volume of air and a parameter called the SAM Number that is shown to correlate to hardened air void analysis and rapid freeze-thaw testing. Results from two different testing laboratories and field data from 303 concrete mixtures are included in this paper. In addition, the measurement variance is shown to be lower than hardened air void analysis and rapid freeze-thaw testing. These specific findings have been made:

- A SAM Number of 0.20 and 0.25 shows a correlation to a Spacing Factor of 200 μm and 250 μm with an 88% and 85% agreement respectively.
- A SAM Number of 0.32 correlates with a Durability Factor between 60% and 80% for over 88% of the data investigated, while a Spacing Factor of 200 μm correlated with a Durability Factor of 70% for only 68% of the data.
- The standard deviation of two SAM Numbers from two different operators using different sets of equipment that were run simultaneously was shown to be 0.049 for concrete and 0.021 when investigating water and a calibration vessel. This lower variability with water suggests that over 50% of the variation in the test is caused by the use of concrete in the test.
- The coefficient of variation of the SAM Number that showed the best correlation to freeze-thaw durability is 15.2%. This value is comparable but lower than similar measurements from hardened air void analysis and rapid freeze-thaw testing.
- A target SAM value of 0.22 or conservatively 0.20 is suggested for design to ensure mixtures have a satisfactory performance in rapid freeze-thaw testing.

References
1. Welchel, D., *Determining the Size and Spacing of Air Bubbles in Fresh Concrete*. 2014, Oklahoma State University.
2. LeFlore, J. *Super Air Meter Test Video*. 2016; Available from: https://www.youtube.com/watch?v=xAcHqMz_m3I.
3. 201.2R, A.C. *Guide to Durable Concrete*. 2016. American Concrete Institute.

2.2 FIELD AND LABORATORY VALIDATION OF THE SAM

For this work, a term called the quality of the air void system will be used to describe a satisfactory void size and spacing in the hardened concrete. The most established method to determine the air void quality is to use a hardened air void analysis and determine a parameter called the Spacing Factor [1, 2]. After the concrete has hardened, it is cut, polished, and the surface is inspected under a microscope to inspect the voids. This process can take weeks and so it cannot be used to provide the immediate feedback needed to modify the fresh concrete. While there are other methods that can measure the volume of air in fresh concrete (ASTM C 231, ASTM C 138, ASTM C 173), the volume of air does not necessarily represent the quality of the air void system [3-5].

2.2.2 Experimental Methods

2.2.2.1 Laboratory Materials & Mixture Design
ASTM C150 Type I Portland cement was used in all of the laboratory concrete mixtures in this report. The local crushed limestone and natural sand meet ASTM C33 standards. The maximum nominal aggregate size of the limestone was 19 mm (3/4"). An intermediate aggregate was also used in some mixtures. The admixtures used met the ASTM C260 and ASTM C494 standards.

Twenty-three different mixture designs were studied for the lab testing. A subset of mixtures was examined with either a polycarboxylate (PC) superplasticizer meeting ASTM C1017, a Type A/F midrange water reducer (WR) meeting ASTM C494, or a Type S shrinkage reducer (SRA) meeting ASTM C494. Some of the mixture designs used a Class C fly ash replacement for 20% of the cement by weight that met ASTM C618 standards. Each mixture design consisted of four to fourteen dosages of AEA to study air contents from 2% to 10%. This allowed 192 mixtures to be investigated. The details are given in the appendix. The US Federal Highway Administration (FHWA) Turner Fairbanks Highway Research Center laboratory in McLean, Virginia, USA also provided data for this report to show an independent assessment of the test method with different materials. This work is summarized in other publications [6].

2.2.2.2 Field Materials & Mixture Design
To investigate the field performance of the SAM, testing was completed by either a Department of Transportation or private testing labs from 21 different States and one Canadian Province. Throughout the entire data set, over 15 users completed the SAM test. This data was collected from more than 110 projects. The nine states that provided detailed information used 34 different mix designs. Within those mix designs, there were 62 different aggregates, 19 different cement sources, 20 different fly ash sources and 39 different admixtures. The mixtures investigated consist of approximately 60% pavement mixtures, 20% bridge deck mixtures, and 20% other air-entrained mixtures including self-consolidating, precast, ready mix, and central mix concrete. Investigating the performance of the SAM on this wide range of materials allows a large number of variables to be investigated that could not be practically completed in a controlled laboratory setting.

2.2.2.3 Laboratory Concrete Mixing and Testing Methods
Aggregates from outdoor storage piles were gathered and moved indoors to a controlled temperature of 23°C. After 24 hours, the aggregates were loaded into the mixer and spun. Samples were collected from the mixer for moisture corrections. After moisture corrections were calculated, all of the aggregate and two-thirds of the water was placed in the mixer and spun for three minutes. This time allowed for evenly distributed aggregates and for the aggregates to be closer to saturated surface dry (SSD).

The residual water, cement, and fly ash were added next and mixed for three minutes. While the mixing drum was scraped, the concrete mixture rested for two minutes. Following the rest time, the mixer was spun and the admixtures were added. The AEA was added 15 to 30 seconds after the PC or WR, then the mixture was spun for three minutes. One hardened air-void analysis (ASTM C457) sample was made from each concrete mixture for testing. Two samples were tested simultaneously with the SAM by different operators. These were used to find the average SAM Number of a mixture.

2.2.3 Results and Discussion

2.2.3.1 Comparing the Spacing Factor and Air Volume

The air content and Spacing Factor was compared for all of the mixtures in this study. The laboratory concrete was shown in Figure 2.2.1 and the field concrete in Figure 2.2.2. A horizontal line was shown with a Spacing Factor of 200 μm as this was the value recommended by ACI 201.2R for freeze-thaw durability [7]. It can be seen in both Figure 2.2.1 and Figure 2.2.2 that the range of air contents needed to provide a Spacing Factor of 200 μm varied from 3.5% to 8% air volume. This wide range shows that it was difficult to develop a specification based on the volume of air to provide freeze-thaw durability. For example, in order to ensure the freeze-thaw durability of some of these mixtures, it would require the air volume in the concrete to be greater than 7.5%. Unfortunately, this would require many mixtures to have much higher air contents than is required. These higher air contents would impact the constructability and the strength of the concrete. This would increase the costs and may reduce the sustainability of a mixture. This reinforces that the air volume and air void quality do not correlate.
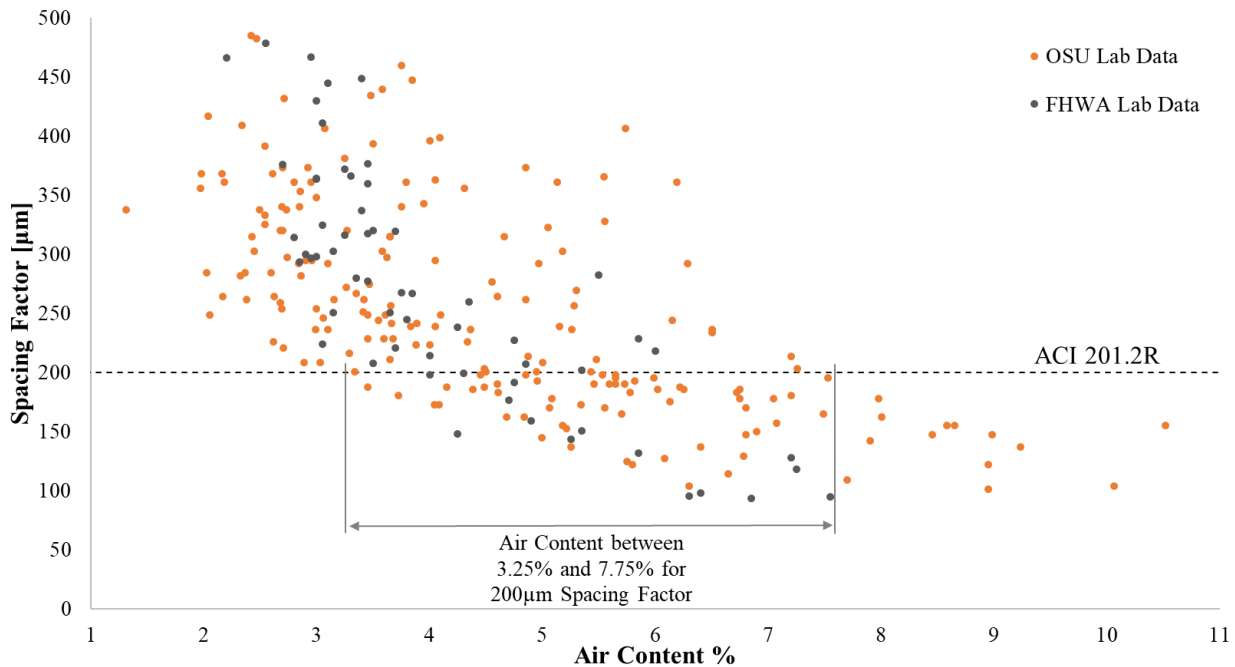
Figure 2.2.1 – Air Content versus Spacing Factor for 257 laboratory concrete mixtures completed by two different research groups.
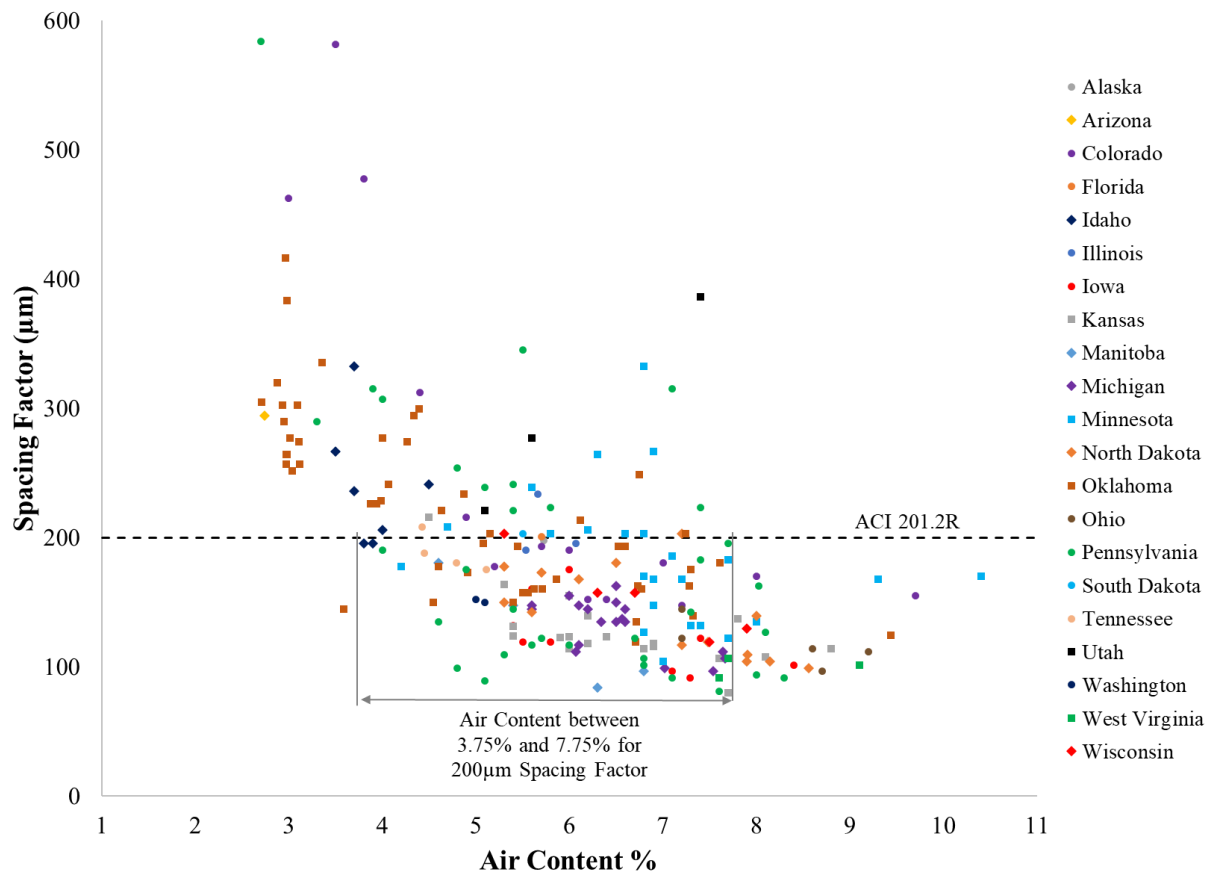
Figure 2.2.2 – Air Content versus Spacing Factor for 231 field concrete mixtures completed by 21 different state DOTs with various aggregates and admixtures.

2.2.3.2 Comparing the SAM Number and Spacing Factor

To further show the utility of the SAM Number, Figure 2.2.3 shows the relationship between SAM Number and Spacing Factor for 257 laboratory concrete mixtures completed by two different labs. Within this set of data, 75% of the mixtures were completed at Oklahoma State University and 25% of the mixtures were completed at FHWA Turner Fairbanks Highway Research Center [6]. Figure 2.2.3 shows that as the SAM Number increases then so does the Spacing Factor. Past recommendations for the Spacing Factor have used a single value to determine if a material is recommended for freeze-thaw durability. This has also been beneficial in aiding industry implementation because it is simple and shows if something is above or below the recommended value.

If target values for the SAM Number and Spacing Factor are used then this will separate the data into four quadrants. The upper right and lower left quadrant show where the SAM Numbers and Spacing Factors agree that the air void system is either satisfactory or unsatisfactory. The upper left and lower right quadrant show where the SAM Number and Spacing Factor do not agree. Past work has suggested that a SAM Number of 0.20 correctly determines if a Spacing Factor is above or below 200 μm for 88% of the data [8]. For this work, the laboratory data showed 85% agreement.

10
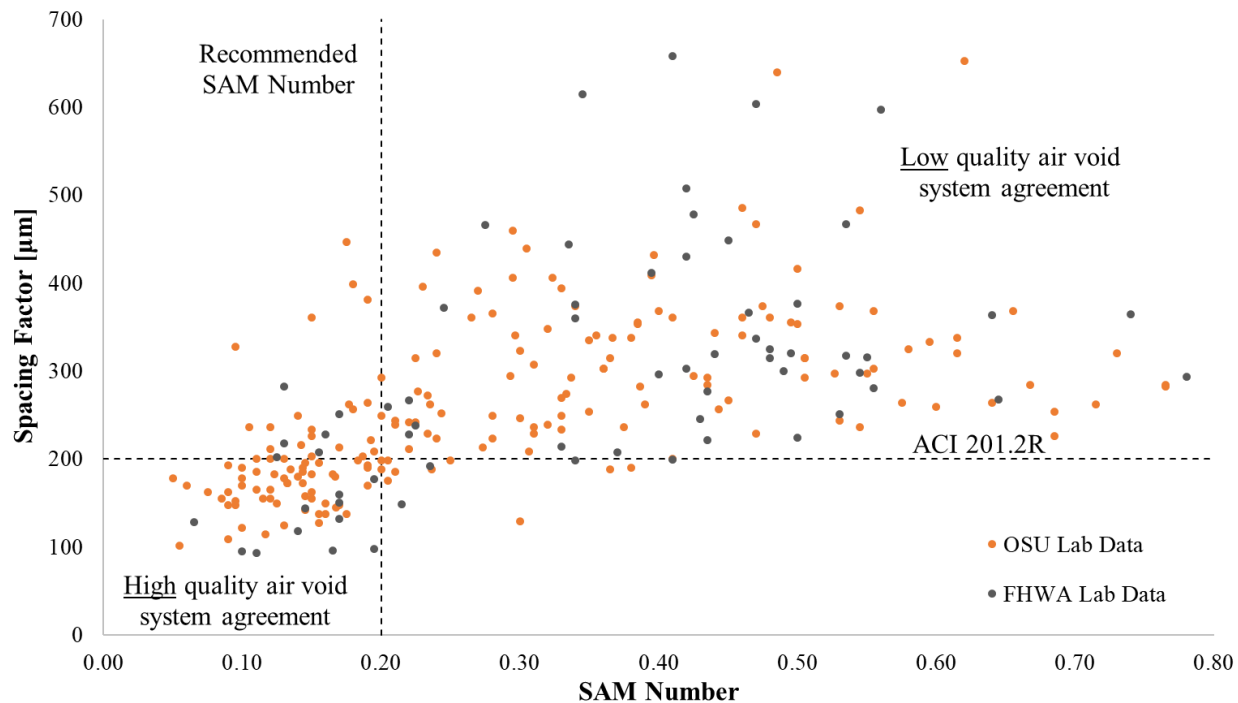
Figure 2.2.3 – SAM Number versus Spacing Factor for 257 laboratory concrete mixtures completed by two different research groups. The results show 85% agreement.

Next, to investigate if the SAM was a useful tool for field usage, the test was used to evaluate 231 different field concrete mixtures from 110 different projects. This work was completed by either a state Department of Transportation or private testing lab from 21 different States and one Canadian Province. A hardened sample was also obtained for ASTM C457 analysis. The SAM Number and spacing factor are plotted together for the field data in Figure 2.2.4. A similar trend is shown in both the laboratory and field data. The spacing factor limit of 200 μm from ACI 201.2R-16 [7] was displayed in Figure 2.2.4 as well as a SAM Number limit of 0.20. The results show 70% agreement for the field data. While this is slightly lower than the laboratory testing, it shows the SAM Number is a useful tool to provide important insights into the quality of the air void system in fresh concrete. This lower agreement may be caused by the increased variability of the field and differences in testing procedures and materials. With the wide range in field users, this new test may also show variability due to unfamiliarity. The field data points in the upper right-hand quadrant of Figure 2.2.4 represent mixtures that would not be recommended for use in freezing climates and consist of 25% of the data (57 Mixtures). These projects may show a reduced lifespan if they are exposed to moisture and freezing temperatures. If these mixtures could have been identified by the SAM to have a low-quality air void system, then they could be adjusted.
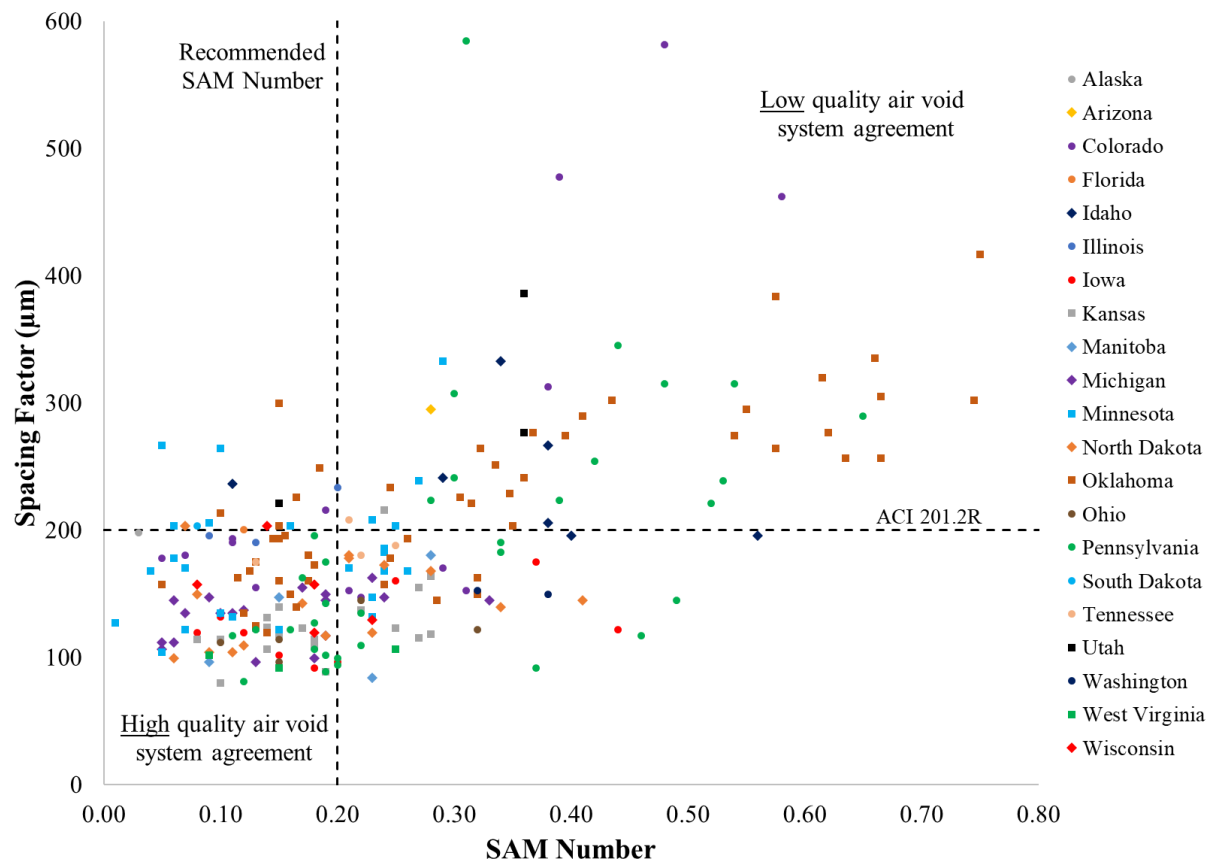
Figure 2.2.4 – SAM Number versus Spacing Factor for 231 field concrete mixtures completed by 21 different State DOTs and one Canadian province with various aggregates and admixtures. The results show 70% agreement.

2.2.4 Conclusion

The SAM seems to meet these needs and provides a tool that shows great potential to be used as a quality control test where freeze-thaw durable concrete is required. This work compares the correlation between the SAM Number, Spacing Factor, and air content for 257 laboratory mixtures and 231 field mixtures with various admixtures, aggregates, devices, and users. The reliability of the method across a data set this diverse shows the reliability and robustness of the SAM test method. These specific findings have been made:

- Air contents between 3% and 8% were needed in order to obtain a Spacing Factor of 200 μm. This shows the inability of a specific air volume to correlate with air void quality.
- For 257 laboratory mixtures, the correlation between a SAM Number of 0.20 and a Spacing Factor of 200 μm agrees with 85% of the laboratory data comparisons.
- For 231 field mixtures, the correlation between a SAM Number of 0.20 and a Spacing Factor of 200 μm agrees with 70% of the field data comparisons.
- For 231 field mixtures, 25% or 57 of them that were placed based on their air volume were shown by the Spacing Factor and SAM Number to have an air void distribution that is not recommended for freeze thaw durability.

References

1. Backstrom, J., et al., *Void spacing as a basis for producing air-entrained concrete.* ACI Journ., 1954. **4**: p. 760-761.
2. Powers, T.C. and T. Willis. *The air requirement of frost resistant concrete.* in *Highway Research Board Proceedings*. 1950.

3. *ASTM C138/C138M-17a Standard Test Method for Density (Unit Weight), Yield, and Air Content (Gravimetric) of Concrete*, A. International, Editor. 2017: West Conshohocken, PA.

4. *ASTM C173/C173M-16 Standard Test Method for Air Content of Freshly Mixed Concrete by the Volumetric Method*, A. International, Editor. 2016: West Conshohocken, PA.

5. *ASTM C231/C231M-17a Standard Test Method for Air Content of Freshly Mixed Concrete by the Pressure Method*, A. International, Editor. 2017: West Conshohocken, PA.

6. *AASHTO TP 118 LRFD Bridge Design Specifications*, A.A.o.S.H.a.T. Officials, Editor. 2017: Washington, D.C.

7. Tanesi, J., et al., *Super Air Meter for Assessing Air-Void System of Fresh Concrete.* Advances in Civil Engineering Materials, 2016. **5**(2): p. 22-37.

8. Ley, M.T., et al., *Determining the Air-Void Distribution in Fresh Concrete with the Sequential Air Method.* Construction and Building Materials, 2017. **150**: p. 723-737.

2.3 TOOLS FOR MIXTURE DESIGN WITH THE SEQUENTIAL AIR METHOD

A historic method that determines the air void quality uses a hardened air void analysis to determine a parameter called the Spacing Factor [1, 2]. After the concrete has hardened then it is cut, polished, and the surface is inspected under a microscope to inspect the voids. This method can take weeks to complete, which does not provide immediate feedback needed to modify the fresh concrete. While there are other methods that can measure the volume of air in fresh concrete (ASTM C 231, ASTM C 138, ASTM C 173), the volume of air does not give insight into the quality or efficiency of the air void system.

In Figure 2.3.1, there are four abstract concrete samples shown. Each sample represents an air content with various bubble sizes and spacing. The quality of the air void system moves low to high (left to right), and the efficiency of the air void system moves low to high (top to bottom). The low efficiency samples show twice the amount of air as the high efficiency images with similar spacing results. This means that with smaller, well-dispersed bubbles, the air void system provides better results with half the amount of air.
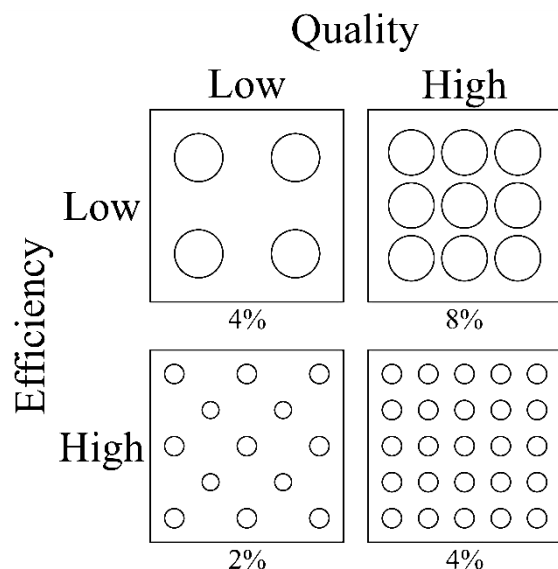
Figure 2.3.5 – Quality and efficiency of air void systems in concrete samples.

The current established tests for freeze thaw durability are not able, within fresh concrete, to measure the quality and efficiency of the air void system. While other methods can measure the volume of air in fresh concrete, studies have shown that the air volume is not the only indicator of freeze thaw durability. The small, well-dispersed bubbles improve the quality and efficiency of the air void system. The Spacing Factor has represented the quality of the air void distribution for a concrete mixture; however, measurement of the Spacing Factor requires hardened air void analysis, which is time consuming and can only be conducted on hardened concrete [1, 2].

The efficiency lines on the air content versus SAM Number figures have been established to provide guidelines for users to understand where their concrete mixture stands in relation to a variety of other concrete mixtures in terms of freeze thaw durability. Using these guidelines, new admixtures and aggregates can be studied and adjusted with the SAM Number to figure out how various materials affect the quality of the air-void distribution.

2.3.2 Experimental Methods

2.3.2.1 Laboratory Materials
All of the laboratory concrete mixtures in this research used a Type I cement that met the requirements of ASTM C150. The aggregates used were locally available crushed limestone and natural sand used in commercial concrete. The crushed limestone had a maximum nominal aggregate size of 19 mm (3/4"). One mixture

contained a blend of the coarse and intermediate aggregate as well. Both the crushed limestone and the sand met ASTM C33 specifications. All the admixtures used met the requirements of ASTM C260 and ASTM C494.

2.3.2.2 Laboratory Concrete Mixture Procedure and Testing

Aggregates were collected from outside storage piles, and brought into a temperature-controlled room at 23°C for at least 24 hours before mixing. Aggregates were placed in the mixer and spun and a representative sample was taken for a moisture correction. Samples were made for hardened air void analysis (ASTM C457). Two 7 L samples were tested with the SAM. These two samples were investigated simultaneously by different operators to determine the average SAM value of a concrete mixture.

2.3.2.3 Estimating Air Void Size by Comparing the Air Volume and SAM Number

Concrete mixtures that contain large air bubbles have been shown to not provide a stable air-void system and not be as effective at providing freeze thaw durability as mixtures with smaller bubbles [3-5]. The industry would benefit from a method that provides immediate feedback so that mixtures could be quickly evaluated to determine the current size of bubbles and how different variables affect the size of the bubbles.

One way to determine the average size or quality of the air-void system in concrete is to look at the combination of the volume of air and the SAM Number in the concrete. Since the SAM provides both of these numbers after completing the test, this information could be used to rapidly determine the air-void size distribution in fresh concrete mixtures. For a given air volume, the mixtures with a higher SAM Number have bubbles that are on average larger than mixtures with a smaller SAM Number. However, a user does not always realize if the SAM Number that they are investigating is a large or small value for the air content found. Historic data could be used to provide this guidance.

To analyze the air volume compared to the SAM Number, a quantile regression method was used. A quantile regression takes a set of data and estimates the upper or lower bound of the data. For example, the 50th quantile separates 50% of the data for two different variables. The 85th quantile gives a line where 15% of the data is above and 85% of the data is below. For this work, quantile lines of 85% and 15% provide useful guidance for users to understand where the SAM Number falls in relation to the air content found. The 15th quantile line (lower limit) will be called the high efficiency line and the 85th quantile line (upper limit) will be called the low efficiency line in this paper.

This analysis is useful, as it uses the air content and SAM Number to produce a graph that shows where a typical mixture falls along with mixtures that have on average larger and smaller air voids. This can be helpful for a user to make an immediate evaluation of the average void size of a mixture as both the air content and SAM Number can be measured in the fresh concrete. This immediate feedback can allow users to learn how different ingredients or construction procedures impact the quality of the bubble size and spacing in the concrete.

2.3.3 Results and Discussion

2.3.3.1 SAM Number and Air Content Relationship

While comparing the SAM Number to the Spacing Factor shows the validity of the SAM test, it would be helpful to give immediate feedback to the user about the quality of the air-void system in the concrete. The two parameters that are measured in the SAM test are the air content and the SAM Number. It may be possible to compare these numbers and give users much better insight on the average size distribution of their air bubbles based on historic data.

The relationship between the air content and SAM Number is shown in Figure 2.3.2 for laboratory mixtures that were completed at Oklahoma State University. Two cubic polynomial lines are included to show the 85th and 15th quantile. These lines represent the efficiency of the SAM Number at a given air content. 15% of the data falls below the High Efficiency line and 85% of the data falls below the Low Efficiency line. These lines are not limitations to the data set, but rather guidelines for the user to understand whether the concrete mixture is efficient for to the volume of air found in the mixture. These two cubic lines were found to be the best

representation of how the data varies. Other trend lines were investigated but they did not provide a useful representation of the investigated data set.

These lines can help SAM users to understand where their concrete mixture falls compared to other SAM Numbers from a wide variety of tests. The closer the SAM Number is to the High Efficiency line, the finer the air-void distribution. If the number is closer the Low Efficiency line, then the air-void distribution is coarser for a specific air volume. These guidelines are based on 192 different concrete mixtures consisting of nine different admixture combinations, seven different water cement ratios (w/cm), and a range of 2% to 10% air contents. It should be noted that these lines are dependent on the mixtures that were investigated. However, the results are helpful as it gives insight into the average size of the bubble system before the concrete has hardened. Due to the wide variety of admixtures, aggregates, and user experience, the two quantile lines help to simplify a range that best represents the SAM Number versus air content instead of a single trend line for all test runs.
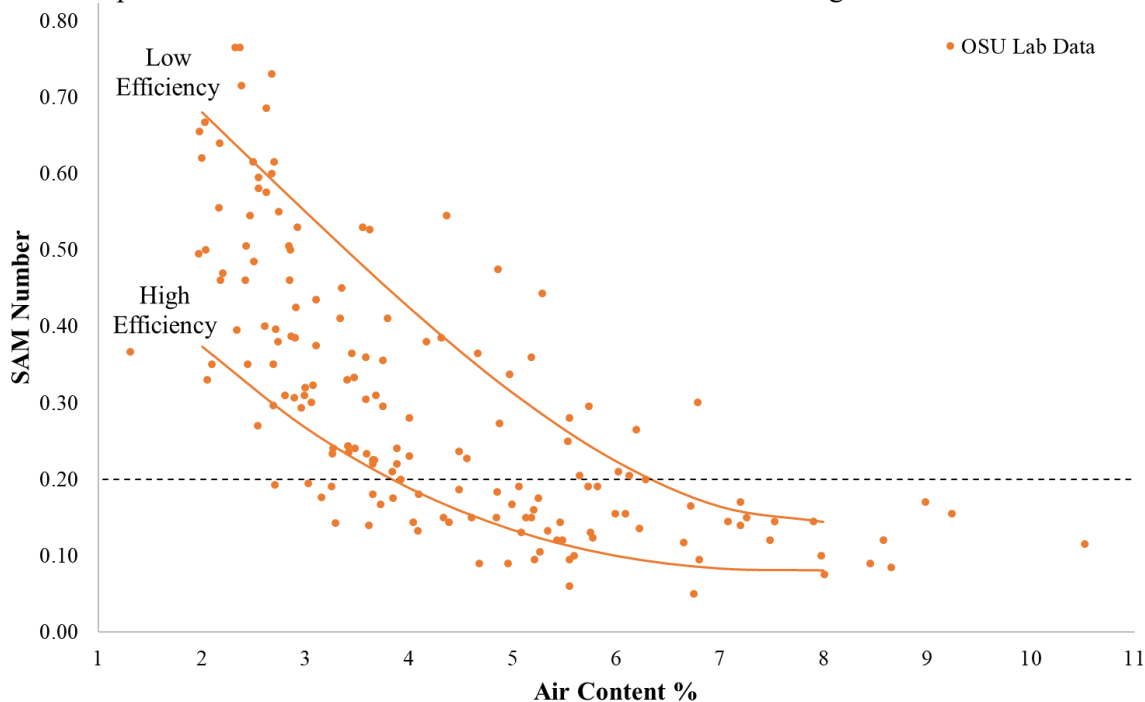
Figure 2.3.2 – Air Content versus SAM Number for 192 laboratory concrete mixtures completed by Oklahoma State University.

In Figure 2.3.3, the comparison between air content and SAM Number is shown for three concrete mixture designs with three different admixture combinations. The guidelines established from the laboratory data were added to show how these lines are helpful to determine how different admixtures effect the air void distribution within concrete mixtures. The mixture containing only air entrainment shows a trend line that falls along the High Efficiency line. The mixtures containing blends of admixtures show one trend that falls between the high and low efficiency lines (PC5) and one trend closer to the low efficiency line. By adding one admixture to the concrete, the air void system quality drastically changes the air content necessary to pass freeze thaw durability. For example, at 5% air content, the mixture with air entrainment only, passes with a SAM Number of 0.11, the mixture with PC5 passes with a SAM Number of 0.20 and the mixture with PC1 fails with a SAM Number of 0.32. This shows that the mixture with the blend of admixtures using PC1 needs a higher air content to pass the 0.20 limit.
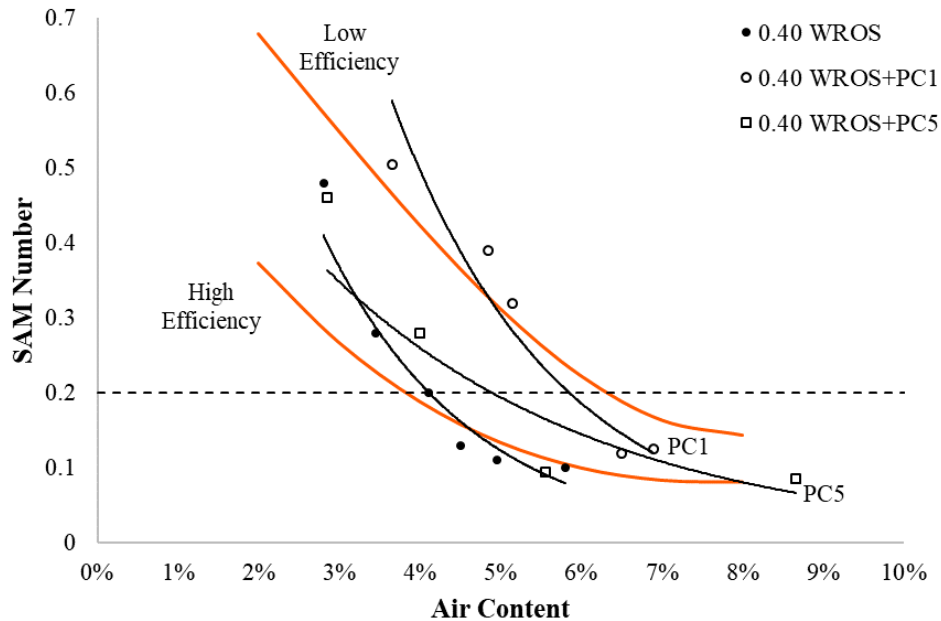
Figure 2.3.3 − Air Content versus SAM Number for two laboratory mixture designs with different admixtures.

2.3.4 Conclusion

This work analyzes laboratory concrete mixtures to determine the reliability of the SAM test method and give guidance to field users. Efficiency lines based on the laboratory data provide helpful insight into the average air void size in fresh concrete mixtures for users to know whether the mixture will meet specifications or not. These curves act as guidelines for field users to relate to data from a wide variety of other mixtures. The cubic quantile lines provides a useful approach to quickly evaluate the average void size in fresh concrete mixtures. This can be used to gain immediate feedback on how the concrete mixtures, material changes, and construction practices impact the average void size in their concrete.

References

1.   Backstrom, J., et al., *Void spacing as a basis for producing air-entrained concrete.* ACI Journ., 1954. 4: p. 760-761.
2.   Powers, T.C. and T. Willis. *The air requirement of frost resistant concrete.* in *Highway Research Board Proceedings.* 1950.
3.   Ley, M.T., et al., *Determining the Air-Void Distribution in Fresh Concrete with the Sequential Air Method.* Construction and Building Materials, 2017. 150: p. 723-737.
4.   Felice, R., J.M. Freeman, and M.T. Ley, *Durable Concrete with Modern Air-Entraining Admixtures.* Concrete international, 2014. 36(8): p. 37-45.
5.   Freeman, J.M., *Stability and quality of air void systems in concretes with superplasticizers.* 2012, Oklahoma State University.

2.4 A RELIABILITY TESTING ALGORITHM FOR THE SUPER AIR METER

The SAM is proving to be a useful device to investigate concrete in both the laboratory and the field. One challenge with the SAM is that a new user has trouble realizing when they have not done the test correctly. While this can be overcome with practice and training, it would be helpful if more feedback could be given to the user based on the results of their tests. This feedback should be simple and let the user know if they have likely completed the test correctly or not. Since the SAM uses many different pressure steps to evaluate concrete then the collection of this information can be compared to past measurements that are known to be of high quality. It would be quite useful if a single algorithm could be used that uses the individual measurements from the SAM test to make this recommendation. This algorithm could serve as a measure of the reliability of the test.

2.4.2 Experimental Methods

To develop this algorithm the research team gathered data from roughly 300 SAM tests that were completed correctly and 300 SAM tests that were not completed correctly. The accuracy of the testing was determined by comparing results from three or more users and identifying results that are outliers as well as those that are close to the mean. Results were also included where errors were intentionally made or a result with an unreasonable SAM number for the given air content. Both the correct and incorrect values were fed into a logistic model. A logistic model was used as it is a simple machine learning algorithm that can use a number of different inputs to provide a single value that predicts the reliability of the test results. A summary of the spreadsheet that uses the algorithm is shown in Table 2.4.1. A spreadsheet is a temporary solution but it allows users to collect data from the field and then use this spreadsheet to evaluate the accuracy of the test. A spreadsheet is easy for everyone to implement and allows quick changes to be made on changes or modifications to the algorithm.

Table 2.4.1 – Overview of the SAM Reliability Spreadsheet

	Date:	10/10/2018	10/10/2018
	Test No.	**Example**	**Example**
First Run	**14.5 psi**	9.93	9.27
	30 psi	23.38	22.30
	45 psi	37.65	36.37
Second Run	**14.5 psi**	10.43	9.49
	30 psi	24.02	22.55
	45 psi	38.32	36.61
Air Content (%)		2.53	3.12
SAM @ 14.5 psi		0.5	0.22
SAM @ 30 psi		0.64	0.25
SAM @ 45 psi		0.67	0.24
SAM's Chance		0.52	0.26
Result:		**Likely Correct**	*Ran Incorrect*

← > 0.50 likely correct
< 0.50 likely incorrect

2.4.2.1 Using the Reliability Model for the SAM

To use the reliability model the six equilibrium pressures recorded during the SAM testing are used to calculate a single reliability parameter. If this parameter is < 0.50 then the test is deemed to be likely incorrect and if the value is ≥ 0.50 then the test is deemed to be likely correct.

2.4.3 Results & Discussion

The accuracy of this prediction based on the correct and incorrect SAM tests is shown in Figure 2.4.1 The orange bars show that when the reliability number is ≥ 0.50 that the tests are consistently correct > 85% of the time. This is a very high number and shows the ability of the reliability factor to give accurate results.
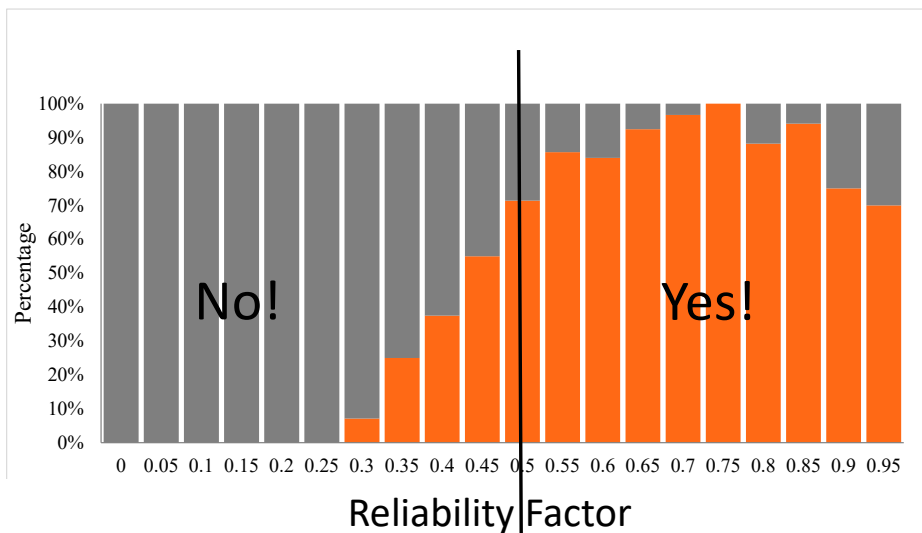
Figure 2.4.1 – The performance of the reliability factor to give an accurate indicator of a SAM test that was completed correctly. The orange bars show the values that are correct and gray bars show the values that were not.

Care should be taken in comparing reliability factors between users or tests to determine which result is better for more accurate beyond how the values compares to the 0.50 limit. If the values are greater than 0.50 then it should be accepted as an accurate test. This is necessary because the logistic model and the data gathered to complete this work does not rank the quality of the data and instead only looks at how correct the measurement was made.

2.4.3.1 Adjustments to the Reliability Model

Based on the feedback from the field and laboratory testing with mistakes several adjustments were made to the model to improve the accuracy. These modifications are still ongoing and show good promise to continue to improve the accuracy of the reliability model. One consistent error that was observed in users that was challenging for the reliability model to capture was not removing all the air bubbles from the bottom chamber when filling with water. To address this the filling of the SAM was adjusted to use a new device called the "shotgun". This is a funnel with a threaded tube at the bottom that will screw into the petcock of the SAM. This funnel is shown in Figure 2.4.2. The shotgun should be filled with water while leaving the petcock closed. The petcock can then be opened and this will introduce the water into the bottom chamber with a continuous flow. This also allows the user to focus on agitating the meter to remove the voids while a continuous stream of water is passing through the meter. Shotguns were provided to all pooled fund members. The addition of the shotgun to the AASHTO test method is being investigated.

Shotgun

Figure 2.4.2 – A funnel and threaded tube that allows water to be continuously added to the bottom chamber while filling.

2.4 Conclusion

Both the reliability factor and shotgun were developed to improve the accuracy of the SAM and give users feedback on how accurate they have completed the test. The SAM continues to evolve and these improvements promise to reduce the variability and make it easier to implement this new tool in the field.

2.5 Effects of Pumping Concrete Based on The Air Void Parameters in Fresh and Hardened Concrete

Pumping of air-entrained concrete for elevated slabs frequently results in quality control issues due to increased pressures and even rejection of the load due to the loss of air content after the concrete was pumped [1-5]. Regardless, many of these bridges remain standing after excessive freezing and thawing cycles. Therefore, this research used Unit Weight (ASTM C138), Super Air Meter (AASHTO TP 118), Freeze-Thaw Resistance (ASTM C666), and Hardened Air Void Analysis (ASTM C457) to investigate how the air void quality and freeze-thaw durability performance of concrete changes due to pumping.

2.5.2 Experimental Methods

The materials used in this work meet the following: ASTM C150 Type I Portland cement, ASTM C618 Class C fly ash, wood rosin based air-entrainer, ASTM C494 Type A/F mid-range water reducer dosed at 7 oz./cwt (467 mL/100 kg), ASTM C1017 Polycarboxylate superplasticizer at a dosage of 2.5 oz./cwt (163 mL/100 kg). Also some laborotoary mixtures contained a food grad citric acid at 0.25% of cementitious material as a hydration stabilizer, set retarder, and water reducer. All of the concrete mixtures had a water-to-cementitious material ratio (w/cm) of 0.45 and 611 lbs./yd^3 (362 kg./ m^3) of total cementitious material with 20% Class C fly ash replacement by weight.

2.5.2.1 Concrete Pumps & Sensors

The Putzmeister TK 50 concrete pump at 1500 RPM was used for the laboratory testing as shown in Figure 2.5.1 and PumpStar AZ34.5-PS220 truck-mounted concrete pump was used for the field research. Multiple GE 5000 pressure sensors were used to measure the concrete pressure near the edge of the pipe for laboratory and field testing. A diagram of the laboratory pipe network has been provided in the appendix of this paper. The field testing used three different configurations of flat, arch, and A-frame arrangements. Both pipe networks had a steel pipe reducer of 5.0 in. I.D. and the rest of the pump lines were 4.0 in. I.D.

Figure 2.5.1. The Putzmeister TK 50 Concrete Pump used for all laboratory testing.

2.5.2.2 Measuring Air

Slump (ASTM C143), Unit Weight (ASTM C138), Super Air Meter (AASHTO TP 118), Freeze-Thaw Resistance (ASTM C666), and Hardened Air Void Analysis (ASTM C457). For this work, durability factors less than 70% after 300 freeze-thaw cycles for ASTM C666 were considered failing

2.5.3 Results

2.5.3.1 Changes in Air Content based on Number of Pump Cycles

Figure 2.5.2 shows the normalized air content versus the number of cycles through the pump. The normalized air content was the ratio of the air before pumping to the air measured after pumping multiplied by 100. All lab

mixtures containing a citric acid and WR showed the most significant decrease in air content between the measurements right after mixing and the measurements after one pumping cycle. After the first pumping cycle, the air content of the citric acid and WR mixtures either decreased at a slower rate or remained approximately constant with additional times through the pump. On average, the citric acid and WR lost approximately 30% of the initial air content after one cycle through the pump with a standard deviation of 4.5% and 7.1% respectively. In contrast, the PC mixture and field mixtures did not show a significant change in air volume after one pumping cycle. These results indicate most of the air lost during pumping occurs during the first cycle for the citric acid and WR mixtures. In addition, the relative proportion of air lost for all citric acid and WR samples was comparable.
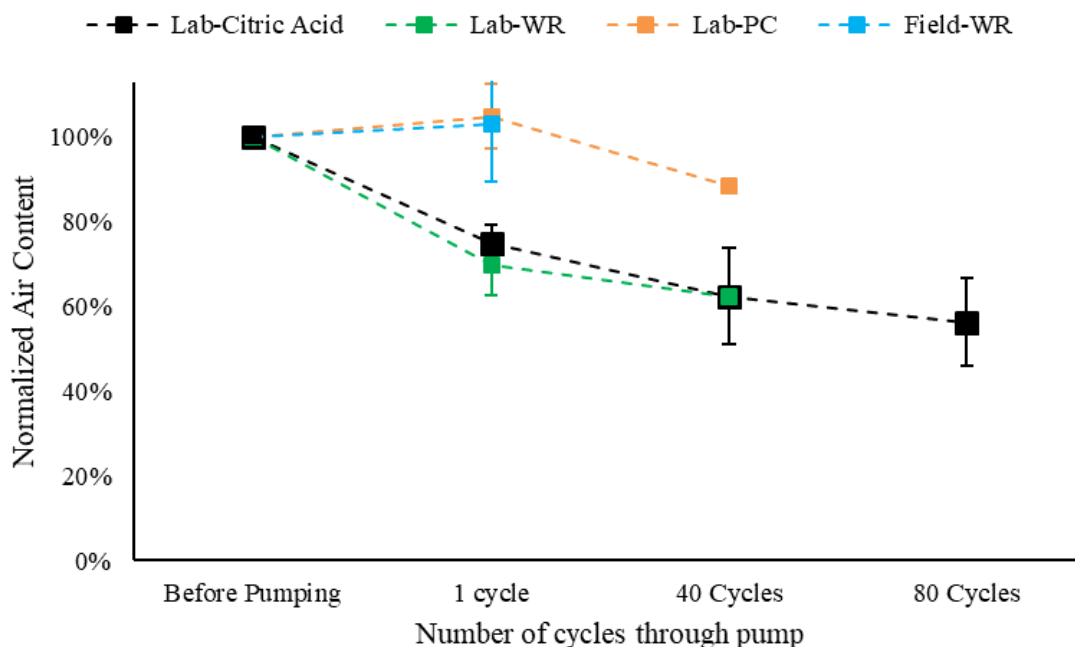
Figure 2.5.2. Plot of Normalized air content vs. Number of cycles through the pump.

2.5.3.2 Air content before pumping vs. Air content after 1 cycle

Figure 2.5.3 shows a plot of the air content before and after one cycle through the pump for the laboratory and field mixtures. The plot shows a line of equality. If a mixture had the same air content before and after pumping then it would be on this line. All of the laboratory mixtures with citric acid and WR showed a decrease in air content after pumping. The PC samples and field samples did not show a significant change in air content. Of the 18 field mixtures, five samples showed a 0.5% change in air volume.
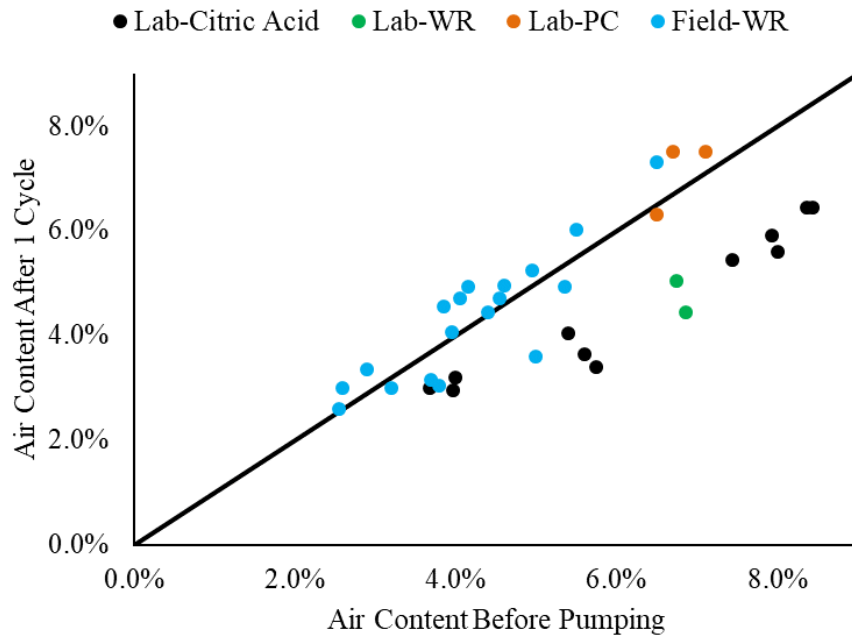
Figure 2.5.3. Plot of Air content before pumping vs. Air content after 1 cycle

2.5.3.3 Air Volume and Super Air Meter After One Cycle

Figure 2.5.4 shows the SAM Number before pumping compared to the SAM Number after one cycle through the pump and pipe network. In all citric acid, WR, and field mixtures, the SAM Number increased by at least 50% for 87% of the mixtures after one cycle through the pump. In the PC samples, the SAM Number slightly decreased after one pumping cycle.
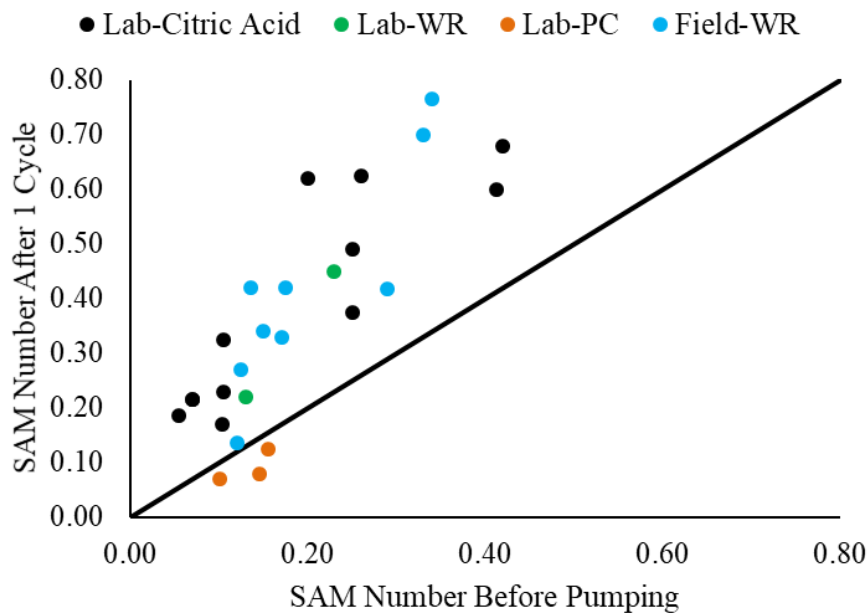
Figure 2.5.4. Plot of SAM Number Before Pumping versus the SAM Number after pumping one cycle through pump and pipe network

2.5.3.4 Hardened Air Void Analysis Results

Figure 2.5.5 shows a plot of the spacing factor before pumping versus the spacing factor after one pumping cycle for laboratory and field samples. Also shown on the graph is a line of equality and lines representing the accepted coefficient of variation for the hardened air void analysis. Just over 80% of the samples fall within the accepted coefficient of variation. This suggests pumping did not significantly change the spacing factor of the hardened concrete samples. Freeze-thaw data was also completed on this work and reinforced these finding further.
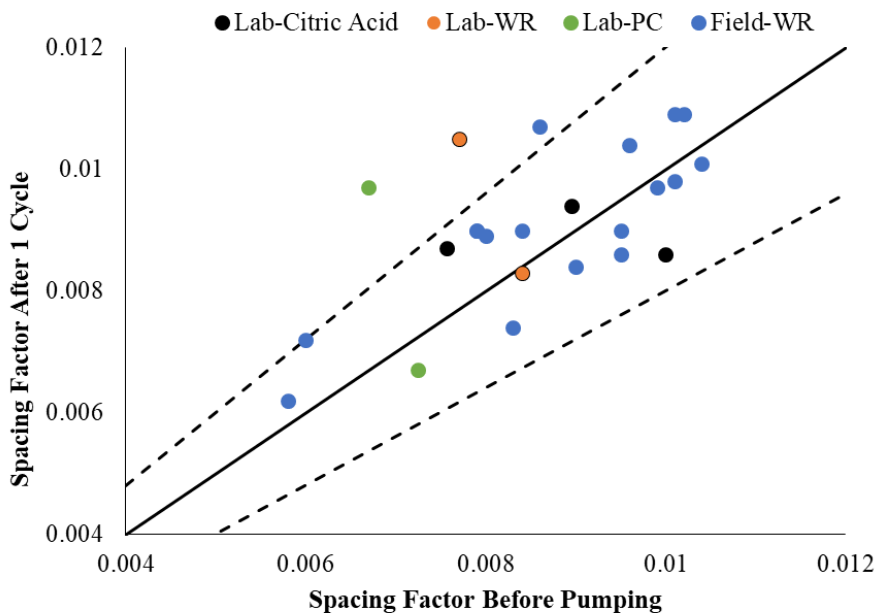
Figure 2.5.5. Plot of spacing factor for samples before pumping and after pumping.

To further understand this, the SAM number of a concrete mixture not being pumped compared to it being pumped over time was investigated. Figure 2.5.6 shows several replicate mixtures with different SAM numbers. The results show that the SAM number increased sharply after pumping and then over time decreased to the SAM number that was present in the concrete prior to pumping. This data in addition to the lack of change in the spacing factor shown in Figure 2.5.5 shows that the small air voids may dissolve right after pumping and then slowly return to the concrete over time.
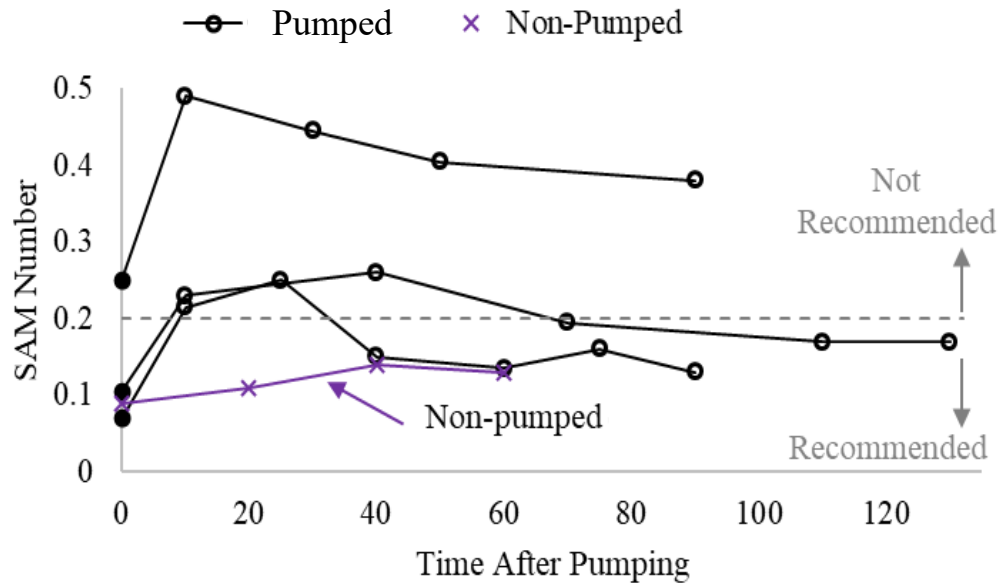
Figure 2.5.7. Plot of SAM Number versus time after pumping one cycle for PC mixtures.

2.5.3.6 Practical Significance

This work suggests that rejecting concrete after pumping for low air content or a high SAM number is not a good practice. Instead, it is suggested to test the concrete before it is pumped for both air volume and SAM number. When the mixtures had an air content > 4% and a SAM number < 0.32 before pumping, all mixtures showed satisfactory freeze thaw durability regardless of any changes in the fresh air content or SAM number due to pumping.

2.5.4 Conclusions

Pumping concrete causes changes in the air void system of the fresh concrete. Regardless of the change in the air void system of the fresh concrete, the hardened air void parameters and freeze thaw performance did not show substantial change of the air void system due to pumping. This suggests that the air content and SAM number after pumping is not representative of what will be in the hardened concrete.

References

1. Elkey W, Janssen DJ, Hover KC. Concrete Pumping Effects on Entrained Air-Voids. Washington State Transortation Center. 1994.
2. [11] Elkey WD, Janssen DJ, Hover KC. Effects of Admixtures on Air-Void Stability of Concrete Subjected to Pressurization. in Concrete Under Severe Conditions 2. 1998.
3. [12] Janssen DJ, Dyer RM, Elkey WE. Effect of Pumping on Entrained Air Voids: role of pressure. in CONSEC 95 Concrete Under Severe Conditions. 1995.
4. [13] Hover K.C., P.R.J. Impact of Concrete Placing Method on Air Content, Air-void System Parameters, and Freeze-Thaw Durability. Transportation Research Record, 1996. **1532**: p. 1-8.
5. [14] NRMCA Association, CIP21 - Loss of Air Content in Pumped Concrete. NRMCA, 2005.

2.6 FIELD INVESTIGATION OF PUMPING AIR ENTRAINED CONCRETE

Pumping air entrained concrete has been a challenging task due to the changings in air content before and after the concrete was pumped[1-5]. This study evaluated concrete in 3 states at 20 site locations with concrete from 62 ready-mix trucks. All testing done in this chapter was performed on-site. Each site had a unique mix design designated to the specific project on hand. All mixes required the use of a concrete pump to place the concrete. Samples were taken directly before the concrete entered the pump and directly after the concrete was dispensed from the outlet of the pump. This allows for the total air volume and the air void distribution effects of the concrete to be compared before pumping the concrete, after pumping the concrete, and also in hardened state. These factors are critical when determining the freeze thaw performance of the concrete mixtures.

2.6.2 Experimental methods

2.6.2.1 Materials & Mix Designs

All the concrete mixtures were prepared at the ready mix plants and transported using ready mix trucks. Each ready mix plant had different sources of aggregate, cement, fly ash, and admixtures. There was a combination of water reducers, retarders, and air entraining admixtures used in these concrete mixtures. The mixture designs were specific to the project at each site. The common factor among all these mixes was that they were designed to be able to be pumped. The slumps ranged from 5 to 10 inches depending on the specification set for the specific project. The air volume of these mixture ranging from 2% to 10%.

2.6.2.2 Sampling and Testing Procedures

There were 18 different models of truck-mounted concrete pumps used on-site to complete this research. The pumping pressures varied based on the specific task, workability of the concrete, and the configuration of the boom as shown in Figure 2.6.1. Two single samples were taken from the middle third of each truck, one before the pump and one after the pump. The samples taken before the pump were obtained directly from the chute of the ready mix trucks. The samples taken after the pump were obtained from the outlet of the pump boom.

Figure 2.6.1. The flat, arch, and A-Frame orientations of the concrete pump.

The Slump (ASTM C143), Unit Weight (ASTM C138), and Super Air Meter (AASHTO TP 118) were gathered to test for the consistency, workability, and air void quality of the fresh concrete. Concrete samples were also made before and after the pump for a hardened air void analysis (ASTM C457).

2.6.3 Results

2.6.3.1 Air Volume Results

Figure 2.6.1 compares the air content before and after the pump with a line of equality. If the air volume stayed the same before and after pumping, then that point would be on this line. The dashed lines represent the variation of +/- 1% off set. This was chosen to account for the air volume range usually specified by the engineers. Seventy percent of the trucks tested did not show a change in air volume by more than 1%. Twenty-three percent of the trucks tested showed more than a 1% decrease in air content after the pumping. Seven percent of the trucks tested showed an increase greater than 1% in air content after pumping.
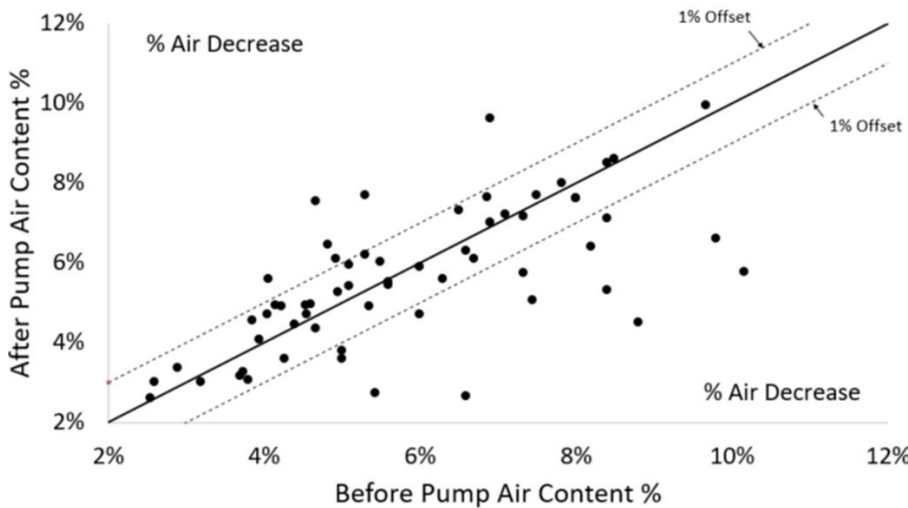
Figure 2.6.1 – Air Content Before/After Pump

2.6.3.2 Super Air Meter

Figure 2.6.2 compares SAM number before and after the pump with a line of equality. If the SAM number before the pump and after the pump were the same then the marker would be on this line. The dashed lines represent a standard deviation of +/- 0.05. This was found from previous work to be the standard deviation between any two SAM test. The SAM test was conducted on 52 different truck mixtures. Fifty-four percent of the SAM numbers increases by more than 0.05 after the pump. Six percent of the SAM numbers decreased by more than 0.05 after the pump. The other 42% of the SAM tests numbers were within 0.05 of each other.
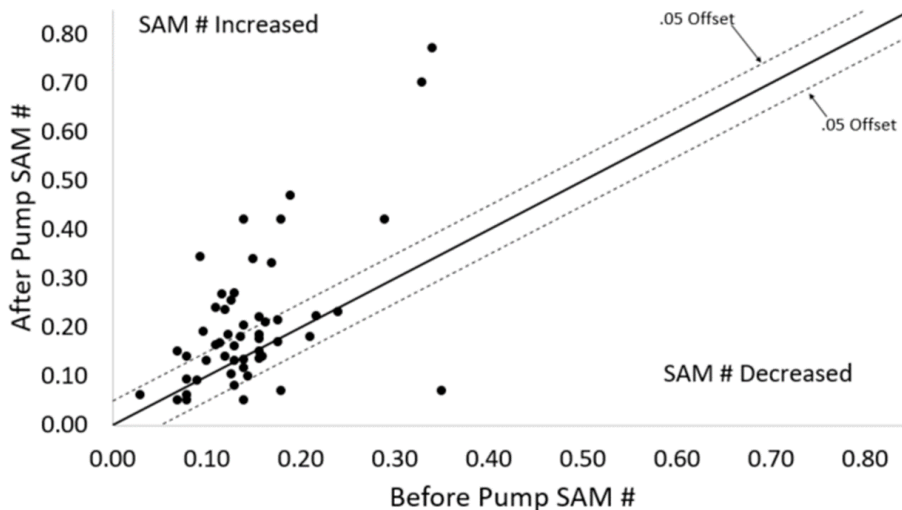
Figure 2.6.2 – SAM numbers Before/After the Pump

2.6.3.3 Effects of Air Content on Pump Configuration

Figure 2.6.3 compares the Air content before and after the pump as well as the different configurations that were tested. There were forty samples tested with known configurations. The configurations that were tested were flat, arch, and a-frame. Zero percent of the flat configurations lost air greater than 1% after pumping, 16% of the arch configurations lost greater than 1 % of air due to pumping, and 39% of the a-frame configurations lost greater than 1% of air due to pumping.
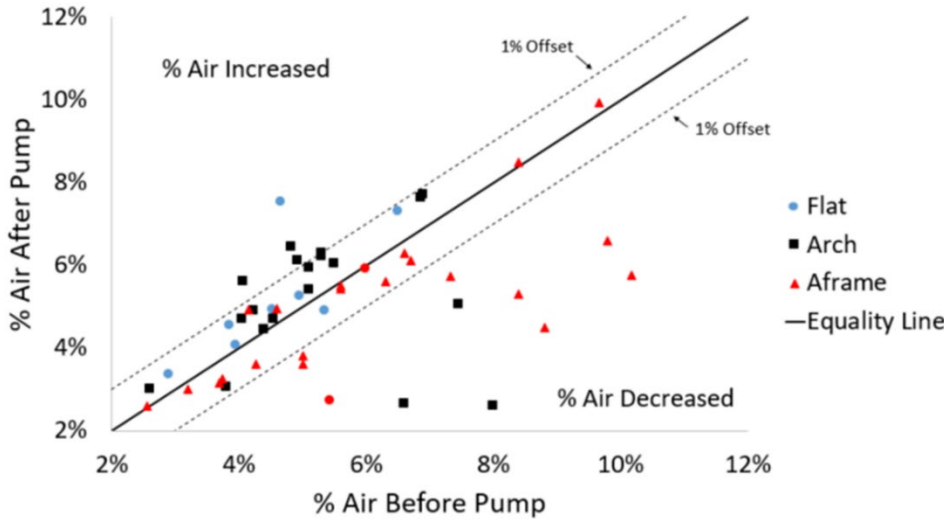
Figure 2.6.3 – Air Content Before and After Pumping with Boom Configurations

The configurations tested were flat, arch, and a-frame. Out of the forty samples total, 40% of the flat configurations, 60% of the arch configurations, and 45% of the a-frame configurations had an increased SAM number increase by more than 0.05 after the pump. Figure 2.6.4 compares the SAM number before and after pumping with three different pipe configurations.
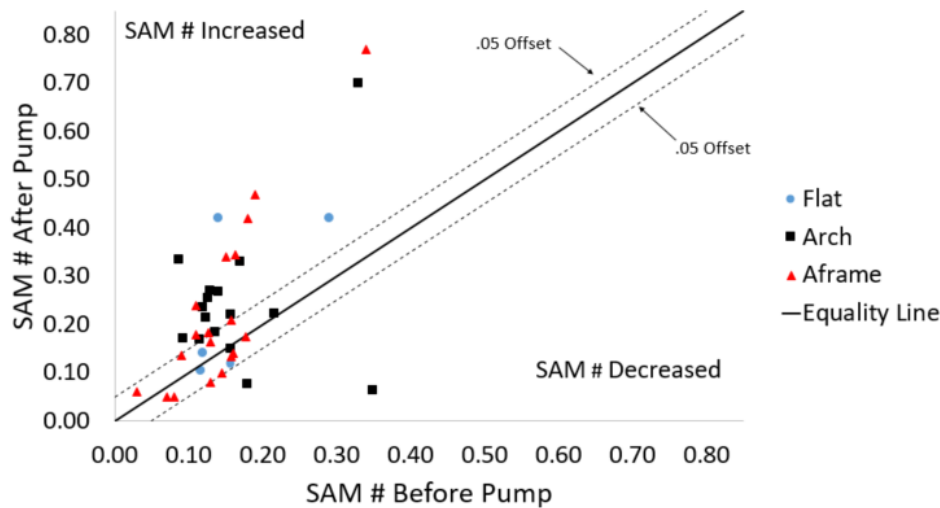
Figure 2.6.4 – SAM number Before/After the Pump with Boom Configurations

2.6.3.4 Hardened air void analysis of the field samples

These samples were also evaluated based on hardened air void analysis. Figure 2.6.5 compares the spacing factor of the field samples. The graph has a line of equality and a +/- 20% coefficient of variation. There was also a comparison of boom configurations in the graph to show how they affect the air void quality of the

concrete. It should be noted that this does not represent all of the data since this research is still in progress. Of the data shown, 82% of the points were within the +/- 20% coefficient of variation line. Further, 71% of the arch configurations, 67% of the a-frame configurations, and 88% of the flat configurations were within the coefficient of variation of the ASTM C 457 results.
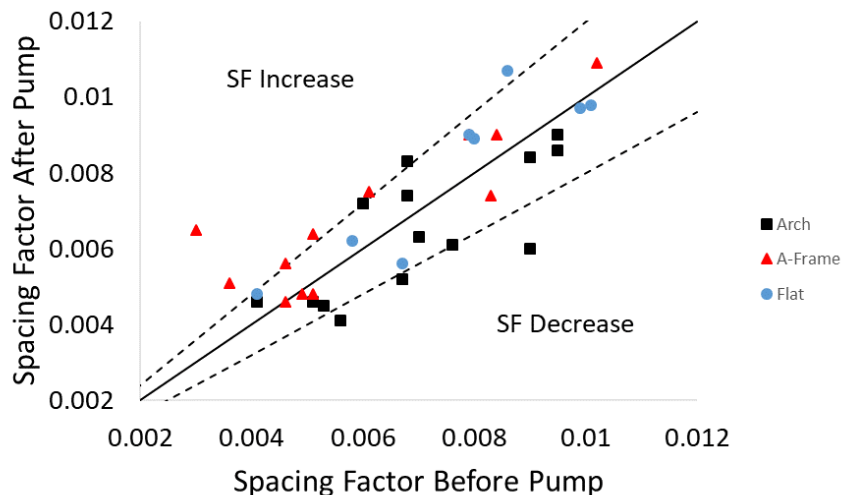
Figure 2.6.5 – Spacing Factor Before/After the Pum. Note: units of spacing factor on x and y-axis is inches.

The air content was also measured during the hardened air void analysis. Figure 2.6.6 compares the air content of the concrete before and after being pumped. The graph has a line of equality represented by the solid line and also a +/- 1% lines. Any point that falls below the line of equality represents that the sample lost air after being pumped. The figure also compares different configurations. The graph shows that 80% of the A-frame samples, 58% of the arch samples, and 57% of the flat samples were within the +/- 1% limit.
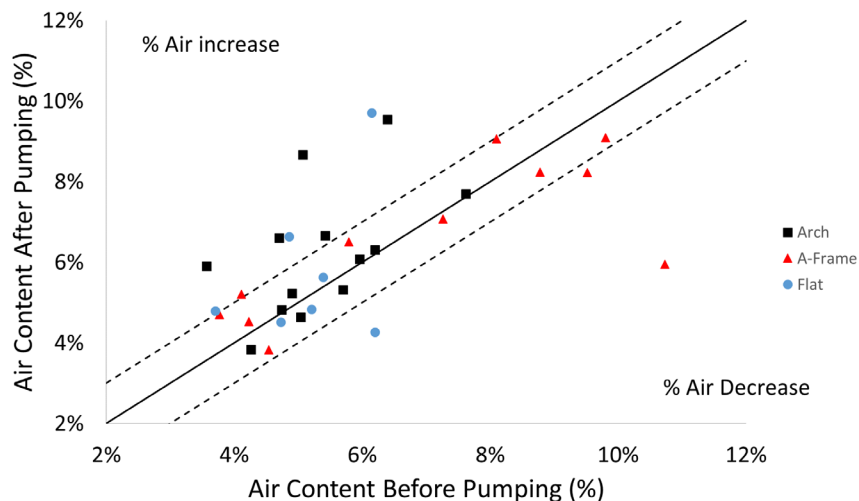
Figure 2.6.6 – Hardened Air Content Before/After the Pump

Also, there are 24 samples compared before pumping and 33 samples compared after pumping. The hardened air volume matched the fresh air volume for the samples before pumping. After pumping, the hardened air content was on average 11% higher than the fresh air content. This shows that on average the hardened air content is higher than the measured fresh air content after pumping. This suggests that the air dissolved during pumping returns over time. This supports previous measurements concerning the air content recovery.

29

2.6.4 Conclusions

The results show the air void system in fresh concrete was regularly disrupted due to pumping. For example, > 30% of the mixtures showed change in air content by more than 1% and > 60% of the mixtures shows an increase in the SAM number by > 0.05. This suggests the air void quality of the concrete was significantly changed by the pumping process. Both the A-frame and the Arch were found to change the air void system the most.

While the fresh properties were shown to change, the hardened air void results suggest a different scenario. Despite the arch and A-frame showing significant changes in the fresh concrete, 71% of the arch, and 70% of the A-frame, and 88% of the flat configurations show that the change in the spacing factor of the hardened concrete did not significantly change before and after pumping. This confirms the recovery of the air void system before the concrete hardens suggested in the previous section.

References
1. Elkey W, Janssen DJ, Hover KC. Concrete Pumping Effects on Entrained Air-Voids. Washington State Transortation Center. 1994.
2. [11] Elkey WD, Janssen DJ, Hover KC. Effects of Admixtures on Air-Void Stability of Concrete Subjected to Pressurization. in Concrete Under Severe Conditions 2. 1998.
3. [12] Janssen DJ, Dyer RM, Elkey WE. Effect of Pumping on Entrained Air Voids: role of pressure. in CONSEC 95 Concrete Under Severe Conditions. 1995.
4. [13] Hover K.C., P.R.J. Impact of Concrete Placing Method on Air Content, Air-void System Parameters, and Freeze-Thaw Durability. Transportation Research Record, 1996. **1532**: p. 1-8.
5. [14] NRMCA Association, CIP21 - Loss of Air Content in Pumped Concrete. NRMCA, 2005.

2.7 IMPACTS OF SAMPLE CONSOLIDATION ON THE AIR VOID SYSTEM OF FRESH CONCRETE

Consolidating concrete can be a challenging task in both field placements and casting test samples in molds. This has been largely attributed to many factors such as the workability of the concrete mixture, the equipment used, methods of placement, and the forms or molds to cast the concrete [1]. The results of inadequate consolidation can negatively impact the aesthetics, structural integrity, and the testing results of concrete. Consolidation of concrete samples is typically done by rodding, internal vibration, or external vibration. However, rodding has been the preferred technique to consolidate concrete samples in the field. However, rodding a low workability concrete mixture may not provide enough energy to properly consolidate the concrete and produce results which may not be represent of the concrete's properties. Both ASTM and AASHTO require cylinders, beams, unit weight and air samples to be vibrated if the slump is less than 1 in (25 mm) while slumps greater than 1 in (25 mm) can be consolidated with either vibration or rodding [2-4]. Unfortunately, not enough guidance is not provided how to uniformly use a vibrator in the field and so this can increase the variability of the results.

Field testing from Wisconsin showed that slip form paving mixtures with a low workability could not be properly consolidated and provided unreliable air content and SAM numbers [5-6]. Consolidation using internal vibration also increased the variability of these measurements and so it was not acceptable.

The aim of this work was to compare the variability of air content and SAM Number to different consolidation techniques at low slumps with a series of laboratory tests. Another goal of this work was to develop a new method of consolidation that would reduce the variability of the SAM when low slump concrete is being tested. After rigorous testing and experimenting, a new method was born out of this work and is based on external vibration. Details about this new technique versus its counterparts will be discussed.

2.7.2 Experimental Methods

2.7.2.1 Mixture Design and Materials

The concrete mixture design was designed to closely resemble a paving mixture used by the Wisconsin Department of Transportation (WisDOT). Table 2.7.1 provides the materials, respective material specification, and mixture design. The concrete mixture was designed with a 0.45 w/cm and had a target air content of 5%. The combined aggregate gradation was plotted using Tarantula Curve in Figure 2.7.1. The ½" sieve size was out of the Tarantula curve, which was a major reason for the harsh workability of the mixture.

Table 2.7.1: Materials used in the mixture design

Material	Description	Mixture Design	
		Weight (lbs./yd^3)	Volume (ft^3)
Coarse Aggregate	57" ASTM C33 crushed limestone	1752	10.6
Intermediate Aggregate	NM 3/8" crushed limestone	250	1.51
Fine Aggregate	ASTM C33 natural sand	1200	7.37
Cement	ASTM C150 Type I	376	1.91
Fly Ash	ASTM C618 Class C fly ash	94	0.60
Water	Potable at 0.45 w/cm	211.5	3.39
Air Entrainer	ASTM C260 Wood rosin based at 5%	0.0525	8.4E^{-4}
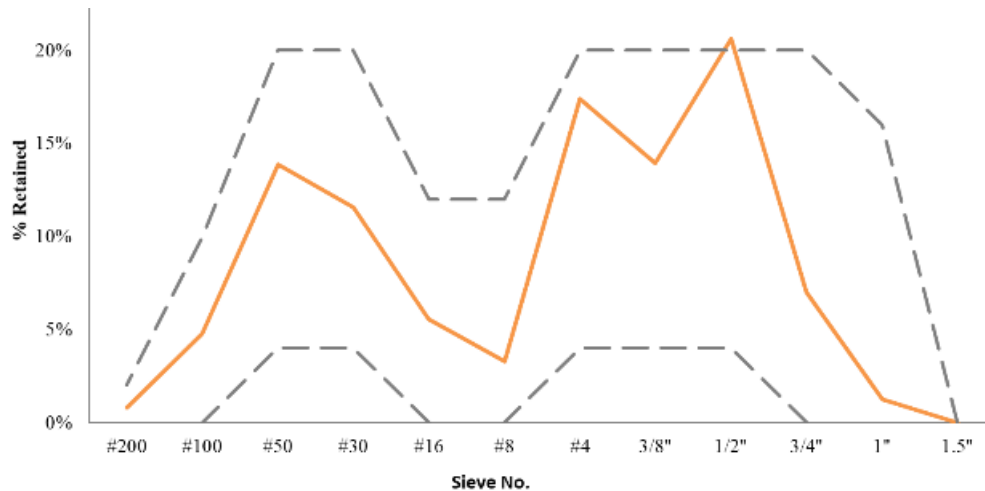
Figure 2.7.1. Approximate WisDOT Mixture Design in Tarantula Curve

2.7.2.2 Mixing Procedure

Aggregates from outdoor storage piles were gathered and moved indoors to a controlled temperature of 23°C. Three samples for each aggregate type were collected from the mixer for moisture corrections. After moisture corrections were calculated, all of the aggregate and two-thirds of the water was placed in the mixer and spun for three minutes. This time allowed for evenly distributed aggregates and for the aggregates to be closer to saturated surface dry (SSD). The residual water, cement, and fly ash were added next and mixed for three minutes. The mixing drum was then scraped and the concrete mixture rested for two minutes. Following the rest time, the mixer was spun and the admixtures were added.

2.7.2.3 Consolidation Methods

Consolidation of concrete samples for quality testing can be completed either by rodding, internal vibration, or external vibration. As shown in Figure 2.7.2 (a) though (d), the consolidation methods investigated were rodding, internal vibration with a 1" diameter portable concrete vibrator at 12,500 vpm, external vibration with a vibrating table, and external vibration with the MinT. The MinT is explained in the next section. These consolidation procedures closely followed ASTM C31 for field samples, ASTM C192 for laboratory samples, and ASTM C138 for unit weight based on the consolidation method.

(a)   (b)   (c)   (d)

Figure 2.7.2 (a) rodding, (b) internal vibration with stinger vibrator, (c) vibrating table, and (d) MinT.

2.7.2.4 MinT

The miniature vibrating table or MinT is new consolidation technique that was developed to provide the benefits of the vibrating table in a portable device. An overview of the MinT is shown in Figure 2.7.3. The MinT consists of a 1ft by 1ft metal table with clamps and a 1" diameter electric vibrator at 12,000 vpm. This work used a Makita XRV01Z battery operated concrete vibrator. A slot in the bottom of MinT provides a pathway to

insert the head of the vibrator and lock it into place with adjustable screws. A clamping system was welded to the top of the metal sheet to keep the pot from moving during vibration.

(a)

(b)   **(c)**
Figure 2.7.3. (a) aerial view of MinT being used, (b) side view of Mint , and (c) underneath view of MinT.

2.7.2.4.1 Procedure for Using MinT
The vibrator head was inserted into the MinT and tightened with the adjustable screws. Then the MinT was placed on a level surface. The unit weight pot was placed in the clamping system and tightened. A layer of concrete of roughly 50% of the volume of the container was scoped into the unit weight pot and then the concrete was consolidated for 50 seconds. This was repeated to fill the container. A number of different consolidation times were investigated but 50 seconds was chosen because after this period large voids were no longer observed to exit from the concrete. Vibration should only occur long enough to adequately consolidate the sample. Over vibrating the concrete can cause segregation of the concrete and loss of entrained air. More quantitative work over the impact of vibration on the air void system is an area for future work.

2.7.2.5 Testing Procedure
Each concrete mixture was evaluated with the following tests: Slump Test ASTM C143/AASHTO T119, Box Test AASHTO test method approved and a test number is pending, Unit Weight ASTM C138/AASHTO T 121, and Super Air Meter (SAM) AASHTO TP 118.

2.7.3 Results and Discussion
The concrete investigated was very stiff and required significant energy to consolidate. The typical slump of the mixtures was 0.75 in. Figure 2.7.4 shows a typical performance in the Box Test of the mixture. Note that the mixture did not consolidate well as there were significant surface voids. This shows the poor workability of the mixture and so the concerns about the need for adequate consolidation methods.

Figure 2.7.4 shows the sample from the Box Test.

One slip form paving concrete mixture with a target air content of 5% was used to compare the sample consolidation of a method on air content and bubble distribution through the SAM number. Rodding, internal vibration, external vibration with a vibration table, and the novel external vibration test with the MinT were conducted using the SAM to measure the air volume and the SAM Number for this mixture. As shown in Table 2.7.2, the number of tests, average SAM number, standard deviation and coefficient of variation are provided. Both rodding and internal vibration had a variability of almost 40%. The vibration table and MinT showed much better performance with a coefficient of variation of 19% and 26% respectively.

Table 2.7.2. Variability of SAM Number Based on Consolidation Method

Consolidation Method	Number of Tests	Average SAM #	Std. Dev.	COV
Rodding	33	0.19	0.075	39%
Vibration Table	26	0.24	0.046	19%
MinT	35	0.19	0.051	26%
Internal vibration*	13	0.21	0.078	37%

*Note: this was conducted with a 1" stinging vibrator.

2.7.3.1 Rodding
Rodding had the highest variation in the SAM Numbers of all the consolidation methods explored. It is worth noting that this form of consolidation required several powerful strikes with the mallet to close the holes created by rodding. This may be why rodding had such a high SAM Number variability because the mixture design was based on a low-slump mixture design; thus, making it difficult for the operator to consolidate the unit weight pot properly. The variability from rodding could be a result of the amount of energy added to the system. Each operator uses the standard rubber mallet to strike the side of the air pot with different energies to close the holes. It is possible that not all operators close the holes properly due to the high amount of energy needed.

2.7.3.2 Internal Vibration
Consolidating using internal vibration was measured to have similar variability as rodding for the SAM measurements. This variability can be attributed to the lack of uniformity with using a high energy vibrator to consolidate the concrete. These challenges seem to be overcome when using external vibration to consolidate the concrete.

2.7.3.3 Vibrating Table
The vibrating table provided the most uniform and consistent consolidation method for measuring the SAM. This could be because the concrete was exposed to a constant vibration during consolidation that shears the concrete in the unit weight pot. Unfortunately, the use of a vibration table in the field has some drawbacks due to the bulkiness of the equipment and the need for a generator. These challenges inspired the development of the MinT.

2.7.3.4 MinT

The MinT was able to provide a coefficient of variation that was slightly higher than the vibrating table and much better than rodding or using an internal vibrator. The MinT is likely successful because it mimics the same action as a vibrating table. The vibrator is mounted below sample and this allows the energy to be transferred to the concrete through shearing. In addition, the MinT is small and easy to move and it uses a battery operated vibrator that is readily available to consolidate the concrete.

2.7.4 Conclusion

For the low slump concrete mixture investigated it required significant energy in order to consolidate the concrete. Consolidation with rodding, internal vibration, and two different vibration tables was investigated. One of these tables was a newly developed device called the MinT that uses a portable electric vibrator that straps to a steel table with clamps for the unit weight pot.

The testing shows that the rodding and use of an internal vibrator had the highest coefficient of variability at close to 40%. The use of a vibrating table and the MinT reduced the coefficient of variability by roughly 50%. Since the MinT is a portable solution to this issue then it may be able to be used in the field to reduce the variability of SAM measurements with low slump concrete mixtures. This needs to be further investigated in field testing.

References

1. Kosmatka, S.H. and M.L. Wilson, *Design and control of concrete mixtures*. PCA. 2016: Stokie, IL.
2. *ASTM C138/C138M-17a Standard Test Method for Density (Unit Weight), Yield, and Air Content (Gravimetric) of Concrete*, A. International, Editor. 2017: West Conshohocken, PA.
3. *ASTM C31/C31M-19a Standard Practice for Making and Curing Concrete Test Specimens in the Field*, A. International, Editor. 2019: West Conshohocken, PA.
4. *ASTM C192/C192M-18a Standard Practice for Making and Curing Concrete Test Specimens in the Laboratory,* A. International, Editor. 2018: West Conshohocken, PA.
5. Ley, M.T., et al., *Determining the Air-Void Distribution in Fresh Concrete with the Sequential Air Method.* Construction and Building Materials, 2017. 150: p. 723-737.
6. *AASHTO TP118-17 Standard Method of Test for Characterization of the Air-Void System of Freshly Mixed Concrete by the Sequential Pressure Method.* AASHTO 2017: Washington, DC.

3.0 PREDICTION OF FREEZE-THAW DURABILITY

3.1 ESTABLISHING A FREEZE-THAW PREDICTION MODEL

A model (based on the time to reach critical saturation, TTRCS) was developed by Fagerlund [1, 2] and has been modified by work of Li et al. [3] and Todak et al. [4]. The time to reach critical saturation model is the backbone of the performance models in AASHTO PP-84 and PASS RIGID and used to determine the time that is required for a concrete to reach critical saturation (a limit state that indicates the potential for damage to occur). This model requires three parameters as shown in Figure 3.1.1 and Equation 3.1.1 [5]. The parameters include:

- **Matrix saturation (DoS_{Matrix}):** Determined either experimentally through Task 1.6a and 1.6b or through a computational model that uses mixture proportions.
- **Secondary sorption (S'_2):** Determined either experimentally using the Task 1.7 standard operating procedure or through the apparent formation factor (F_{APP}),
- **Critical degree of saturation (DoS_{CR}):** Determined either experimentally through Task 1.8 or through a fitted equation that works for a wide range of concrete mixtures.

Figure 3.1.1 The comparison of theoretical and experimentally measured porosity of concrete with different air contents.

$$t = \left(\frac{DoS_{CR} - DoS_{Matrix}}{\varphi S'_2}\right)^2 \qquad (3.1.1)$$

where, φ is a parameter to account for the drying exposure conditions and t (year) is the time for the concrete to reach critical saturation. The φ can be taken as 1 when concrete is in continuous contact with water at a constant temperature.

A recent paper [6] has shown that the service life of concrete exposed to freezing and thawing may be able to be predicted (as a limit state) from mixture proportions; however, additional work is needed to fully evaluate and calibrate the models. This report outlines several advancements in the modeling prediction. Specifically, the results are summarized as they relate to each of the aforementioned parameters.

This section is a series of work that combines a series of testing to develop a predictive freeze-thaw model. This work used a shared number of mixtures and methods to gain new insights. This model starts by making basic property measurements and then testing these mixtures in a more fundamental way to determine water uptake and damage once that concrete is at a point of critical saturation. Finally, a parametric model is developed that could serve as a foundation for a freeze-thaw model that could predict field performance.

3.1.2 MATERIALS AND MIXTURE PROPORTIONS

Type I ordinary portland cement (ASTM C150-17) was used with a specific gravity of 3.15 and a Blaine fineness of 386 m^2/kg. The chemistry and mineral compositions, as provided by material producers, are listed in the appendix in the respective chapters. The appendix also contains the details for the concrete mixtures. Three water to cement ratios (w/c = 0.40, 0.45 and 0.50) and a wide range of the air contents were investigated. The mixture proportions were adjusted to yield.

The fine aggregate was a natural river sand with a specific gravity of 2.61 and an absorption rate of 0.44%. Two coarse aggregates were used with specific gravity of 2.75 and 2.72. The coarse aggregates were crushed limestone with an absorption of 0.73% and a maximum size of 19.1 mm (0.75 in.). A wood rosin air entraining admixture (AEA) was used to achieve different air contents. In addition, a polycarboxylate (PC)-based high range water reducing admixture (HRWRA) was used as it has been shown to alter the air void distribution.

For length change measurements, the same materials were used to prepare concrete with varying air void content and air void quality. After the air void content and SAM were measured on the fresh concrete. Mortar was obtained from the fresh concrete by sieving coarse aggregates out of it.

3.1.3 EXPERIMENTAL MEASUREMENTS

3.1.3.1 Porosity

This section compares the measured porosity with the theoretically calculated porosity [7]. The theoretical and experimental data for concrete mixtures with different w/c, air volume, and air quality is shown in Figure 3.1.2. There is a correlation (within ± 10 % variation) between the theoretical values and the experimental data. The theoretical porosity is slightly higher than the experimental data, and the difference is approximately 1.1 - 1.3 % (which is similar to the porosity of the aggregate). This may indicate the difficulty to saturate the normal weight aggregates within the hardened concrete even at a high vacuum level (7 ± 2 Torr). It appears reasonable to assume the total porosity as the sum of the paste matrix porosity and air content in the air-entrained concrete with normal weight aggregates; however, more work is needed to confirm this observation. The results show that the porosity of concrete mixtures can be predicted using the mixture design as an input.
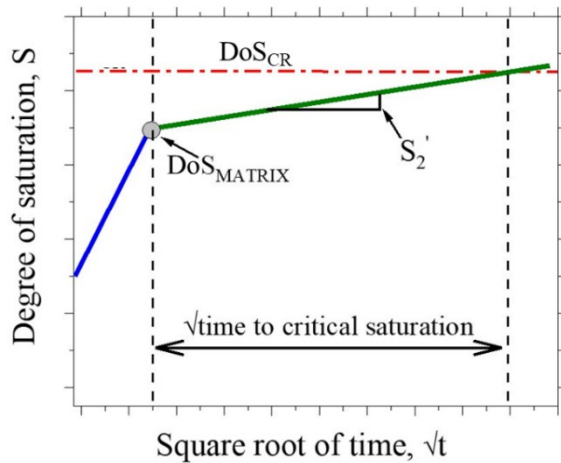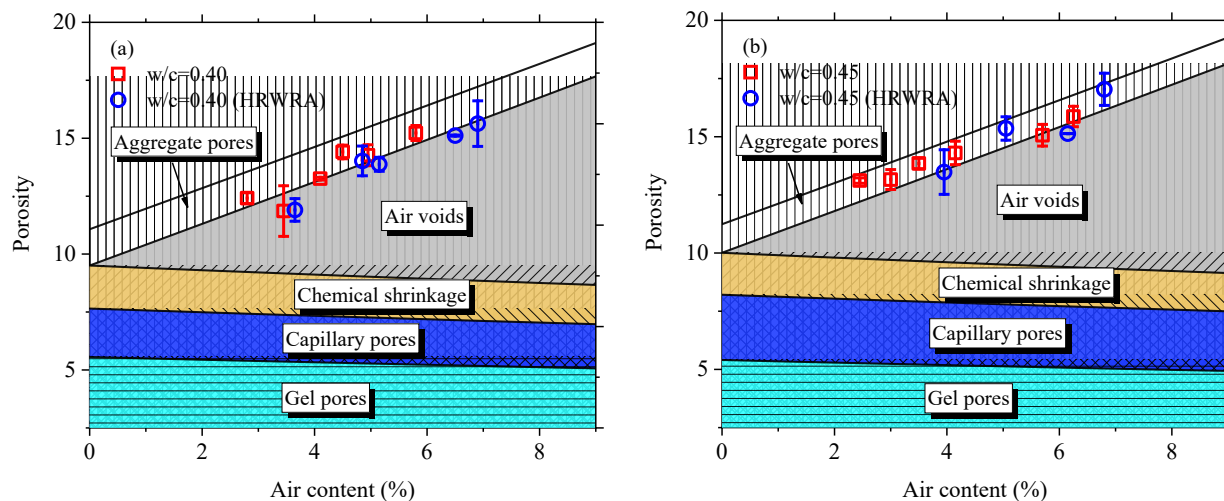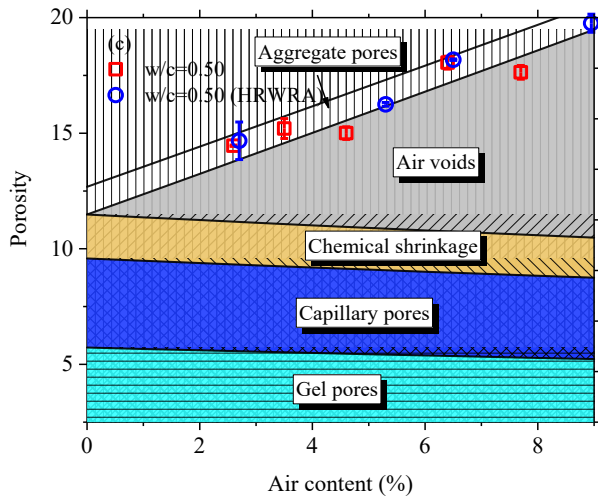
Figure 3.1.2. The comparison of theoretical and experimentally measured porosity of concrete with different air contents.

3.1.3.2 Matrix degree of saturation (DoS_{Matrix})

The matrix degree of saturation (DoS_{Matrix}) plays an important role in freeze-thaw performance of concrete. The DoS_{Matrix} of concrete is defined as the degree of saturation when the capillary, gel, and chemical shrinkage pores are filled with water, but the air voids (entrained and entrapped) only contain vapor [6, 7]. The DoS_{Matrix} was experimentally determined using the 'Bucket test at Nick Point' (according to a procedure that is being standardized as the AASHTO TP-119, option A procedure). Figure 3.1.3 shows the two-stage absorption from the amount of absorbed water and the electrical resistivity of the concrete as functions of the square root of time. The Nick Point occurred at Day 4 - Day 7 for the samples with varying w/c and air content, as illustrated in Figure 3.1.3, and DoS_{Matrix} can be calculated as shown in Figure 3.1.2.

$$DoS_{Matrix} = \frac{m_{NK} - m_{OD}}{m_{SAT} - m_{OD}}$$ (3.1.2)

where, m_{NK}, m_{OD} and m_{SAT} denote the mass (g) at Nick Point, oven dry and saturation, respectively.

Figure 3.1.4 compares the measured values of DoS_{Matrix} with the calculated values [7]. The experimental values are comparable to the theoretical values (within ± 10%). As shown in Figure 3.1.4, the value of DoS_{Matrix} decreases as the air content increases, since a greater volume of air voids needs to be filled during the secondary absorption. At a similar air content, the concrete with a higher w/c generally has a greater value of DoS_{Matrix} since a greater volume of matrix pores need to be filled during the initial absorption. However, the amount of air in concrete (i.e., volume of air) is the most influential factor on DoS_{Matrix}.
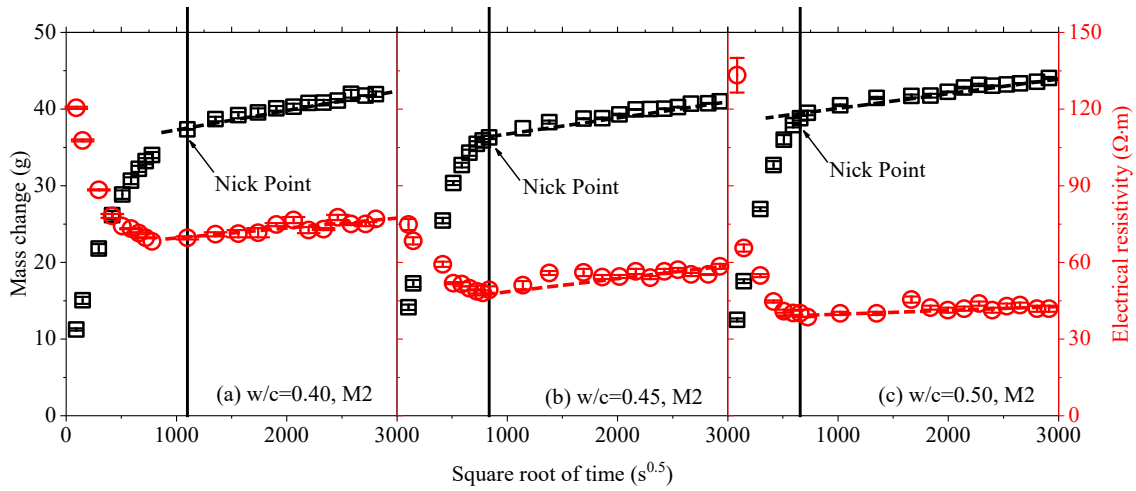
Figure 3.1.3. Determination of DoS_Matrix during the 91-day immersion test.
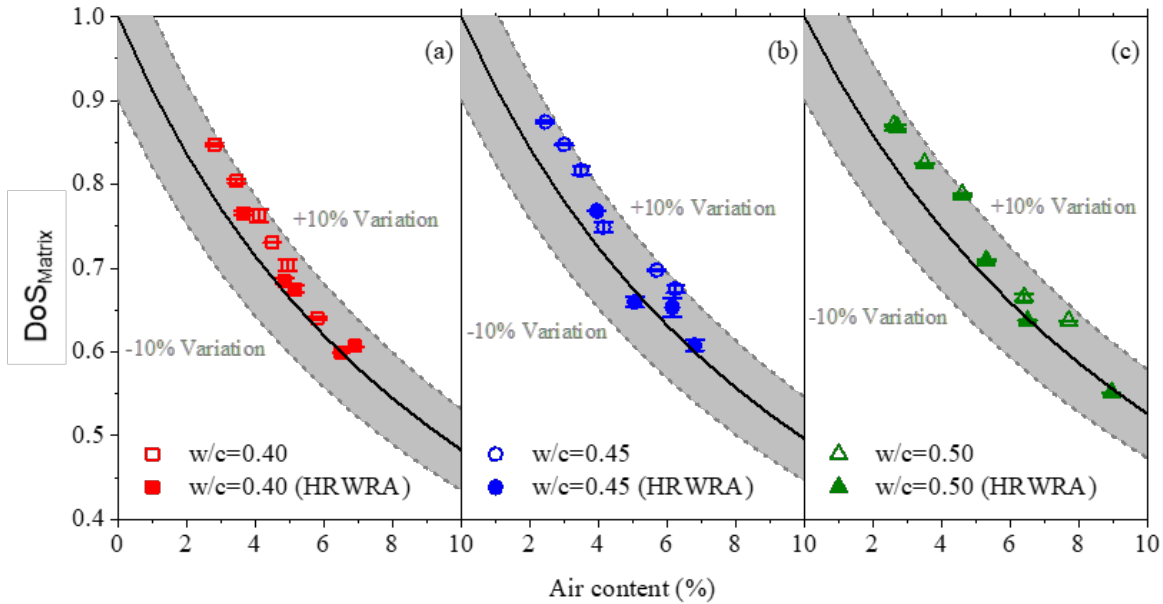
Figure 3.1.4. The measured DoS_Matrix from bucket test (The solid lines represent the theoretical values).

3.1.3.3 Electrical resistivity and formation factor

The bulk electrical resistivity of the concrete mixtures was measured according to AASHTO TP-119-17 at two different saturation levels: (1) conditioning according to AASHTO TP-119 Option A (i.e., matrix saturation) and (2) conditioning according to AASHTO TP-119 Option C (vacuum saturation). As a microstructural descriptor, the formation factor has historically been defined as the vacuum saturated sample (F_{SAT}) as shown in Equation 3.1.3a. However, the formation factor of the sample at matrix saturation level (F_{APP}, apparent formation factor) as shown in Equation 3.1.3b appears to be more practical. The formation factor for the saturated and matrix saturation cases are defined as the ratio of the electrical resistivity of the concrete (ρ_C) to that of the pore solution (ρ_{ps}) at vacuum saturation and matrix saturation levels, respectively [7]:

$$F_{SAT} = \frac{\rho_{C-SAT}}{\rho_{ps-SAT}} \qquad\qquad (3.1.3a)$$

$$F_{APP} = \frac{\rho_{C-APP}}{\rho_{ps-APP}} \qquad\qquad (3.1.3b)$$

Figures 3.1.5 and 3.1.6 show the measured F_{SAT} and F_{APP} of the air-entrained concrete as a function of air content. As the air content increases, the value of F_{SAT} linearly decreases due to the increased porosity of the entrained air but the F_{APP} does not change. As the w/c increases, F_{SAT} decreases due to the increased porosity and pore connectivity. This shows the usefulness of using F_{APP}. This is likely caused by the filling of the air voids. Practically, this further confirms the observations of Bu et al. [8] that showed that electrical properties like the rapid chloride permeability (RCPT) index are dependent on the air content because the samples are vacuum saturated before testing; thereby, accounting for some of the variation associated with quality control testing with this test method. The independence of F_{APP} on the air content is expected since the pore solution at DoS_{Matrix} only occupies the matrix pores which are similar in volume and microstructure in the same group of concrete. The F_{SAT} can be related to F_{APP} via the degree of saturation, as shown in Equation 3.1.4 [7].

$$f(DoS_{Matrix}) = \frac{F_{SAT}}{F_{APP}} = DoS_{Matrix}{}^{n} \qquad (3.1.4)$$

The experimental data of $f(DoS_{Matrix})$ is fitted using Equation 3.1.4. The fitted value of exponent n is 2.97 (approximately 3), and the majority of the experimental data lies within $\pm 15\%$ variation.
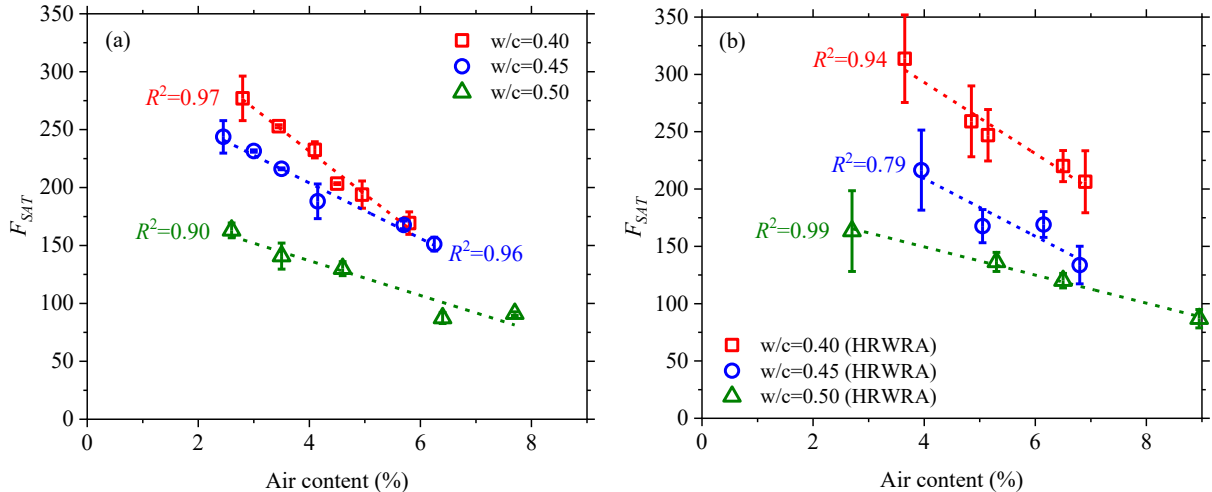
Figure 3.1.5. Formation factor of vacuum saturated concrete (F_{SAT}) as a function of air content.
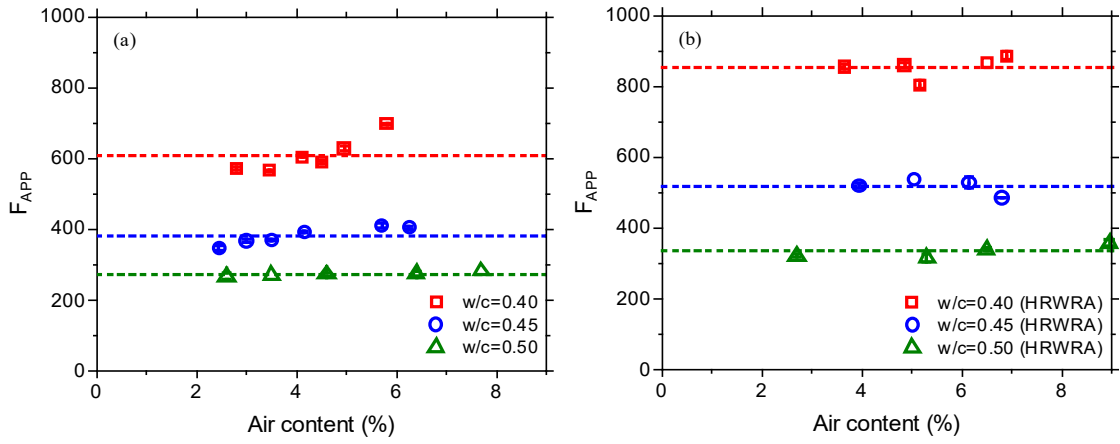
Figure 3.1.6. The apparent formation factor of concrete (F_{APP}) at matrix saturation level (i.e., DoS_{Matrix}).

3.1.3.4 Initial and secondary absorption rates

The impact of entrained air voids (air content and quality) on fluid transport (water absorption) was examined for concrete with varying water-to-cement (w/c) ratios. Neutron Radiography (NR) was used to measure water absorption in concrete samples with high spatial resolution. The samples were conditioned at $50 \pm 2\%$ RH and

25 ± 1 °C [9]. ASTM C 1585-13 identifies absorption as the change in mass divided by the product of the exposed area of the sample and density of water. This formulation is shown in Equation 3.1.5.

$$i = \frac{\Delta m}{\rho_w A} \qquad (3.1.5)$$

where, i is the absorption and A is the cross-sectional area of the flow (i.e., the exposed area of the sample to water).

Equations 3.1.6 and 3.1.7 were used to determine initial and secondary absorption rates (S_1 and S_2) of the samples. S_1 and S_2 are determined as the slope of the absorption versus square root of the time ($\sqrt{t}$) curves during the first 5 h and 1 d – 7 d, respectively (ASTM C 1585-13 definition).

$$i\left(t_{5min}^{5h}\right) = S_1\sqrt{t} \qquad (3.1.6)$$

$$i\left(t_{7d}^{1d}\right) = S_2\sqrt{t} + B_1 \qquad (3.1.7)$$

where, t is the time and B_1 is the regression constant.

Figure 3.1.7 shows the S_1 and S_2 as a function of air content calculated based on Equations 3.1.6 and 3.1.7 for concrete mixtures with varying w/c. The values of S_1 and S_2 are independent of the air content. The addition of HRWR reduces the measured values of S_1 and S_2 by approximately by 25% for mixtures with the same w/c due to a refined capillary pore structure.
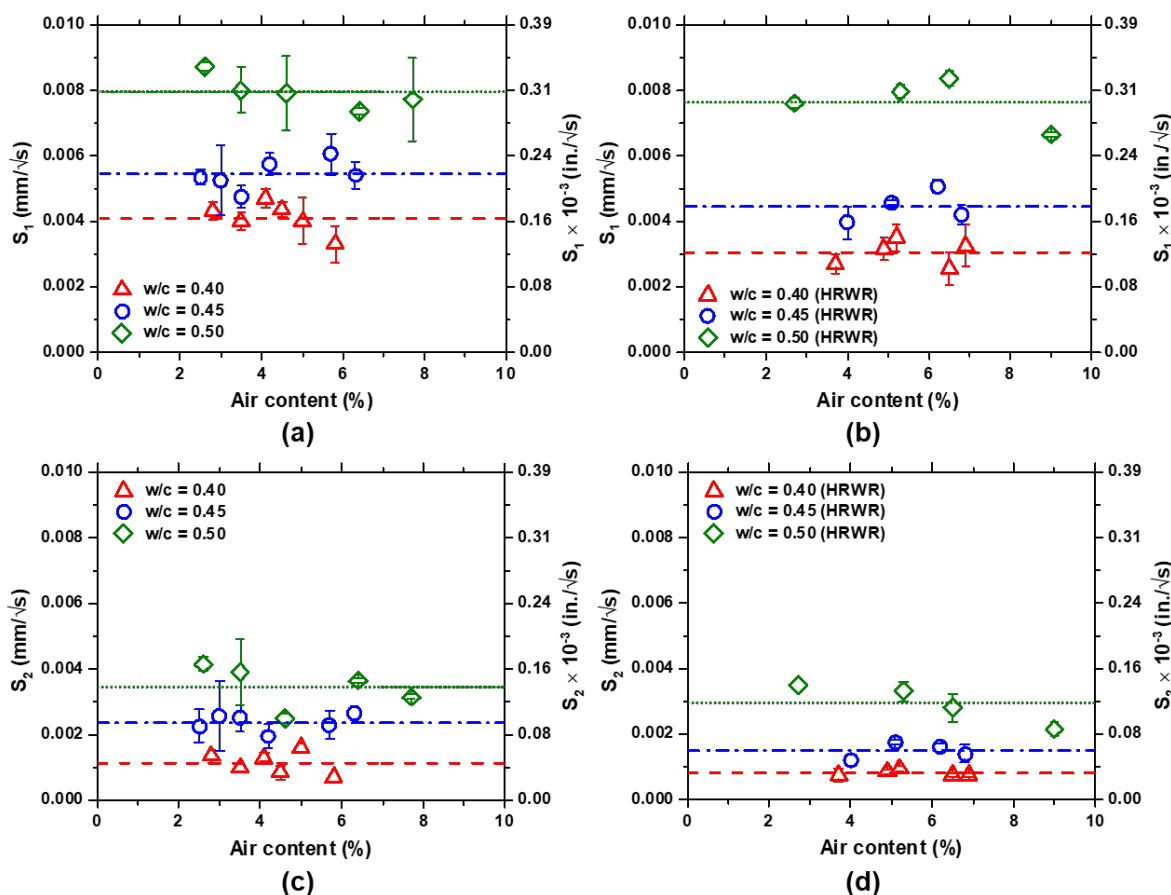

Figure 3.1.7. Initial and secondary absorption rate versus air content for the samples with varying w/c with and without HRWR based on absorption vs. $\sqrt{t}$ curves (S_1, S_2) – ASTM C 1585-13 definition. (Note: the "mm" in S_1 and S_2 units is not representative of actual depth of penetration.)

41

3.1.3.5 Relating water absorption to the apparent formation factor

A linear relationship exists between the rate of water absorption and the reciprocal of the square root of the formation factor ($\sqrt{(1/F)}$) based on both theoretical derivations and experimental measurements [9, 10]. Figure 3.1.8 shows S_1 and S_2 versus F_{APP}. A linear relationship exists between S_1 and S_2 and $\sqrt{F_{APP}}$. This linear relationship is insensitive to air content. These results are consistent with previous findings by Khanzadeh Moradllo et al. [10] which also included a theoretical derivation describing the fundamental underpinnings of this relationship.

This linear relationship can be used to predict S_1 and S_2 based on F_{APP} and thereby saving substantial time in sample preparation and testing. This relationship provides a powerful tool in quality control to obtain F_{APP} (AASHTO TP-119 Option A). The secondary rate of fluid absorption (S_2) is a key parameter in service life prediction of concrete (Equation 3.1.1).
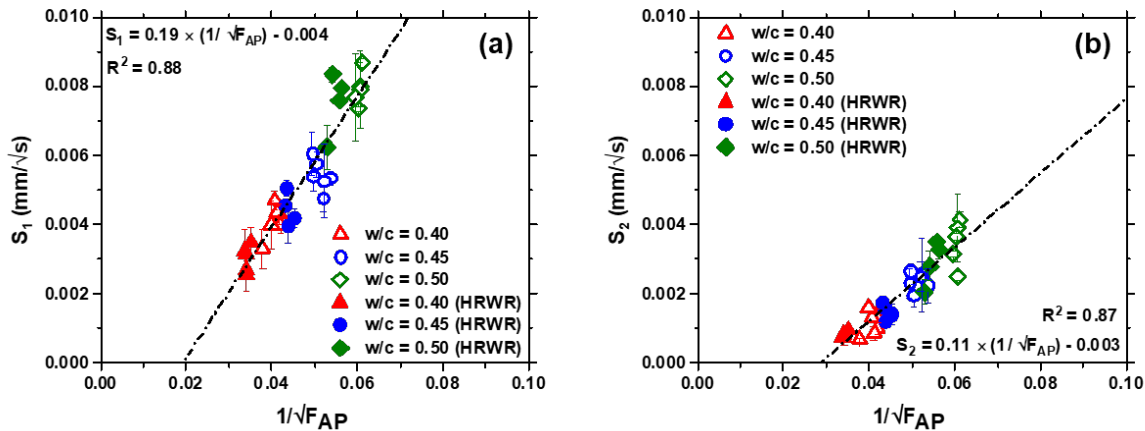

Figure 3.1.8. (a) and (b): Initial and secondary absorption rates vs. apparent formation factor calculated based on absorption vs. $\sqrt{t}$ curves for the samples with varying w/c and air content with and without HRWR.

3.1.3.6 A simple model to quantify the volume of water filled air voids using NR

In air entrained concrete, the fluid absorption can be divided into two parts: 1) water that is absorbed by the matrix pores (capillary, chemical shrinkage and gel pores) and 2) water that is absorbed in the entrained and entrapped air voids. Conventional testing methods for measuring fluid absorption (e.g., ASTM C 1585-13, AASHTO Task 1.7) measure the mass of the total cumulative fluid uptake into the concrete. As such, ASTM C 1585-13 is not able to distinguish where the absorbed water is in the sample or to determine the amount of water that is absorbed by the different types of pores (i.e., matrix pores and entrained air voids) in the concrete. Therefore, it is useful to provide information about the spatial distribution of filled pores in the concrete to better understand this absorption progress and its influence on time-dependent DoS.

This section describes how NR and the Beer-Lambert Law [11] can be used to quantify the rate of water absorption by the matrix pores and the air voids. Figures 3.1.9 and 3.1.10 outline the steps to determine the volume fraction of pores filled with fluid. Figure 3.1.9 (a through c) provides a schematic diagram of time-dependent volumetric water content profiles obtained from NR. Figure 3.1.9 illustrates the volume of pores initially filled with water (i.e., volume of filled pores after conditioning at 50% RH), volume of matrix pores, and the total volume of pores. The volume of initially filled pores ($\theta_{Initial}$) and total pores (θ_{Total}) are determined from reference and vacuum-saturated radiographs, respectively. The volume of matrix pores (θ_{Matrix}) is calculated [11]. Figure 3.1.9b shows the initial sharp water front that moves into the sample upon wetting. The initial absorbed water content is below the θ_{Matrix}. Therefore, the area shown in Figure 3.1.9b between $\theta_{Initial}$ and the time-dependent θ profile (θ_t) represents the volume of water filled matrix pores ($\theta_{Matrix-Fill}$). Water infiltrates the air voids when the θ_t values are larger than the θ_{Matrix} (Figure 3.1.9c). The volume of water filled air voids ($\theta_{Air-Fill}$) can be determined by subtracting the θ_{Matrix} from θ_t over the sample depth (green area, Figure 3.19c).

The mathematical expressions of the volume of water filled matrix pores and air voids are presented in Equations 3.1.8a and 3.1.8b.

$$\theta_{Matrix-Fill} = \theta_t - \theta_{Initial} \ \textbf{and} \ \theta_{Air-Fill} = 0 \ \textbf{\textit{if}} \ \ \theta_t \leq \theta_{Matrix} \tag{3.1.8a}$$

$$\theta_{Matrix-Fill} = \theta_{Matrix} - \theta_{Initial} \ \textbf{and} \ \ \theta_{Air-Fill} = \theta_t - \theta_{Matrix} \ \textbf{\textit{if}} \ \theta_t > \theta_{Matrix} \tag{3.1.8b}$$

where, θ_t and $\theta_{Initial}$ are the time-dependent and initial volumetric water contents of the sample at depth d_i (measured by NR), respectively; and θ_{Matrix} is the calculated volume of matrix pores [7, 11, 12].

A schematic of the time-dependent volume of water filled air voids profiles is presented in Figure 3.1.10a. To determine the percentage of filled air voids (i.e., DoS of air voids), the volume of filled air voids was divided by the estimated volume of air voids over the sample depth (Figure 3.1.10b). More details and examples can be found in [11].

As shown in Figure 3.1.9, the air voids filling process is slower than the filling of the matrix pores. The water absorption front by matrix pores is significantly sharper than that of the air voids. This is attributed to the higher capillary pressure in matrix pores when compared to the air voids.
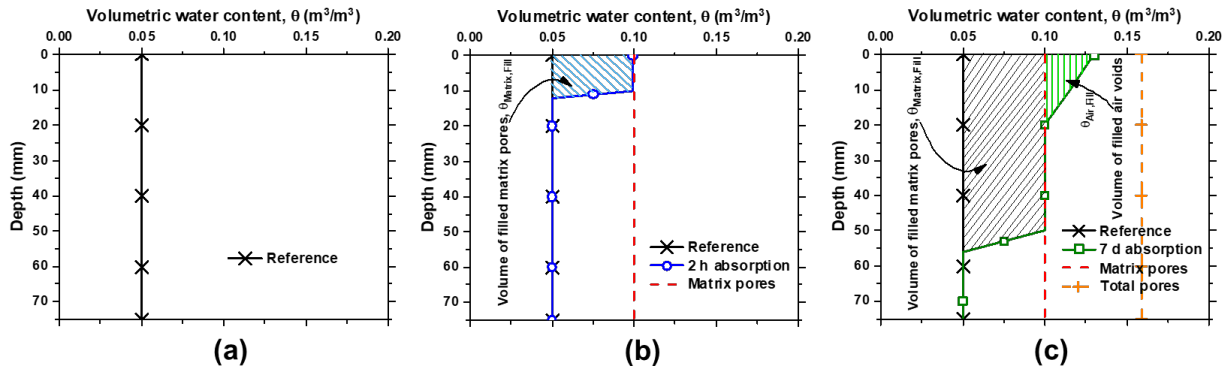
Figure 3.1.9. A procedure of determining volume of water filled pores: (a) An example of initially filled pores after conditioning at 50% RH obtained from reference radiograph, (b) an example of matrix pores filling during absorption at early ages, and (c) an example of concurrent matrix pores and air voids filling during the absorption experiment. (Note: Volume of total pores obtained from a vacuum-saturated radiograph).
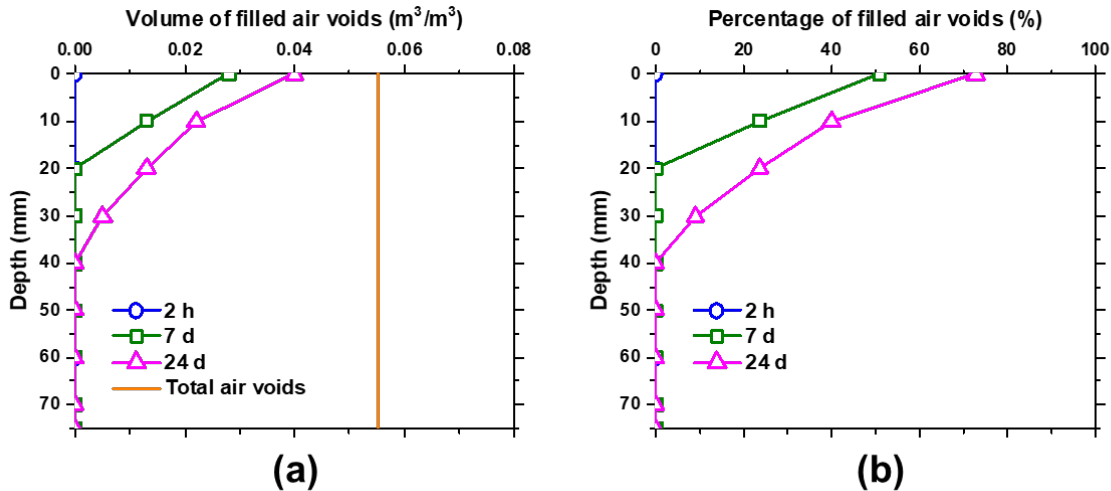
Figure 3.1.10. An example of smoothed: (a) Time-dependent profiles of volume of water filled air voids and (b) time-dependent percentage of water filled air voids (i.e., DoS of air voids).

43

3.1.3.7 Rate of water absorption by air voids (S_2')

The time-dependent absorbed water mass described in Equation 3.1.9 was used to determine the rate of fluid absorption by air voids as shown in Figure 3.1.11. The water absorption rate by air voids (S_2') was assumed to be the slope of the absorbed water by air voids versus the square root of time curve during the 3 d – 40 d as shown in Figure 3.1.11.

$$m_a\left(t_{40d}^{3d}\right) = S_2'\sqrt{t} + B_1 \qquad (3.1.9)$$

where, m_a (g) is the time-dependent mass of water absorbed by air voids; t (s) is the time; and B_1 is the regression constant.

Figure 3.1.12 shows the S_2' versus air content and SAM Number calculated for concrete mixtures with varying w/c with and without HRWR. Reducing the w/c of the mixture lowers the value of S_2'. This can be attributed to the refined microstructure of the sample with a lower w/c where the fluid progress through the capillary pores is slower. The entrained air voids are connected by the capillary pore system of the cement paste matrix [7, 9]. Therefore, the process of air void filling will require a longer time in a low w/c mixture. Figure 3.1.12 also indicates that the impact of air content on S_2' is minimal, while the S_2' decreases with reduction of the SAM Number. The relationship between S_2' and SAM Number is stronger in the samples with HRWR. A lower SAM Number is shown to correlate to better air void quality (i.e., lower spacing factor) [13].
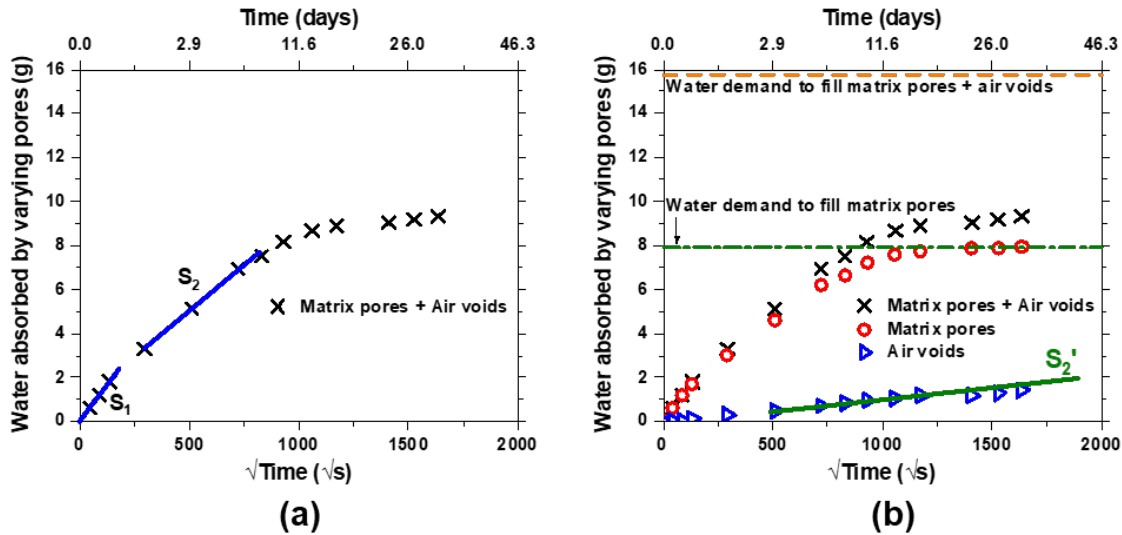
Figure 3.1.11. An example of the time-dependent water mass absorbed by matrix pores and air voids from NR: (a) represents the initial and secondary absorption rates (S_1 and S_2) based on ASTM C 1585-13 definition and (b) represents the filling rate of air voids (S_2') based on Equation 3.1.9.
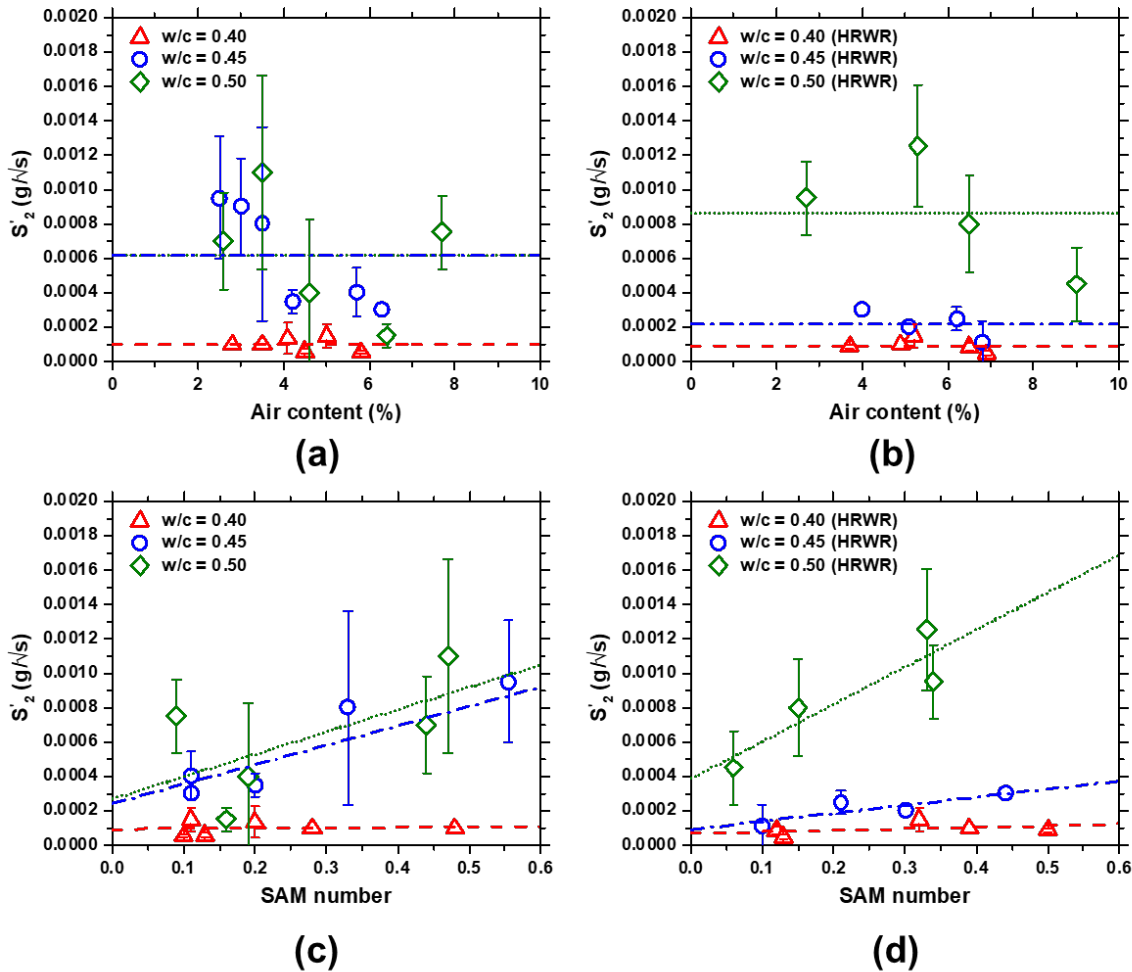
Figure 3.1.12. The calculated water absorption rate by air voids (S_2') versus air content and SAM number for the samples with varying w/c with and without HRWR.

3.1.3.8 Relating SAM Number to the air content

The air content and SAM Number of the freshly mixed concrete were measured using AASHTO TP 118-17. Figure 3.1.13 shows the relationship between air content and SAM Number for the mixtures with and without HRWR. This relationship depends on the quality of the air void system in a given concrete. The samples without HRWR have a better air void distribution (i.e., a smaller SAM Number) when compared to the samples with HRWR at a given air content. As a result, to achieve the same SAM Number, a higher volume fraction of air is required for the samples with HRWR.

Figure 3.1.13. The relationship between air content and SAM Number for the mixtures with varying w/c and with and without HRWR.

3.1.3.9 Critical degree of saturation (DoS_{CR}): relationship with SAM Number & air content

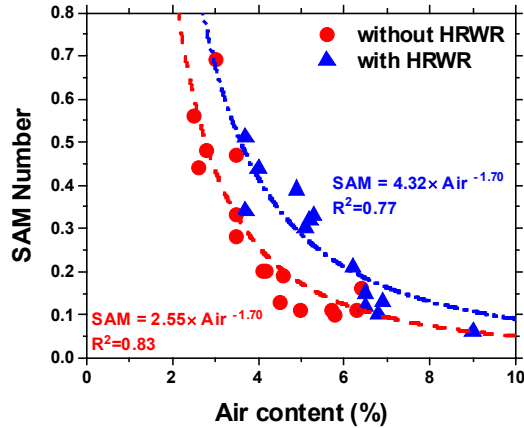The DoS_{CR} can be defined for each mixture and when the DoS in the concrete exceeds DoS_{CR}, damage will develop during freezing and thawing [1]. The DoS_{CR} is one of the important factors in freeze-thaw performance of concrete. In this study, the DoS_{CR} of concrete mixtures was estimated using the measured damage index from ultrasonic pulse velocity (UPV) measurements. A cold plate was used to expose the samples to three freeze-thaw cycles between 23 ± 1 °C and -20 ± 1 °C. Details on the experimental procedure can be found in [14].

The air void quality has the most important impact on DoS_{CR} [1-3]. Weiss et al. [5] and Todak et al. [4] proposed that the DoS_{CR} can be related to the SAM Number based on Equation 3.1.10 which was obtained as a fitted lower bound to experimental data.

$$DoS_{CR} = 87 - 10 \cdot SAM \qquad (3.1.10)$$

Figure 3.1.14 illustrates the measured DoS_{CR} using UPV as a function of SAM Number for the mixtures with and without HRWR. It can be noticed that Equation 3.1.10 shows good agreement with the experimental results of the mixtures without HRWR. However, the mixtures with HRWR have a lower DoS_{CR} compared to the mixtures without HRWR and the intercept value of Equation 3.1.10 needs to be reduced to 82% in order to represent the lower bound of experimental data, as shown in Figure 3.14b. The lower DoS_{CR} in the samples with HRWR can be explained by the lower filling rate of air voids (i.e., lower S'_2) in these samples due to higher tortuosity of the matrix [9, 14].

When the SAM Number (i.e., air quality) of the concrete mixture is unknown, Equation 3.1.11a and 3.1.11b can be used to estimate the DoS_{CR} based on volume fraction of air.

$$DoS_{CR} = 87 - 10 \cdot A \cdot Air^{-5/3} \; , \; without \; HRWR \qquad (3.11a)$$

$$DoS_{CR} = 82 - 10 \cdot A \cdot Air^{-5/3} \; , \; with \; HRWR \qquad (3.11b)$$

Figure 3.15 compares the measured DoS_{CR} values as a function of the air content using UPV with the estimated trend based on Equation 3.11. Based on Figure 3.1.13, the 'A' values of 2.55 and 4.32 were used in Equation 3.1.11(a) and (b) for the mixtures with and without HRWR, respectively. It can be noted that Equation 3.1.11(a) and (b) illustrates a lower bound to experimental data.
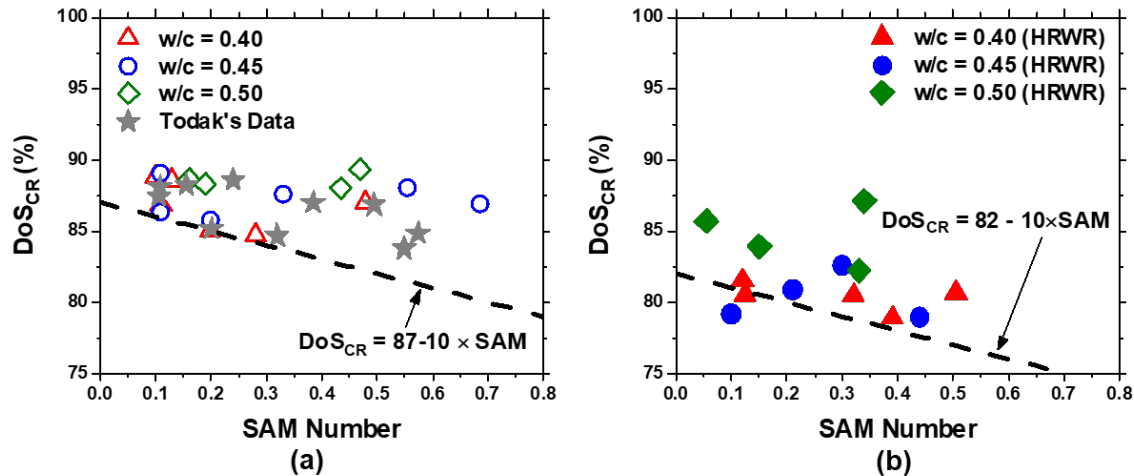
46

Figure 3.1.14. The measured *DoS_CR* (based on UPV measurements) versus SAM Number for the mixtures with varying w/c: (a) with and (b) without HRWR. Note: A comparison with Todak's data [4] is presented in (a).
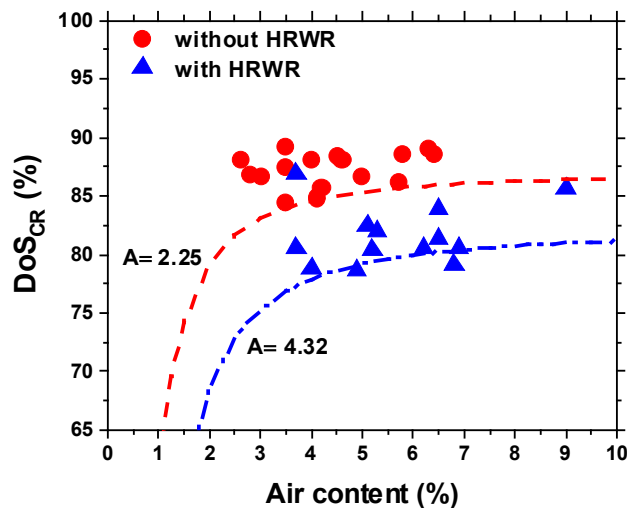
Figure 3.1.15. The relationship between DoS_CR and air content for the mixtures with varying w/c and with and without HRWR based on Equation 3.11.

3.1.3.10 Length change measurements

Length change measurements were used to quantify the *DoS_CR*. Experimental results indicate that specimens with a DoS higher than *DoS_CR* showed length expansion at freezing temperature, length reduction at melting temperature, permanent length change, and damage after the freeze-thaw cycle (Figure 3.1.16a). Alternatively, mortar samples with a lower DoS show a linear length change during cooling and did not develop any damage after the Freeze-thaw cycle (Figure 3.1.16b). A linear regression may be used to determine the DoS_CR by extrapolating it to the DoS at which any of residual strain is higher than 0μm/m (Figure 3.1.17).

Figure 3.1.18 (a) shows the residual strain values versus the damage index determined from another test method (i.e., using UPV measurements on the mortar samples). The threshold for the damage index was determined experimentally based on the variability in the ultrasonic wave speed and is found to be equal to 8%. This study demonstrated a systematic methodology to determine the critical DoS accurately based on length change measurements. This method can be used as an alternative method to determine the DoS_CR to use in DoS models.
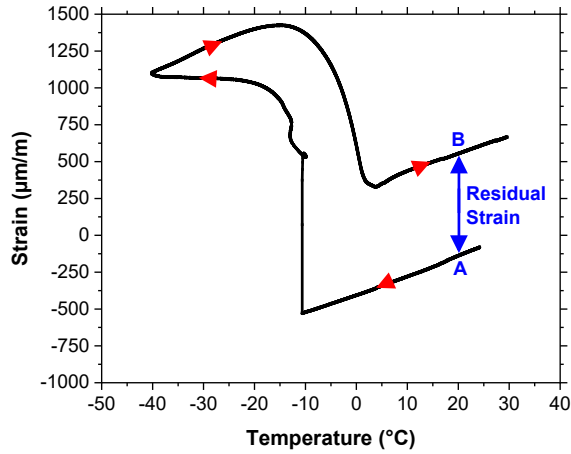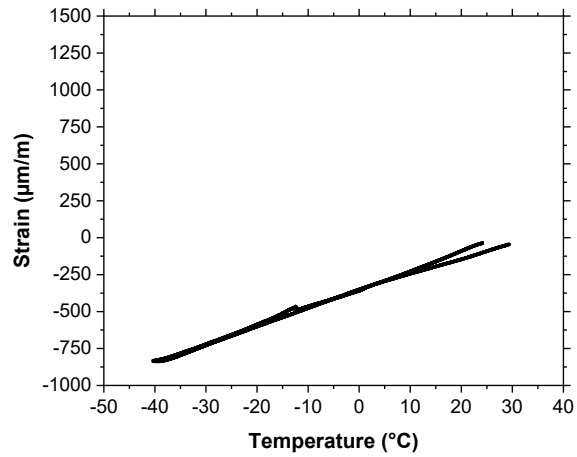
(a) DoS > DoS_CR   (b) DoS<DoS_CR

Figure 3.1.16. Strain evolution with respect to temperature: (a) *DoS > DoS_CR*; (b) *DoS < DoS_CR*.

Figure 3.1.17. Determination of *DoS_CR* based on length change measurements.

(a)   (b)

Figure 3.1.18. Comparison of the freeze-thaw damage obtained from length change with the one obtained using UPV on mortar samples with varying air volume and quality.

48

References

[1] G. Fagerlund, The critical degree of saturation method of assessing the freeze/thaw resistance of concrete, Matériaux et Construction 10(4) (1977) 217-229.

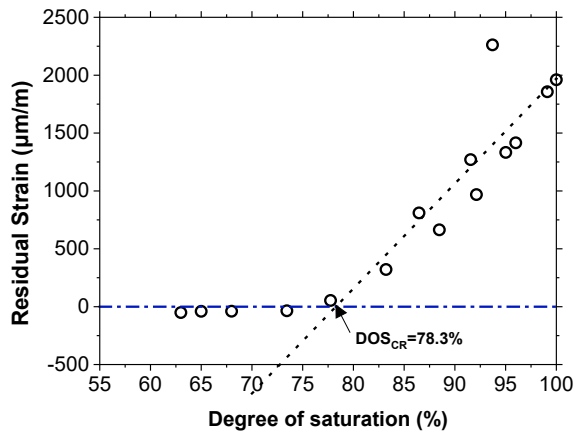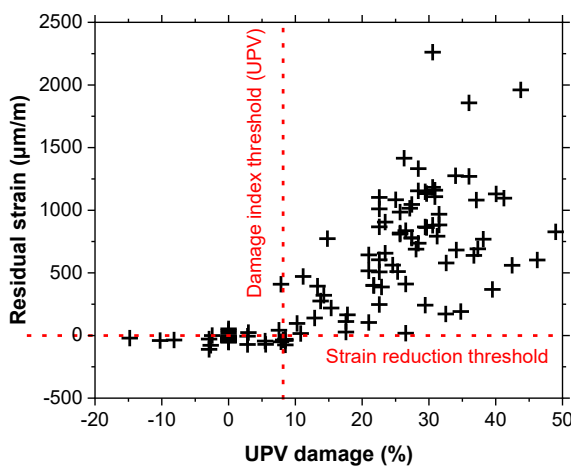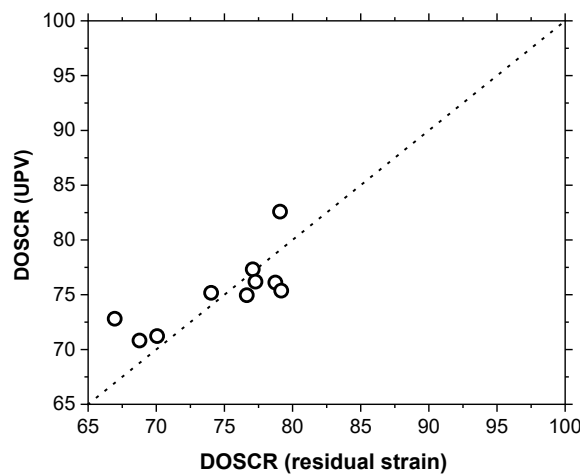[2] G. Fagerlund, A service life model for internal frost damage in concrete, Lund University, Lund, Sweden, 2004, p. 139 pp.

[3] W. Li, M. Pour-Ghaz, J. Castro, J. Weiss, Water absorption and critical degree of saturation relating to freeze-thaw damage in concrete pavement joints, Journal of Materials in Civil Engineering 24(3) (2011) 299-307.

[4] H.N. Todak, Durability assessments of concrete using electrical properties and acoustic emission testing, Purdue University, 2015.

[5] W.J. Weiss, T. Ley, O.B. Isgor, T. Van Dam, Toward performance specifications for concrete durability: using the formation factor for corrosion and critical saturation for freeze-thaw, Proceedings of the 96th Annual Transportation Research Board, Washington, DC, USA (2017) 8-12.

[6] K. Bharadwaj, D. Glosser, M. Khanzadeh Moradllo, B. Isgor, J. Weiss, Toward the Prediction of Pore Volumes and Freeze-Thaw Performance of Concrete Using Thermodynamic Modelling, Cement and Concrete Research 124 (2019).

[7] C. Qiao, M.K. Moradllo, H. Hall, T. Ley, J. Weiss, Electrical Resistivity and Formation Factor of Air Entrained Concrete, ACI Materials Journal 116(1) (2018).

[8] Y. Bu, J. Weiss, Saturation of air entrained voids and its implication on the transport of ionic species in concrete, (2014).

[9] M.K. Moradllo, C. Qiao, M. Keys, H. Hall, M.T. Ley, S. Reese, W.J. Weiss, Quantifying Fluid Absorption in Air Entrained Concrete Using Neutron Radiography, ACI Materials Journal in press (2019).

[10] M.K. Moradllo, C. Qiao, B. Isgor, S. Reese, W.J. Weiss, Relating the Formation Factor of Concrete to Water Absorption, ACI Materials Journal 115(6) (2018) 887-898.

[11] M. Khanzadeh Moradllo, C. Qiao, H. Hall, M.T. Ley, S. Reese, J. Weiss, Quantifying Fluid Filling of the Air Voids in Air Entrained Concrete Using Neutron Radiography, Cement and Concrete Composites in press (2019).

[12] T.C. Powers, T.L. Brownyard, Studies of the physical properties of hardened Portland cement paste, Journal Proceedings, 1946, pp. 101-132.

[13] M.T. Ley, D. Welchel, J. Peery, S. Khatibmasjedi, J. LeFlore, Determining the air-void distribution in fresh concrete with the Sequential Air Method, Construction and Building Materials 150 (2017) 723-737.

[14] M. Khanzadeh Moradllo, C. Qiao, R.M. Ghantous, M. Zaw, H. Hall, M.T. Ley, J. Weiss, Quantifying the Freeze-Thaw Performance of Air-Entrained Concrete Using the Time to Reach Critical Saturation Modelling Approach Cement and Concrete Composites Under review (2019).

3.2 TIME TO REACH CRITICAL SATURATION (TTRCS) MODEL

The model for the time to reach critical saturation (TTRCS) relies on three main parameters: critical degree of saturation (DoS_{CR}), matrix degree of saturation (DoS_{Matrix}), and the air void filling rate (i.e., secondary rate of absorption (S_2')) [1-3].

A common form of the TTRCS model is shown in Equation 3.2.1 [1-3].

$$DoS = DoS_{Matrix} + \varphi S_2' \sqrt{t} \leq DoS_{CR} \tag{3.2.1}$$

where, φ is a parameter to account for the drying exposure conditions and t (year) is the time for the concrete to reach critical saturation. The φ can be taken as 1 when concrete is in continuous contact with water at a constant temperature. Further work is needed to better understand the impact of drying and wetting as well as temperature change on this term.

The time to reach critical saturation can be written using Equation 3.2 where S'_2 has been replaced with F_{APP} and the constant c_1 (described earlier).

$$t = \left(\frac{DoS_{CR} - DoS_{Matrix}}{\varphi \cdot c_1 \sqrt{\frac{1}{F_{APP}}}} \right)^2 \tag{3.2.2}$$

The time to reach critical saturation can be normalized (using c_1 and φ), as shown in Equation 3.2.3 [6, 14]. This normalized time to reach critical saturation is based on the DoS_{Matrix}, DoS_{CR}, and F_{APP} and it is a unitless quantity. A simple experimental procedure to measure these parameters is described in Section 3.1.

$$t \cdot (\varphi \cdot c_1)^2 = F_{APP}(DoS_{CR} - DoS_{Matrix})^2 \tag{3.2.3a}$$

$$t \cdot (\varphi \cdot c_1)^2 = F_{APP} \cdot \Delta^2 \tag{3.2.3b}$$

where, Δ (%) is the difference between the DoS_{CR} and DoS_{Matrix}. The Δ is an indicator of freeze-thaw resistance of concrete and it primarily depends on the air void quality and volume.

3.2.1 Impact of air content and air quality on 'Δ'
This section examines the impact of air content and air quality on Δ in concrete mixtures with and without HRWR. Several observations can be made from Figure 3.2.1.
- First, samples with a lower SAM number have a greater Δ and therefore a greater time to reach critical saturation.
- Second, samples with a SAM number greater than 0.30 show very little difference in performance as the curves flatten.
- Third, samples with and without HRWR present a similar trend (i.e., statistically similar) for Δ as a function of the SAM Number.
- Fourth, the value of Δ is however statistically different when this is shown as a function of air content for samples with and without HRWR. This highlights that the SAM Number considers both air volume and spacing for providing an indicator of freeze-thaw resistance. As a result, the SAM Number is a better indicator of freeze-thaw resistance irrespective of the admixture combination when compared to air volume.

Equation 3.2.4 (developed from experimental data in Figure 3.2.2a) can be used to estimate the Δ based on the SAM Number.

$$\Delta = C \cdot SAM^{-D} \tag{3.2.4}$$

where, 'C' and 'D' are constants. Based on experimental data, the values of 'C' and 'D' are 6.03 and -0.645, respectively for the materials in this work. While it initially appears that the constants are independent of mixture

50

proportions. However, further work is needed to examine Equation 3.2.5 for the mixtures with different materials.

When the SAM Number of the concrete mixture is unknown, Equation 3.2.5 can be used to estimate the Δ based on volume fraction of air.

$$\Delta = C \cdot (A \cdot Air^{-B})^{-D} \tag{3.2.5}$$

As discussed, it seems that the values of 'B', 'C', and 'D' are independent of mixture proportions. By replacing these constants (B=1.70, C=6.03, and D=-0.645) based on experimental results, Equation 3.2.6 can be simplified as following:

$$\Delta = 6.03 \cdot A^{-0.645} \cdot Air^{1.10} \tag{3.2.6}$$

The predicted Δ as a function of air content based on Equation 3.2.6 for varying values of 'A' (i.e., air quality) is presented in Figure 3.2.1.
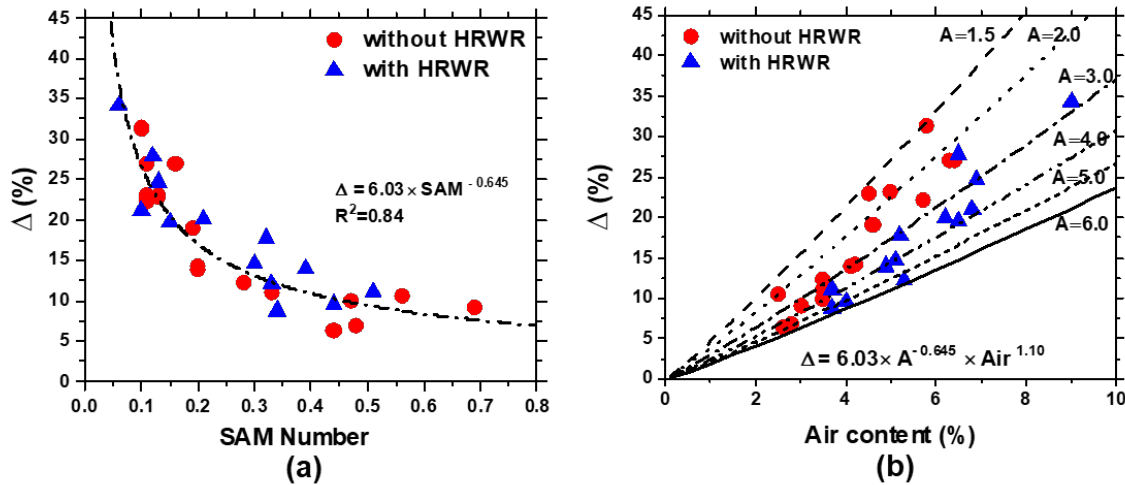
Figure 3.2.1. The 'Δ' versus (a) SAM Number and (b) air content for the samples with and without HRWR.

3.2.2 Impact of w/c, air content, and air quality on time to reach critical saturation

The normalized time to reach critical saturation (based on Equation 3.2.7 (TTRCS model)) as a function of the SAM Number and air content is illustrated in Figures 3.2.2 and 3.2.3 (experimental data points), respectively. In addition, Equations 3.2.7 and 3.2.8 are used to predict the normalized time to reach critical saturation using SAM Number and air volume (dashed lines), respectively.

$$t \cdot (\varphi \cdot c_1)^2 = F_{APP} \cdot (6.03 \cdot SAM^{-0.645})^2 \tag{3.2.7}$$

$$t \cdot (\varphi \cdot c_1)^2 = F_{APP} \cdot (6.03 \cdot A^{-0.645} \cdot Air^{1.10})^2 \tag{3.2.8}$$

The average F_{APP} for the mixtures with different w/c was used in Equations 3.2.7 and 3.2.8 to estimate the time to reach critical saturation. Based on Figure 3.1.13, the 'A' values of 2.55 and 4.32 were used in Equation 3.2.9 for the mixtures with and without HRWR, respectively.

Following observations can be made from Figures 3.2.2 and 3.2.3:
- The normalized time to reach critical saturation exponentially increases with a decrease in the SAM Number (i.e., better air quality).
- All samples with SAM Number below 0.20 exhibited a normalized time to reach critical saturation greater than 10.
- The samples with a higher air volume have a longer time to reach critical saturation due to the increase in the Δ value.

51

- Reducing the w/c slightly improves the freeze-thaw performance in the samples with HRWR.
- The predicted time to reach critical saturation shows reasonable agreement with the calculated values (TTRCS model).
- The results indicate that the SAM Number can be used to improve the understanding the performance of concrete in freeze-thaw environment, especially in modern concrete with combination of chemical admixtures.
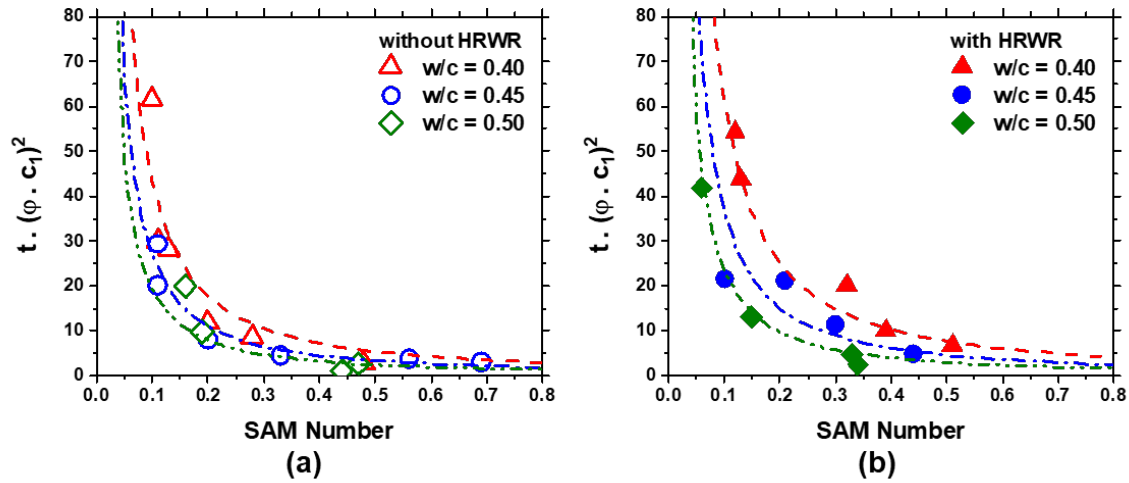
Figure 3.2.2. The normalized time to reach critical saturation as a function of the SAM Number for the mixtures with varying w/c and (a) with and (b) without HRWR. Note: The lines present the predicted values based on Equation 3.18.
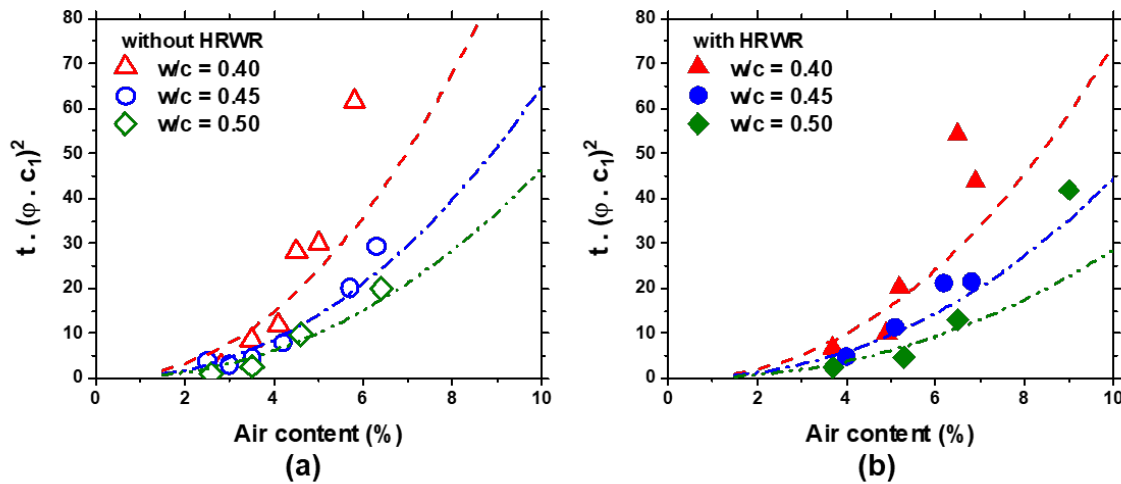
Figure 3.2.3. The normalized time to reach critical saturation as a function of the air content for the mixtures with varying w/c and (a) with and (b) without HRWR. Note: The lines present the predicted values based on Equation 3.19.

A summary of proposed equations to estimate the time to reach critical saturation and the critical degree of saturation based on SAM Number and air content is reported in Table 3.2.1. The derived constants in these equations based on experimental work are also reported in Table 3.2.1. However, more research is needed to examine these equations for other materials and mixture designs.

Table 3.2.1. Summary of proposed equations to estimate time to reach critical saturation and DoS_{CR}.

Relationship	Equation	Constants
Time to reach critical saturation	$t \cdot (\varphi \cdot c_1)^2 = F_{APP}(DoS_{CR} - DoS_{Matrix})^2$	
Time to reach critical saturation based on SAM Number	$t \cdot (\varphi \cdot c_1)^2 = F_{APP}. (C \cdot SAM^{-D})^2$	A= 2.55 (no HRWR) A= 4.32 (with HRWR) B= 1.70 C= 6.03 D= 0.645
Time to reach critical saturation based on air volume	$t \cdot (\varphi \cdot c_1)^2 = F_{APP} \times (C. A^{-D}. Air^{B \cdot D})^2$	
Critical degree of saturation based on SAM Number	$DoS_{CR} = 87 - 10 \cdot SAM$, no HRWR $DoS_{CR} = 82 - 10 \cdot SAM$, with HRWR	
Critical degree of saturation based on air volume	$DoS_{CR} = 87 - 10 \cdot A \cdot Air^{-B}$, no HRWR $DoS_{CR} = 82 - 10 \cdot A \cdot Air^{-B}$, with HRWR	

3.2.3 Time to reach critical saturation versus durability factor from ASTM C 666

This section compares the estimated time to reach critical saturation based on TTRCS model to the measured durability factor using ASTM C 666-15 for thirty different concrete mixtures. The normalized time to reach critical saturation as a function of the durability factor is presented in Figure 3.2.4. Based on this figure:

- The durability factor is greater than 75% and the normalized time to reach critical saturation is greater than 10 ($\approx$2.5 years with assumptions of c_I=2.1 $\frac{1}{\sqrt{year}}$ and φ=1.0) for all the mixtures with air content above 4.5% and a SAM Number below 0.30.
- While 86% of the mixtures with air content above 4.5% and a SAM Number below 0.30 have a normalized time to reach critical saturation of above 20 ($\approx$5 years with assumptions of c_I=2.1 $\frac{1}{\sqrt{year}}$ and φ=1.0), over 80% of the mixtures with air content below 4.5% and a SAM Number above 0.30 demonstrate a normalized time to reach critical saturation of below 10 ($\approx$2.5 years with assumptions of c_I=2.1 $\frac{1}{\sqrt{year}}$ and φ=1.0).
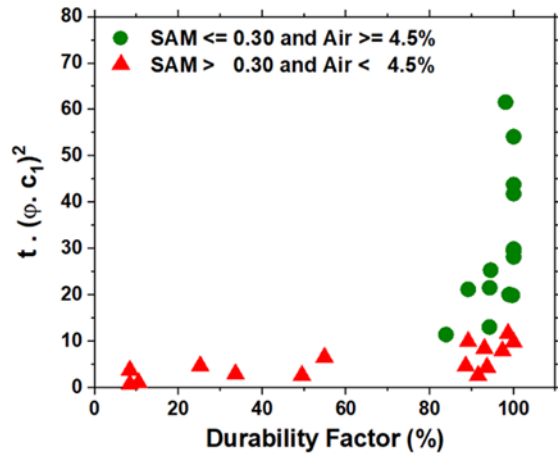
Figure 3.2.4. The measured durability factor (ASTM C 666-15) versus the normalized time to reach critical saturation (TTRCS model) for the mixtures with varying w/c, air content, and air quality.

3.2.4 Practical implications

This work provides data for a numerically based model to predict freeze-thaw durability that uses the air quality, air content, and quality of the matrix (i.e., formation factor). These mixture parameters have been shown to be easily derived from currently available measurement methods and the predicted results have been shown to correlate well to two different types of rapid freeze-thaw testing with significantly different storage and freezing rates. This model can allow the prediction of freeze-thaw service life of concrete mixtures based on mixture designs. Further, this could serve as a tool to adjust performance expectations of field concrete based on the

provided materials versus what was required in design. This could help determine the change in service life and therefore determine reasonable bonuses or penalties. This would be a valuable way to more closely tailor the design of concrete for the environment and service life expectations of the owner.

References

[1] W.J. Weiss, T. Ley, O.B. Isgor, T. Van Dam, Toward performance specifications for concrete durability: using the formation factor for corrosion and critical saturation for freeze-thaw, Proceedings of the 96th Annual Transportation Research Board, Washington, DC, USA (2017) 8-12.
[2] K. Bharadwaj, D. Glosser, M. Khanzadeh Moradllo, B. Isgor, J. Weiss, Toward the Prediction of Pore Volumes and Freeze-Thaw Performance of Concrete Using Thermodynamic Modelling, Cement and Concrete Research 124 (2019).
[3] M. Khanzadeh Moradllo, C. Qiao, R.M. Ghantous, M. Zaw, H. Hall, M.T. Ley, J. Weiss, Quantifying the Freeze-Thaw Performance of Air-Entrained Concrete Using the Time to Reach Critical Saturation Modelling Approach Cement and Concrete Composites Under review (2019).

3.3 USING X-RAY COMPUTED TOMOGRAPHY TO INVESTIGATE MORTAR SUBJECTED TO FREEZE-THAW CYCLES

This work uses X-ray computed micro tomography (XCT) to investigate the role of critical DoS and air void system on the crack propagation of Portland cement mortar subjected to freeze-thaw cycles. X-ray CT uses X-rays to look inside of a sample and take 3D images. The technique is non-destructive and so it can be used to investigate concrete before and after different events. For this 3D scans were made before and after freezing mortars that were cast with and without air entraining agent. These mortars were saturated to different levels or to different DoS. This was done to simulate different moisture content for concrete in the field. Next, the samples were subjected to a single freeze thaw cycle and then they were scanned again.

The work made two very important findings. First, cracks were observed only for the sample without air entrainment and with a very high DoS. These cracks were observed to extend from existing cracks and form at the transition between aggregates and paste. An example of this damage is shown in Figure 3.3.1.
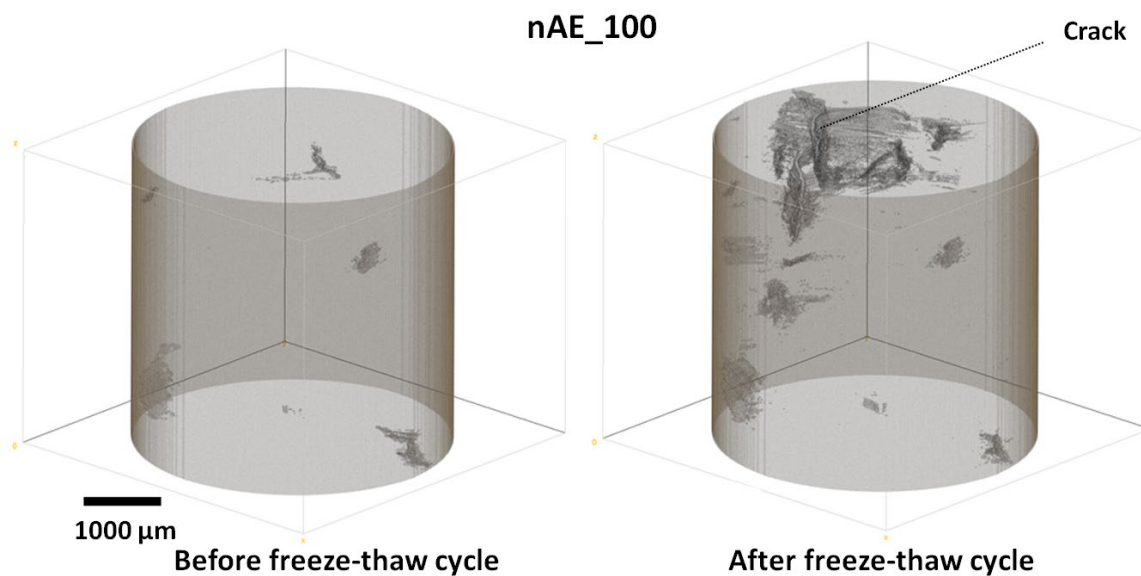
Figure 3.3.1. An example of the 3D rendering of cracks for saturated sample both before and after freeze-thaw damage for nAE_100.

The second important finding is that the voids within the mortar samples that were not saturated showed that the voids filled with solids after freezing. An example of the filled voids can be seen in Figure 3.3.2.
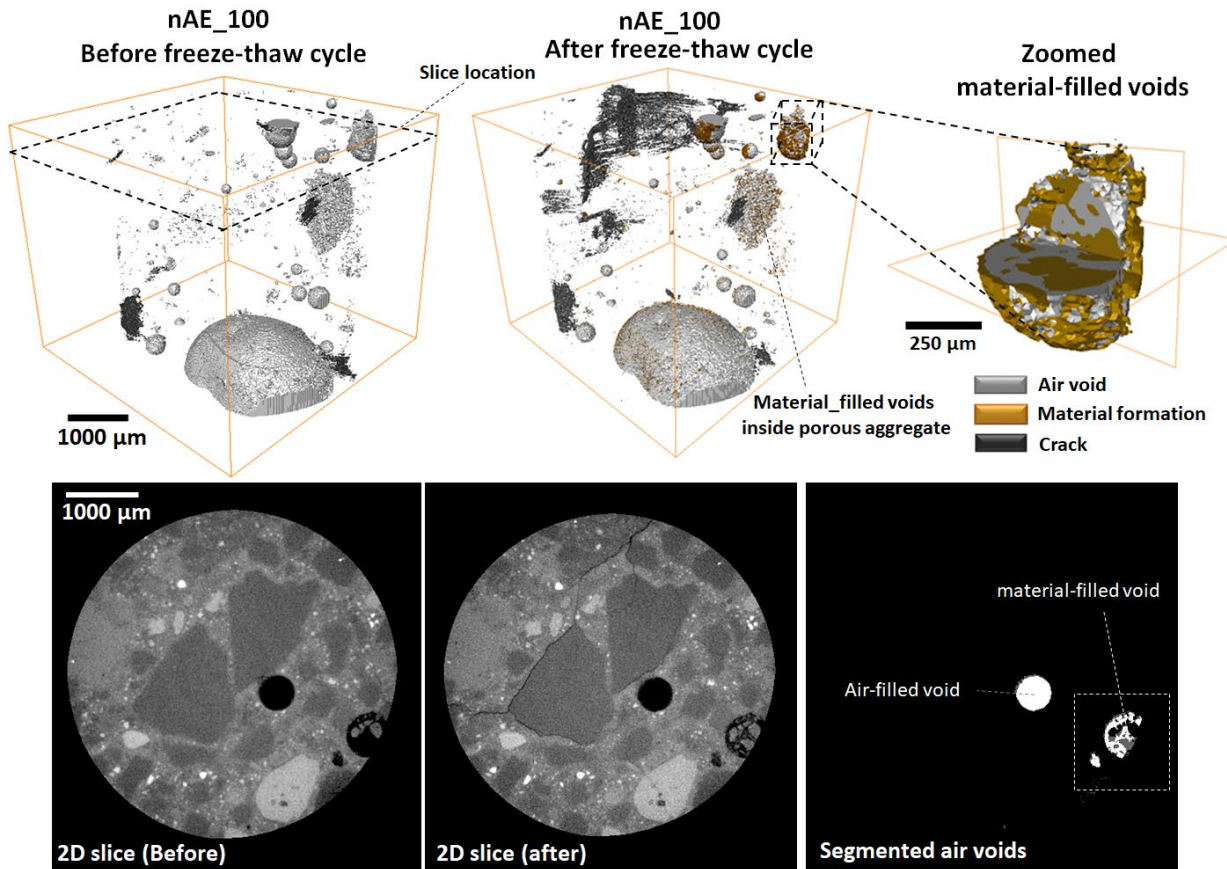
Figure 3.3.2. An example of a 3D rendering of the air voids, cracks, and infilled voids for the saturated sample (DoS=100%) before and after freeze-thaw testing.

The filling occurred in all size voids but the majority of the solids formed in the voids < 50 μm in diameter. In fact, > 75% of the voids < 50 μm in diameter lost at least 20% of their volume. More details can be seen in Figure 3.3.3. The samples nAE were not air entrained and the samples AE were. The numbers in the legend in Figure 3.3.3 are the DoS of the concrete.
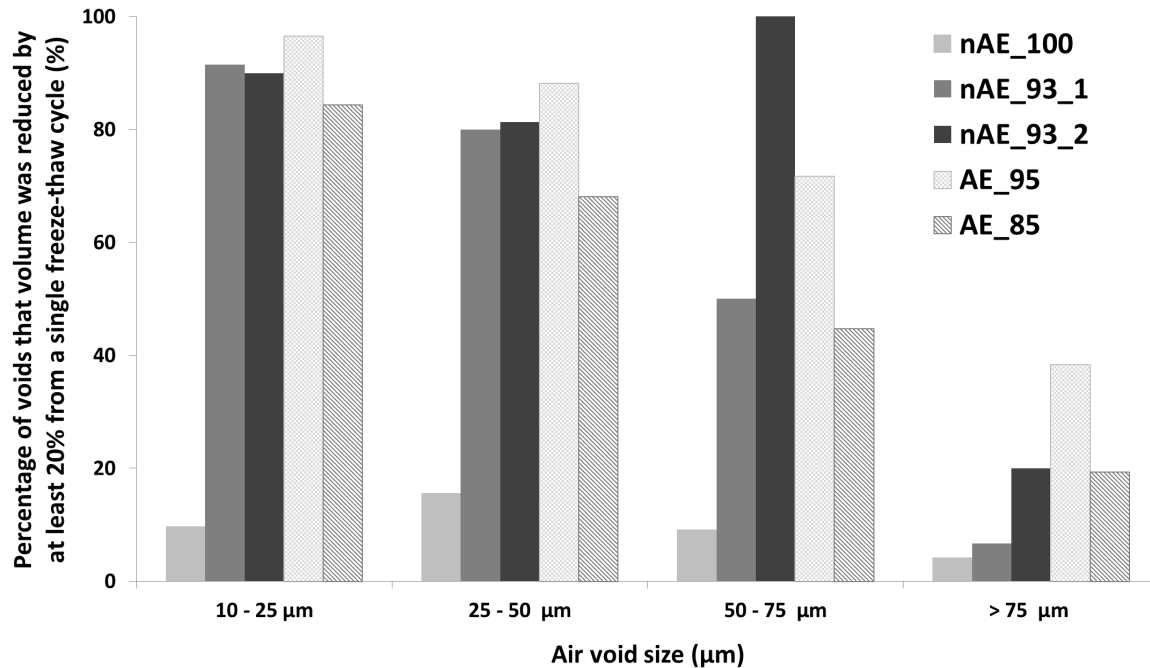
Figure 3.3.3. Percentage of voids that volume was reduced by at least 20% from a single freeze-thaw cycle

The material formed in the voids was investigated with scanning electron microscopy and X-ray fluorescence microscopy. The chemical makeup of the material was found to be high in calcium with some silicon and aluminum. The material seems to be calcium hydroxide or some other calcium salt.

This finding is important because these small voids are the most important for resisting freeze thaw damage and they are losing volume from the freezing cycles. No one in the current literature has looked at concrete both before and after a freeze thaw cycle with this imaging technique to learn how the material changes. This air void filling could be a critical part of the freeze thaw durability mechanism.

More details about this work can be found in Appendix in this report. It is recommended that more testing be done for a larger number of freeze thaw cycles and different mixture designs to gain more insight into the impact of the air void filling and the distribution of cracking in concrete subjected to freezing. These findings will be an important addition to the freeze thaw model proposed for phase 2 of this work.

3.4 INSTRUMENTATION FOR MEASURING FIELD ENVIRONMENT CONDITIONS

The temperature and moisture of concrete plays an important role in freeze thaw damage. Concrete that is near saturation when a freezing event occurs will have a higher probability of experiencing damage. This means that different locations will have different propensity for freeze thaw damage. Currently, most state DOTs use a constant air content of 6% regardless of the location. This assumes that the danger for freeze thaw damage is the same in every region. While this is not likely true, it is not possible to make changes to current specifications without extensive data.

This work is focused on developing an instrumentation box and set of samples that can measure the moisture and subsequent freezing events in different environments. The data from this testing can provide the critically needed data that will truly allow different environments to be compared. With this new information and subsequent laboratory testing it may be possible to better design concrete for the local weather conditions. The aim of this part of the project is to build these devices and then supply them to the different supporting states. The long term measurement of these devices will be done under future testing.

3.4.1 Experimental Methods

The configuration of the sample and data logger is shown in Figure 3.4.1. Each pallet contains two mortar samples that are surrounded in concrete to protect them and an instrument box. Two mortar samples are used to get replicate measurements and also to anticipate some of the instrumentation failing in the field. The surface of the specimen is 1" lower than the mold top to promote accumulation of water on the top. This is important because freeze thaw damage typically occurs in the areas of poor drainage in the field. This space between the surface of the mortar samples and the surface of the block force any water that falls to be retained and to evaporate naturally. Again, this will mimic areas with poor drainage. The mortar samples are surrounded by a layer of concrete. This concrete is helpful to protect the wires, keep the samples from falling over or being taken, and to insulate the mortar samples.
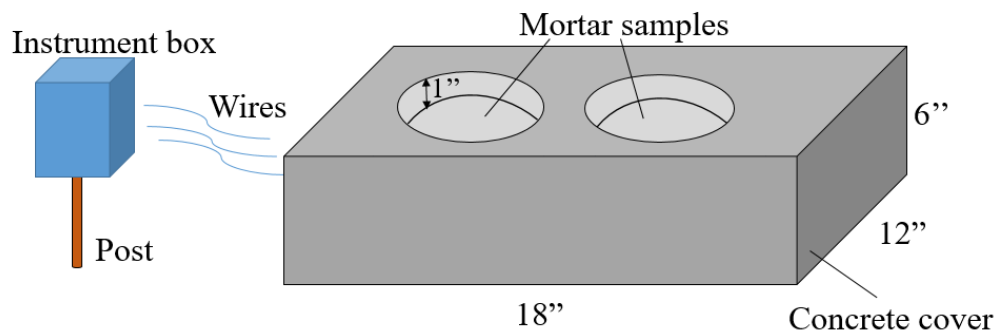
Figure 3.4.1. Overview of the samples and instrument box.

3.4.1.1 Concrete and Mortar Materials & Mixture Design

The mixture in the 6 in. x 6 in. molds was a standard mortar mixture with a water-to-cement ratio of 0.45. The cement met the requirements of a ASTM C150 Type I Portland cement. The fine aggregate was a natural sand and met the requirements of ASTM C33. The mixture surrounding these 6x6 molds was a standard concrete mixture with reinforced concrete fibers. The samples are all > 90 days old when sent to the field.

3.4.1.2 Measurements

Each sample has 8 pairs of stainless steel threaded rods with a diameter of 1/8" and four type T thermocouples that are placed into the mold along its depth as shown in Figure 3.4.2 and Figure 3.4.3. Two samples were cast together in concrete to protect and solidify this sample setup as shown in Figure 3.4.4. The impedance is measured between each pair of stainless steel rods at a consistent height. Since the mortar is > 90 days old and

did not use a fly ash or slag then the electrical signal should not change over time. This means that the only changes will be from a change in moisture which will change the impedance of the mortar. A thermocouple and set of stainless steel rods is also placed just above the surface of the sample. Since the stainless steel rods are in the air then they will not allow an impedance signal unless there is water on the surface. The thermocouple will give information about the surface temperature of the sample. Next thermocouples are placed at four different depths. This information will be used to find the temperature profile in the samples over time.
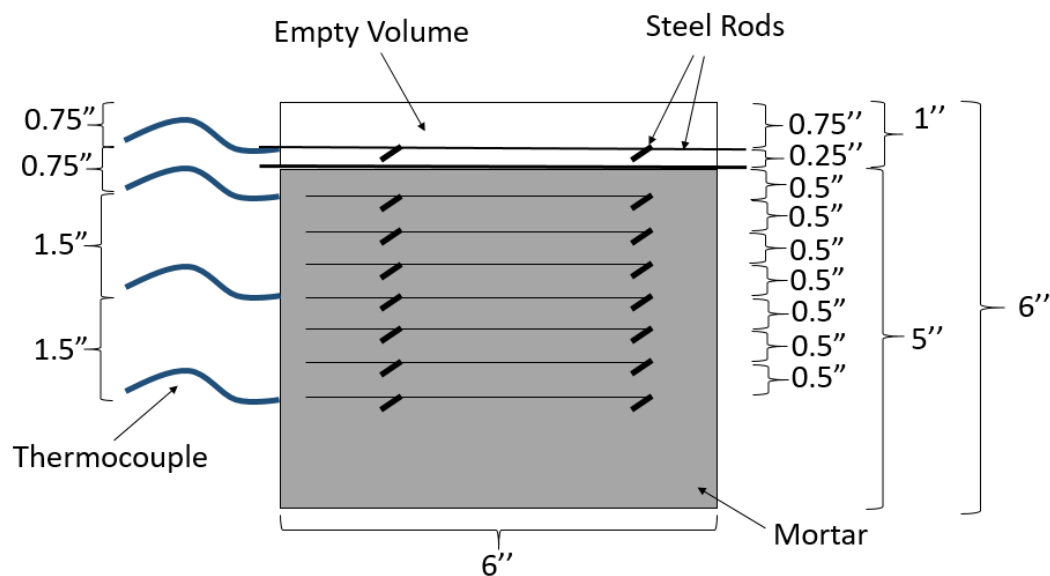

Figure 3.4.2. Layout of stainless steel rods and thermocouples in mold.

Figure 3.4.3. Mortar sample molds.

Figure 3.4.4 – An overview of the mortar samples being prepared and also surrounded by the concrete cover and ready for the instrumentation box.

3.4.1.3 Instrument box

The instrument box is a collection of equipment that was built for this project to monitor the samples. A solar panel is used to provide power. The box also contains a battery and circuit board. Figure 3.4.5 shows an overview of the assembled box. A data logger developed by the research team is used to investigate the samples and store the data. The outside box will protect the equipment in the field.

Figure 3.4.5. Instrument box with solar panel

Measurements are expected to be made every 30 minutes in the field for the temperature and impedance from 12 different sensors in the samples. The data will be stored on a USB drive within the box. The DOTs will be asked to gather the data every few months and send it to a website.

3.4.2 Evaluation of the system

Before starting the tests a set of experiments were completed to evaluate the performance of the system. This test consisted of subjecting the concrete to different wetting and drying cycles to see how the system responds. A thin layer of water was added on the top of the samples to simulate water accumulation in the field. Then the samples were left to the air. During this process, the water penetrated into the samples and the surface became dry again later. This impedance measurement was conducted over a period of 36 continuous days, during which the specimens underwent 3 cycles.

The time-dependent impedance response of different layers is shown in Figure 3.4.6 and the differential or change in impedance is shown in Figure 3.4.7. The layer number from 2 to 8 is corresponded to the different

depth of the rods from top to bottom with layer 2 being the top surface of the sample. Layer 1 isn't shown in this graph because it is put in the air, not inside the samples.

It can be seen from Figure 3.4.7 that the impedances of layer 2 and 3 change immediately when the water is added to the top of the specimens. Layer 2 and 3 are much more sensitive compared with layers from 4 to 8. Layers at a lower depth generally have a lower impedance value, which means they have higher moisture contents and maintain humidity longer. There is a lag in the response between the lower depth and the top part of a sample when the environment changes at the surface.

Figure 3.4.6 and 3.4.7 shows that the rate of penetration of water inside the sample is faster than that of evaporation of water. Accordingly, the samples get saturated easier than they dry. The change of moisture content at different depths is not consistent from top to bottom. This system shows great promise and will provide important results from the field testing.
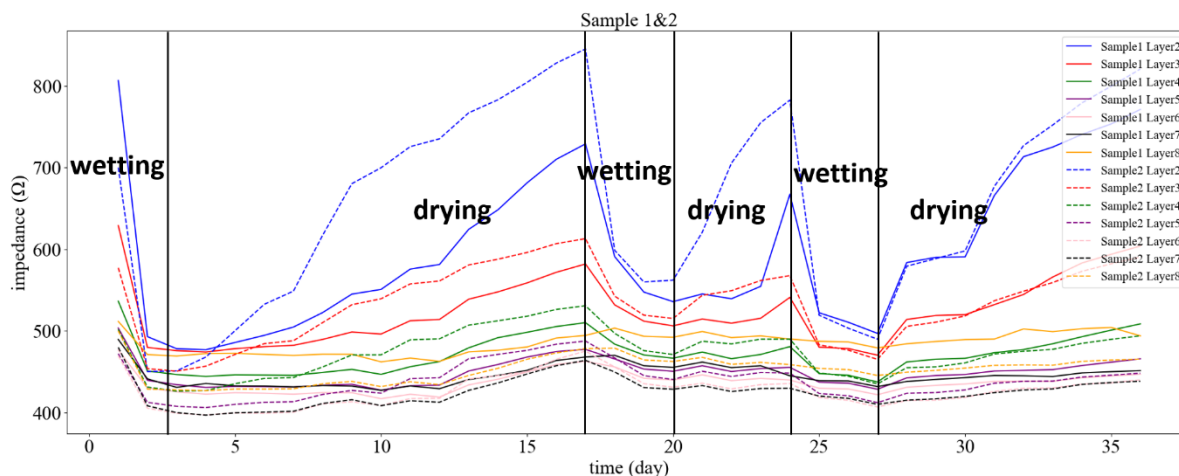
Figure 3.4.6. Time-dependent curve of impedance response
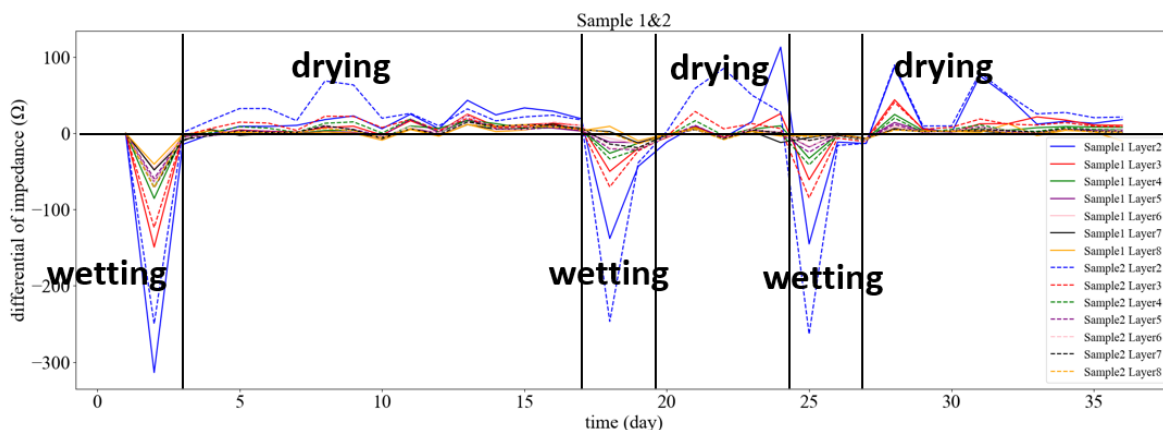
Figure 3.4.7. Time-dependent curve of differential of impedance

3.4.3 Implementation of device in field

Several specimens will be loaded on pallets and sent to different states to be used in the field. Each state is asked to take the pallets to distinctly different weather conditions in their state and then power the data logger. This will allow the moisture and freeze thaw cycles of the samples to be obtained from these different locations and the results can be compared. The research team will use the local weather station data to compliment the measurements made in the field. This test will also potentially help us get more information about drying, curling, and shrinkage.

3.4.4 Conclusion

A new method has been presented to measure different weather conditions on concrete and quantify different freeze thaw environments. The lab testing shows that this system will provide valuable information about the change in moisture and temperature over the depth of the samples for very different exposure environments. This promises to provide outstanding data to provide insight into specification development and also to create improved freeze thaw prediction models. This work shows great promise and will be a major focus of future work.

4.1 RECOMMENDATIONS

4.2 MEASURING AIR VOID SYSTEMS IN FRESH CONCRETE

This work presents a new method to measure the air void quality in fresh concrete by using sequential pressures. The test can determine both the volume of air and a parameter called the SAM number that is shown to correlate to hardened air void analysis and rapid freeze-thaw testing. Results from two different testing laboratories and field data from 303 concrete mixtures are reported. In addition, the measurement variance is shown to be lower than hardened air void analysis and rapid freeze-thaw testing. Also, the SAM continues to evolve and these improvements promise to reduce the variability and make it easier to implement this new tool in the field.

Establishing the SAM test method
1. A SAM Number of 0.20 and 0.25 shows a correlation to a Spacing Factor of 200 μm and 250 μm with an 88% and 85% agreement respectively.
2. A SAM Number of 0.32 correlates with a Durability Factor between 60% and 80% for over 88% of the data investigated, while a Spacing Factor of 200 μm correlated with a Durability Factor of 70% for only 68% of the data.
3. A target SAM value of 0.32 or conservatively 0.30 is suggested for design to ensure mixtures have a satisfactory performance in rapid freeze-thaw testing.
4. The standard deviation of two SAM Numbers from two different operators using different sets of equipment that were run simultaneously was shown to be 0.049 for concrete and 0.021 when investigating water and a calibration vessel. This lower variability with water suggests that over 50% of the variation in the test is caused by the use of concrete in the test.
5. The coefficient of variation of the SAM Number that showed the best correlation to freeze-thaw durability is 15.2%. This value is comparable but lower than similar measurements from hardened air void analysis and rapid freeze-thaw testing.

Use of SAM in the field
6. Air contents between 3% and 8% were needed in order to obtain a Spacing Factor of 200 μm for the 257 laboratory and 231 field mixtures investigated. This shows the inability of a specific air volume to correlate with air void quality.
7. For 257 laboratory mixtures, the correlation between a SAM Number of 0.20 and a Spacing Factor of 200 μm agrees with 85% of the laboratory data comparisons.
8. For 231 field mixtures, the correlation between a SAM Number of 0.20 and a Spacing Factor of 200 μm agrees with 70% of the field data comparisons.
9. For 231 field mixtures, 25% or 57 of them that were accepted based on their air volume were shown by the Spacing Factor and SAM Number to have an air void distribution that is not recommended for freeze thaw durability.

Using tools to improve the reliability and usefulness of the SAM
10. The cubic quantile lines provides a useful approach to quickly evaluate the average void size in fresh concrete mixtures. These lines can be used to gain immediate feedback on how the concrete mixtures, material changes, and construction practices impact the average void size in their concrete.
11. The shotgun has proven to be a helpful tool to help users continuously fill the bottom chamber of the SAM. This can be done more rapidly and also with less error than the conventional methods.
12. The reliability factor can help improve the accuracy of the SAM by giving users immediate feedback on how accurate they have completed the test.

Using the SAM to evaluate pumped concrete
13. Based on laboratory studies, the pumping of concrete causes changes in the air void system of the fresh concrete. Regardless of the change in the air void system of the fresh concrete, the hardened air void

parameters and freeze thaw performance did not show substantial change of the air void system due to pumping. This work shows the air content of fresh concrete cannot be accurately measured after being pumped based on laboratory testing.

14. Based on field studies, the air void system in fresh concrete was regularly disrupted due to pumping. For example, > 30% of the mixtures showed change in air content by more than 1% and > 60% of the mixtures shows an increase in the SAM number by > 0.05. This suggests the air void quality of the concrete was significantly changed by the pumping process. Both the A-frame and the Arch were found to change the air void system the most.

15. While the fresh properties in the field were shown to change, the hardened air void results suggest a different scenario. Despite the arch and A-frame showing significant changes in the fresh concrete, 71% of the arch, and 70% of the A-frame, and 88% of the flat configurations show that the change in the spacing factor of the hardened concrete did not significantly change before and after pumping. This confirms the recovery of the air void system before the concrete hardens suggested in the previous section.

Measuring the SAM in low workability concrete

16. For the low slump concrete mixture investigated it required significant energy in order to consolidate the concrete. Consolidation with rodding, internal vibration, and two different vibration tables was investigated. One of these tables was a newly developed device called the MinT that uses a portable electric vibrator that straps to a steel table with clamps for the unit weight pot.

17. The testing shows that the rodding and use of an internal vibrator had the highest coefficient of variability at close to 40%. The use of a vibrating table and the MinT reduced the coefficient of variability by a factor of two. Since the MinT is a portable solution to this issue then it may be able to be used in the field to reduce the variability of SAM measurements with low slump concrete mixtures. This needs to be further investigated in field testing.

4.3 PREDICTION OF FREEZE THAW DURABILITY

The following section outlines the major findings from the prediction of freeze thaw durability. The sections provided in this report provide some details while the detailed sections in the appendix provide even more insight.

SAM Air Number and Air Content

1) A generalized relationship was found between the SAM Number (SAM) and the air content (V_{AIR}). The general form of the equation is shown in equation 2

$$SAM = C_1 \, V_{Air}^{C_2}$$

where, C_1 and C_2 are constants that describe the quality of the air void system. C_1 was found to range between 1 and 6 with lower numbers referring to a better air void system while C_2 was typically observed to be -5/3.

Matrix saturation (*DoS_Matrix*):

2) The matrix saturation was measured for a wide range of mixtures using Task 1.6a and 1.6b (Appendix A) which have been recommended to AASHTO for approval. These testing procedures can be used as part of either mixture approval or for quality control testing.

3) The theoretical porosity of the air-entrained concrete can be estimated based on the mixture proportions using a computational model. This model can be based on Powers assumptions for OPC (ordinary portland cement) systems for GEMS for systems with OPC and SCM

(supplementary cementitious materials). In both of these cases the model is scaled to concrete by accounting for aggregate volume [1-3]. The theoretical porosity was found to be comparable to the experimental data using the matrix saturation.

4) The matrix degree of saturation at the Nick Point (DoS_{Matrix}) decreases as the air content increases. The experimentally measured values of DoS_{Matrix} is comparable to the theoretical values (i.e., ± 10 % variation).

Secondary sorption (S'_2) and the Formation Factor (F):

5) The formation factor was defined in two moisture states: complete saturation (F_{SAT}) and matrix saturation (F_{APP} or the apparent formation factor. The formation factor at complete saturation is the conventional definition; however, it is argued that this is not how concrete typically exists in service and the values are dependent on the air content. The apparent formation factor (F_{APP}) of concrete at matrix saturation (i.e., also referred to as the Nick Point) is independent on the air content. As such it is recommended that the F_{APP} should be used as the quality control value describing a mixture. This can be determined using AASHTO TP 119 or 358 and the pore solution chemistry. F_{SAT} and F_{APP} can be correlated using a saturation function in a form of a power function with a fitted exponent of approximately 3.

6) The initial and secondary absorption rates are relatively independent of air content.

7) The addition of HRWR reduces the mean initial and secondary absorption rates at a given w/c, particularly at low w/c mixtures. This can be attributed to the refined microstructure that reduces connectivity of the pore network.

8) A linear relationship exists between the initial and secondary absorption rates and the reciprocal of the square root of the apparent formation factor. Therefore, the apparent formation factor appears to be used to predict the water absorption and may serve as a replacement of the water absorption test. The coefficient can be related to the conditioning of the sample (i.e., the size of the pores emptied in drying) and the average pore size of the mixture.

9) A method to estimate the water absorption by the matrix pores and air voids of concrete mixtures was established using NR. This method can help to improve the predictive capabilities of service life modeling methods for concrete elements and structures subjected to freeze-thaw cycles. This is because while the filling rate of air voids is a crucial factor in estimating service life of air-entrained concrete in cold environments, there is lack of previous studies to quantify this factor.

10) The air void filling process is substantially slower than the filling of the matrix pores. The water absorption front by matrix pores is significantly sharper than that of the air voids. This is attributed to the higher capillary pressure in matrix pores when compared to the air voids.

11) Samples with a lower w/c (i.e., 0.40) showed a lower rate of absorption by air voids (S_2') when compared to the samples with a higher w/c. This is due to the lower permeability of the matrix in low w/c samples (i.e., samples with higher F_{APP}).

12) The air volume has a minimal impact on rate of air void filling at a given w/c. However, as the air content increases, the percentage of the air void volume that is filled decreases regardless of the w/c for a given period of exposure. This lowers the DoS in the sample and delays the time to reach a critical saturation. As a result, concrete with a greater air content has a longer time to reach critical saturation

13) The impact of SAM Number on S_2' appears to depend on the quality of the paste matrix. For very high F_{APP} (i.e., low permeability), the impact cannot be seen in this study since the absorption rate is so low. However, result shows that the sample with good air quality or low SAM Number has a lower rate of fluid absorption by air voids.

Critical degree of saturation (DoS_{CR}):

14) Experimental data was used to develop an equation to estimate the DoS_{CR} based on SAM Number. The general form of the equation is shown below:

$$DoS_{CR} = DoS_{Constant} - 10\,SAM$$

where, $DoS_{Constant}$ was 87 for conventional mixtures and 82 for mixtures with HRWR. It is not clear as to why this value is not the same for both mixtures.

15) The samples with and without HRWR showed a similar trend for the '$\Delta = DoS_{CR} - DoS_{Matrix}$' as a function of the SAM Number. Therefore, an exponential relationship was developed to estimate the Δ based on the SAM Number. This relationship can be used in TTRCS model to predict the time to reach critical saturation just using SAM Number and apparent formation factor. However, further work is needed to examine this equation for the mixtures with different materials.

16) The time to reach critical saturation exponentially increases as the SAM Number decreases (i.e., better air quality). All samples with SAM Number below 0.20 exhibited a normalized time to reach critical saturation greater than 10. In addition, the samples with higher air content have a longer time to reach critical saturation.

17) The addition of HRWR increased the normalized time to reach critical saturation in the mixtures with a low w/c at a given SAM Number (i.e., air quality). This is primarily attributed to the influence of the addition of HRWR on tortuosity of the samples (i.e., F_{APP}) with a lower w/c (w/c=0.40) which reduces the filling rate of air voids.

General Mixture Observations

18) The mixtures with a HRWR used in this study required a higher volume fraction of entrained air (≈6% air content) to satisfy the recommended limit for durability factor (75%) than the mixtures without HRWR (≈4% air content).

19) Based on TTRCS model and ASTM C 666 results, 86% of the mixtures with air content above 4.5% and a SAM Number below 0.30 have a normalized time to reach critical saturation of longer than 20 and durability factor that is higher than 75%.

20) A systematic methodology has been developed to determine DoS_{CR} of mortar samples based on length change measurements using a thermomechanical analyzer. This methodology uses small specimens that can be conditioned rapidly, which enables specific scientific features to be studied more quickly for a larger number of samples with a high accuracy. This approach may be very valuable for testing a much wider range of matrix compositions.

21) The quality of the air void system (volume, size and distribution of these air voids) inside the mortar samples has a significant impact on the freeze-thaw performance. Based on the length change measurements, samples with a high quality of air void distribution (SAM<0.20) show a higher resistance to freeze-thaw cycles compared to samples with a poor air voids quality.

4.4 FUTURE WORK

While the authors believe that this work has provided great advancement for the measurement and modeling of freeze thaw durability, they recommend that additional work be performed to:

1. Quantify how different weather conditions impact the freeze thaw performance of concrete with low-cost data loggers. This work has been started under this existing project but these samples should be distributed in the field and used to quantify the combination of saturation and freeze thaw cycles in different states.
2. Investigate the freeze thaw performance of existing structures in different climates with different air void qualities. In combination with quantifying the weather in different environments, structures should be found in these structures with different quality of air void systems to determine how they perform. This will provide true case studies of field performance in a quantified exposure.
3. Expand the freeze thaw model to a larger range of mixtures to see if the trends still hold.
4. Further evaluation of the accuracy of the modeling predictions for determining the matrix saturation and the relationship between the secondary sorption and formation factor.
5. Better understand the damage propagation after critical saturation is reached.
6. Extension of this work to include salts such as those that result in calcium oxychloride to further improve the computational modeling predictions.
7. Determine how air void filling impacts the durability of concrete from freeze thaw cycles.
8. Develop freeze thaw specifications based on concrete quality, air void system, and local weather conditions.
9. Determine how construction methods such as pumping, mixing time, paving vibration, and hand held vibrators impact the air void spacing within concrete
10. Improve the SAM by making the measurement more consistent through developing a semi-automated testing procedure and improving reliability prediction.
11. Further refine a rapid test method that measures the uptake and fluid and resistivity of the concrete to determine the freeze thaw durability of concrete

This proposed work will answer a number of important questions and will create several new tools to help determine the freeze thaw durability of concrete. Further, this work will create new specifications for DOTs based on their local weather conditions and quality of their concrete. These new efforts will create a new level of understanding and produce practical tools and guidance that will help DOTs change their specifications and consistently produce more durable concrete.